Long-term evaluation of VDES R-Mode

GA3.2/3.3 project report

Issue: 1.1

Issue Status: Approved

Issue Date: 01/05/2022

	Name	Partner	Signature
Provided	Lead Author	Krzysztof Bronk (NIT)	
Review	Work Package Leader	Krzysztof Bronk (NIT)	
Approval	Project Manager	Stefan Gewies (DLR)	

Document Information

Project Title	R-Mode Baltic 2
Work Package No.	GA 3.2/3.3
Document Title	Long-term evaluation of VDES R-Mode
Description	The major topic of the document is the analysis of the data from long-term positioning monitoring VDES R-Mode
Date	01/05/2022
Lead Author	NIT
Lead Author's Contact Information	National Institute of Telecommunications Wireless Systems and Networks Department Telephone: (+48) 58 341 71 21 E-mail: K.Bronk@itl.waw.pl
Contributing Author(s)	Krzysztof Bronk, Magdalena Januszewska, Adam Lipka, Patryk Koncicki, Rafał Niski, Błażej Wereszko
Approval	Yes

Track Changes

Issue	Date	Pages	Change	Author, Company
0.13	01/03/2022	71	Draft	NIT
1.0	11/03/2022		Internal review	NIT (Adam Lipka)
1.1	15/03/2022	95	Internal approval	GA 3.3 Leader (Krzysztof Bronk)

SHORT DESCRIPTION OF PROJECT

The R-Mode Baltic 2 project is co-financed by the European Regional Development Fund within the Interreg Baltic Sea Region Programme.

This report is available for download on the project website https://www.r-mode-baltic.eu.

Contents

1 Introduction 10
2 VDES R-Mode 2 campaign preparations 12
2.1 Location of the receiving station on the Hel Peninsula 12
2.2 Technical parameters of the VDES R-Mode 2 stations 20
3 R-Mode Baltic 2 measurement campaign 24
3.1 Selection of the measurement scenario 24
3.2 Collected data in the measurement campaign 28
4 VDES R-Mode 2 static "long-term" ranging results 30
4.1 Analysis of RMS fluctuations depending on the measurement time (day/night) 33
4.2 Analysis of the power and quality of correlation of received signals 48
4.3 The relation between the RMS and the prevailing meteorological conditions 49
4.4 The phenomenon of tropospheric ducts in measurements 66
5 VDES R-Mode Baltic 2 static "long-term" positioning results 69
5.1 Comparison of the positioning accuracy depending on RMS changes with the measurement time (day/night) 70
5.2 Fluctuations of positioning accuracy and fluctuations of the range measurement accuracy due to weather conditions 78
5.3 Comparison of the positioning accuracy for various correlators 78
6 Real-time positioning demonstrator application 82
6.1 Description of the software 82
6.2 Range measurement emulation 83
6.3 Analysis of dynamic scenarios 84
6.3.1 Line scenario with disappearing reference signal 84
6.3.2 Non-line scenario with HDOP changing 87
7 Summary and conclusions for the next measurement campaign 91
References 94

List of Tables

Table 2-1: Technical conditions relevant to the installation of a VDES receiver 14
Table 2-2: VDES antenna height measurement by Trimble RTK receiver, type BX982 19
Table 2-3: Technical parameters of the R-Mode Gdynia base station 20
Table 2-4: Technical parameters of the receiver.....21
Table 2-5: Maximum useful and interfering ranges of the R-Mode Gdynia base station. 21
Table 3-1: Coordinates of the emulated stations as well as the transmitter and receiver.....26
Table 3-2: Measurement data collected in summer.....28
Table 3-3: Measurement data collected in autumn.....29
Table 3-4: Measurement data collected 30
Table 4-1: RMS summary for given periods of the day - 19.06.2021.....39
Table 4-2: RMS summary for given periods of the day - 20.06.2021.....40
Table 4-3: RMS summary for given periods of the day - 22.06.2021.....41
Table 4-4: RMS summary for given periods of the day - 24.06.2021.....42
Table 4-5: RMS summary for given periods of the day - 26.06.2021.....43

List of Figures

Figure 2-1: The location of the VDES transmitter in the Port of Gdynia and the potential locations of the receiver in Jastarnia or in Hel 12
Figure 2-2: Location of the Hel Lighthouse in relation to the Gdańsk Bay water line towards Gdynia....13
Figure 2-3: The Hel Lighthouse and the roof of the engine room with the antenna of the RTK station. 13
Figure 2-4: View of the Jastarnia harbor and the existing RTK and VHF antenna installations on the roof....15
Figure 2-5: View of the harbor office in Jastarnia from the south - the entrance to the port...15
Figure 2-6: View from the roof of the Jastarnia harbor. In the foreground, the RTK station mast, which can be used to mount the rod antenna of the VDES receiver. Two additional RF cables were led to it. 16
Figure 2-7: RTK cabinet and power sockets. Below is the place for the devices (rack) of the VDES receiver. 17
Figure 2-8: View of the entry of antenna cables through the roof with a vertical pipe - bottom view....18
Figure 2-9: View of the antenna cables exit on the roof - top view. 18
Figure 2-10: Map of the useful range of the R-Mode Gdynia station 22
Figure 2-11: Map of the interfering range of the R-Mode Gdynia station 23
Figure 3-1: Receiving station in Jastarnia 24
Figure 3-2: Transmitting station in the port of Gdynia [3-1] 25
Figure 3-3: Measurement scenario for four emulated broadcasting stations 25
Figure 3-4: Frame structure VDES 26
Figure 3-5: R-Mode ranging signal 26
Figure 3-6: VDES transmitter block diagram (Gdynia Port)....27
Figure 3-7: VDES receiver block diagram (Jastarnia Harbor) 28
Figure 4-1: Concept of collecting data from four emulated broadcasting stations 30
Figure 4-2: Measurement data samples recording....31
Figure 4-3: USRP platform 31
Figure 4-4: Recorded sample slots and corresponding correlation functions 32
Figure 4-5: Signal correlation application - ranging....32
Figure 4-6: The results obtained from 5-minute segments of measurements....33
Figure 4-7: Results for measurements that lasted 11 days - the obtained RMS for each day during the summer campaign 34
Figure 4-8: RMS for different times of day for summer measurements (subtracting mean error calculated for the first day only) 35
Figure 4-9: RMS for different times of day for summer measurements (subtracting mean error calculated for each day) 36
Figure 4-10: Determined RMS for each measuring hour for summer data 37
Figure 4-11: Determined RMS for each measuring hour for summer data and measurement errors....38
Figure 4-12: Detailed analysis of the RMS observed for one day depending on the consideration of the mean error - 19.06.2021 39
Figure 4-13: Detailed analysis of the RMS observed for one day depending on the consideration of the mean error - 20.06.2021 40
Figure 4-14: Detailed analysis of the RMS observed for one day depending on the consideration of the mean error - 22.06.2021 41

Figure 4-15: Detailed analysis of the RMS observed for one day depending on the consideration of the mean error - 24.06.2021 42
Figure 4-16: Detailed analysis of the RMS observed for one day depending on the consideration of the mean error - 26.06.2021 43
Figure 4-17: Results for measurements - the RMS obtained for each day during the summer and autumn campaign 45
Figure 4-18: Measurement errors with respect to the GNSS receiver for summer and autumn measurements 46
Figure 4-19: Measurement errors with regard to the GNSS receiver for summer and autumn measurements 47
Figure 4-20: Comparison of the received signals strength for the summer and autumn campaigns 48
Figure 4-21: Comparison of the SNRs obtained during summer and autumn measurements 48
Figure 4-22: Correlation quality for summer and autumn measurements 49
Figure 4-23: The obtained RMS values per day during the summer campaign (including meteorological data) 50
Figure 4-24: RMS for different times of day for summer measurements (subtracting mean error calculated for the first day only, including meteorological data) 51
Figure 4-25: RMS values for each hour during the summer campaign, including meteorological data 52
Figure 4-26: Analysis of the observed RMS depending on the meteorological conditions (20.06.2021) 1/2 53
Figure 4-27: Analysis of the observed RMS depending on the meteorological conditions (20.06.2021) 2/2 54
Figure 4-28: Analysis of the observed RMS depending on the meteorological conditions (26.06.2021) 1/2 55
Figure 4-29: Analysis of the observed RMS depending on the meteorological conditions (26.06.2021) 2/2 56
Figure 4-30: Detailed analysis of the RMS (upper graph) and distance error characteristic for various meteorological factors (bottom graph) -14.10.2021 (1/2) 58
Figure 4-31: Detailed analysis of the RMS (upper graph) and distance error characteristic for various meteorological factors (bottom graph) 14.10.2021 (2/2) 59
Figure 4-32: Detailed analysis of the RMS (upper graph) and distance error characteristic for various meteorological factors (bottom graph) 15.10.2021 (1/2) 60
Figure 4-33: Detailed analysis of the RMS (upper graph) and distance error characteristic for various meteorological factors (bottom graph) 15.10.2021 (2/2) 61
Figure 4-34: Detailed analysis of the RMS (upper graph) and distance error characteristic for various meteorological factors (bottom graph) 16.10.2021 (1/2) 62
Figure 4-35: Detailed analysis of the RMS (upper graph) and distance error characteristic for various meteorological factors (bottom graph) 16.10.2021 (2/2) 63
Figure 4-36: Detailed analysis of the RMS (upper graph) and distance error characteristic for various meteorological factors (bottom graph) 17.10.2021 (1/2) 64
Figure 4-37: Detailed analysis of the RMS (upper graph) and distance error characteristic for various meteorological factors (bottom graph) 17.10.2021 (2/2) 65
Figure 4-38: Influence of the multipath phenomenon on the shape of the correlation function [4-4] 66
Figure 4-39: The phenomenon of tropospheric ducts 67
Figure 4-40: The phenomenon of tropospheric ducts - 26.06.2021 67

Figure 4-41: Signal attenuation (yellow line) and RMS (blue bars) for each day in the summer campaign 68
Figure 4-42: Signal average attenuation (yellow line) and RMS (color bars) for each day in the summer campaign 68
Figure 5-1: Geometry of the reference stations' location for long term static analysis 69
Figure 5-2: Summer campaign – RMS positioning errors for each day 70
Figure 5-3: Summer and autumn campaign – RMS positioning errors for each day 70
Figure 5-4: Summer campaign – RMS positioning errors for each hour 71
Figure 5-5: Summer and autumn campaign – RMS positioning errors for each hour 72
Figure 5-6: Summer and autumn campaign – positioning errors 73
Figure 5-7: Positioning errors observed on 22.06.2021 74
Figure 5-8: Measurements on 22.06.2021 - RMS positioning errors for each hour 75
Figure 5-9: Measurements on 22.06.2021 - RMS positioning errors for each hour 76
Figure 5-10: Measurements on 22.06.2021 - RMS positioning errors for each hour 77
Figure 5-11: Summer campaign – RMS positioning errors for each day and the precipitation data 78
Figure 5-12: The geometry of reference stations distribution in the scenarios: a) scenario 1 – four stations and good geometry HDOP=3.39; b) scenario 2 - three stations and good geometry HDOP=3.73; c) scenario 3 - three stations and poor geometry HDOP=9.20 ..79
Figure 5-13: Scenario 1 - TOA positioning error for: basic correlator (green), narrow correlator (red), double delta correlator with second pair spacing = 0.1 chip (blue) and double delta correlator with second pair spacing = 0.2 chip (orange) 80
Figure 5-14: Scenario 2 - TOA positioning error for: basic correlator (green), narrow correlator (red), double delta correlator with second pair spacing = 0.1 chip (blue) and double delta correlator with second pair spacing = 0.2 chip (orange) 80
Figure 5-15: Scenario 3 - TOA positioning error for: basic correlator (green), narrow correlator (red), double delta correlator with second pair spacing = 0.1 chip (blue) and double delta correlator with second pair spacing = 0.2 chip (orange) 81
Figure 6-1: Real-time positioning demonstrator application window 82
Figure 6-2: Range measurements emulator window 83
Figure 6-3: Station edit window 84
Figure 6-4: Line scenario with disappearing reference signal 85
Figure 6-5: Line scenario positioning errors, geometry (HDOP) and number of available reference signals 86
Figure 6-6: Non-line scenario with HDOP changing 87
Figure 6-7: Non-line scenario positioning errors and geometry (HDOP) 88
Figure 6-8: Non-line scenario R-Mode ranging positioning errors and geometry (HDOP) 89

Abbreviations

AIS	Automatic Identification System
ERP	Effective Radiated Power
E	Electric field intensity
EGNOS	European Geostationary Navigation Overlay Service
GNSS	Global Navigation Satellite System
GPS	Global Positioning System
GSM	Global System for Mobile Communications
h	Antenna height
HF	High frequency
KSBM	Krajowy System Bezpieczeństwa Morskiego
LNA	Low Noise Amplifier
LOS	Line Of Sight
LPF	Low-pass filter
LTE	Long Term Evolution
MF	Medium Frequency
MOG	Maritime Office in Gdynia
NF	Noise Figure
NIT	National Institute of Telecommunications
NLOS	Non Line Of Sight
PNT	Position, Navigation and Time
R-Mode	Ranging Mode
RMS	Root Mean Square
RRC	Root Raised Cosine
SDR	Software Defined Radio
SNR	Signal to Noise Ratio
SWR	Standing Wave Ratio
TOA	Time of Arrival
USRP	Universal Software Radio Peripheral
VDES	VHF Data Exchange System
VHF	Very High Frequency

1 Introduction

The following report summarises the activities of the National Institute of Telecommunications in the R-Mode's GAs 3.2 and 3.3 [1-1]. The main topic of the document is the description of the tasks that led to the creation of the R-Mode Baltic 2 long-term positioning monitoring [1-2,1-3] . This report also refers to previous documents "AIS and VDES Ranging – concept and signal design"[1-4], "AIS and VDES Ranging – measurements results" [1-5], "R-Mode positioning system demonstrator" [1-6] that were prepared for the R-Mode Baltic project, therefore there will be some references to these reports in the text.

The title of the GA's 3.2 task was: Static long-term evaluation of R-Mode test bed. As part of this task, long-term static measurements were carried out using the R-Mode Baltic position monitoring system. The tests were carried out using the installed transmitting station in Gdynia and the receiving station in Jastarnia. The purpose of this task was to determine the accuracy of the monitoring system operation and to measure the impact of variable weather conditions. For the purposes of the project, the R-Mode software was updated and a signal consisting of Gold code and an alternative sequence was implemented. The Gdynia VDES R-Mode transmitter has been updated in terms of hardware, i.e. software defined radio and filters. The influence of the time of day, season and weather conditions was analyzed. The results will be prepared in the form of a paper for scientific publication.

The title of the GA's 3.3 task was: Dynamic long-term evaluation of R-Mode test bed. The main goal of this GAis a long-term evaluation of the R-Mode system performance in dynamic conditions. The evaluation will be carried out in the target operational environment of the system (i.e.: at sea, within a dedicated test bed) using measurement platforms developed in the R-Mode Baltic project which will be adapted for that purpose. Tasks carried out under GA3.3 are based on the achievements of the R-Mode Baltic project. In the initial stage of activities, the test platform developed by NIT in the R-Mode Baltic project was used, in which the R-Mode transmitter was located in the Port of Gdynia (Poland). As part of this task, the VDES R-Mode Baltic system was implemented, which determines the position of the receiver in real time based on the determined pseudoranges.

The report is comprised of seven chapters (including this introduction).

In the second chapter, the most attention was paid to the preparations for the R-Mode 2 measurement campaign. All the technical parameters of the stations used were presented. The locations of the transmitting and receiving stations are also described. The third chapter presents a set of all recorded data, ready for processing in the next step. A measurement scenario was also proposed, according to which the subsequent measurements were conducted in the campaign. Chapter four focuses on the static analysis of long-term range measurements. All the analyzes were based on the calculated RMS errors and respective measurement periods in order to be able to draw correct conclusions later. The analyzed RMS was correlated with the meteorological data on the selected measurement days. Their influence on the pseudo-range error was assessed. It was also shown how the occurrence of the tropospheric ducts phenomenon could affect the temporary increase in the RMS error. The next chapter shows how the obtained pseudoranges changed the RMS of the receiver position. Similarly to the previous chapter - the results were analyzed for different periods of time and correlated with the meteorological conditions during the measurement campaign. The sixth chapter focuses on the description of the real-time position demonstration application. A simulation of dynamic measurements was presented, including the generation of pseudo ranges. The analysis of the results is presented for the linear scenario of the

motion in a circle. The last chapter presents conclusions resulting from the conducted measurement campaign. Plans for the future development of the R-Mode system and the upcoming measurement campaigns were also discussed.

2 VDES R-Mode 2 campaign preparations

The R-Mode Baltic project ended on 03/31/2021, but on 04/01/2021, its continuation began in the form of the Ranging Mode Baltic Sea test bed evaluation project, under the acronym R-Mode Baltic 2 [1-3]. The main goal of the R-Mode Baltic 2 project is a long-term evaluation of the R-Mode Baltic test stand and further testing of new R-Mode concepts. To this end, the project consortium will increase the monitoring capabilities of the R-Mode Baltic test stand and equip vessels with R-Mode-ready receivers and marine applications from the R-Mode Baltic project. This expanded network of static and dynamic monitoring stations was used for extensive R-Mode performance studies over a project period of nine months. The results are essential for further development of the proposed solution and its ultimate transformation into a reliable and internationally accepted backup system for maritime navigation. This project allows to observe stability in long-term measurements conducted in varying weather conditions.

2.1 Location of the receiving station on the Hel Peninsula

The first task here was the selection of a stationary VDES receiver's location on the Hel Peninsula in order to conduct long-term stability studies of the distance measurement (range) in signal transmission over the sea under various propagation conditions.

The VDES transmitter is installed on the mast of the beacon Gdynia facility in the port of Gdynia, and the receiver should be installed in a place ensuring an uninterrupted (as far as possible) signal transmission over the water, with a minimum land section [2-1].

On the basis of preliminary considerations, two alternative sites have been proposed at the facilities of the Maritime Office in Gdynia:

• At the Harbor of Jastarnia,

• In the engine room of the Hel Lighthouse.

The geographical location on the map and the distance from the broadcasting point of the two potential locations of the VDES receiver are shown in Fig. 2-1.

Figure 2-1: The location of the VDES transmitter in the Port of Gdynia and the potential locations of the receiver in Jastarnia or in Hel

The preliminary assessment on the map shows that the harbor in Jastarnia is located slightly further (20.24 km) than the engine room of the Lighthouse in Hel (18.28 km) (Figure 2-2, 2-3). The on-site inspection also showed that the harbor in Jastarnia is closer to the waterline than the building of the Lighthouse in Hel.

Figure 2-2: Location of the Hel Lighthouse in relation to the Gdańsk Bay water line towards Gdynia.

Figure 2-3: The Hel Lighthouse and the roof of the engine room with the antenna of the RTK station.

Table 2-1 summarizes the essential parameters and features of the two considered objects. Taking into account the location of the receiver in relation to the water line in the south direction (towards the port of Gdynia) and the height of the receiving antenna installation, which is more favorable for the position in Jastarnia, the focus was on the technical conditions of installation in the Jastarnia harbor. This location allows to receive the VDES signal in a straight line (LOS), i.e. it is possible to maintain optical visibility between transmitting and receiving antennas despite the curvature of the Earth.

Table 2-1: Technical conditions relevant to the installation of a VDES receiver

ID	Specifications / technical features	Location Jastarnia	Location Hel	Comments
1	Geographic location / Distance from the transmitter	54˚41' 43,7" 018˚ 40' 23,5" 20,24 km	54˚35' 58,37" 018˚ 48"45,16" 18,28 km	Map in fig. 2-1
2	VDES signal path	In a straight line, LOS	Covering with trees on the land section	
3	The route over land	Approx. 100m	Approx. 0,5 km	
4	Antenna mounting height	17,1 m	15 m	a.s.l.
5	Ease of installation	Flat roof + existing 2m mast	Lattice mast h=15m (difficult to access)	
6	Length of the VHF antenna cables	10-12 m	Approx. 25 m	
7	Length of the GPS cable	5 m - without the need for external assembly	The cable should be extended	
8	Power availability	AC240V, UPS	AC240V, UPS	Power consumption up to 25W
9	Routing antenna cables	Easy, there are RF cables for use	Difficult, none	
10	Object availability	12/24h	24/24h	Service rooms UMG

11	Presence of other VHF interfering ELM fields	Yes, weak, distance approx. 10m	Yes, strong, AIS 50m, VHF 50m, UHF 2m	There are many KSBM installations in the Hel Lighthouse
12	Optical fiber availability	Yes, directly	Yes, indirectly	Sharing with RTK system (Jastarnia) or AIS (Hel)

Based on the assessment on the map and the photographic documentation, the technical conditions were checked at the location of the Jastarnia harbor (Figure 2-4, 2-5, 2-6).

Figure 2-4: View of the Jastarnia harbor and the existing RTK and VHF antenna installations on the roof

Figure 2-5: View of the harbor office in Jastarnia from the south - the entrance to the port

Figure 2-6: View from the roof of the Jastarnia harbor. In the foreground, the RTK station mast, which can be used to mount the rod antenna of the VDES receiver. Two additional RF cables were led to it.

The visit to the boatswain's office showed that in the attic rooms (photo Fig. 2-7), the VDES receiver station could be placed. There is already an installation of the RTK reference station devices for which AC power (240V, 50Hz) and DC 24V power supply via UPS power supply are provided. There is enough space to accommodate a small 19” rack to accommodate VDES receivers, with a Procom input filter next to it. The selected location on the VDES rack is shown in Figure 2-7 below the RTK rack.

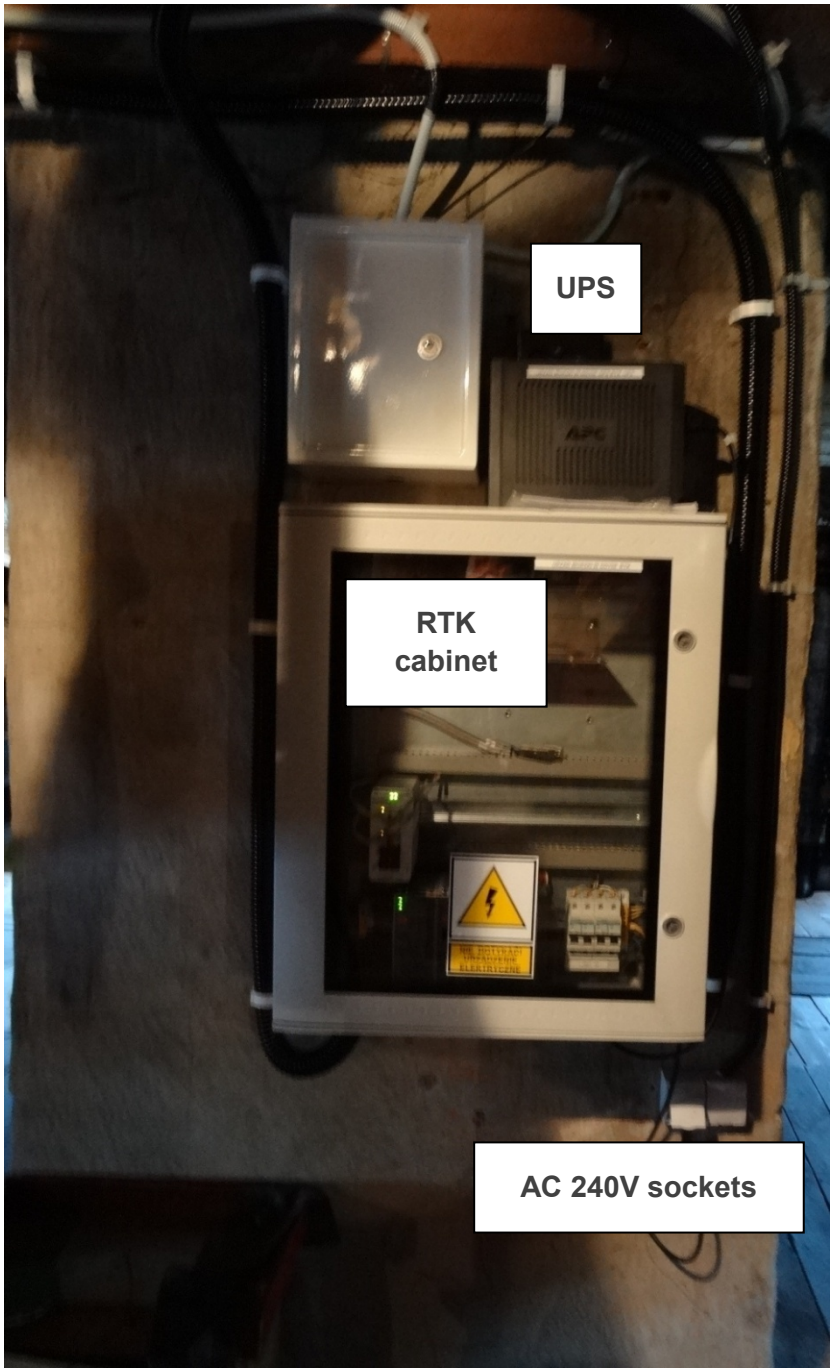

Figure 2-7: RTK cabinet and power sockets. Below is the place for the devices (rack) of the VDES receiver.

An input filter and a VDES rack can be inserted in the space under the RTK equipment cabinet. The antenna cable path is connected to the RTK cabinet, which can be used for the VHF antenna cable of the VDES antenna.

It has been found that two redundant RG58 RTK cables were also available there. One of them can be used for the VDES antenna, which would greatly simplify the installation. Nevertheless, the accessibility of the passage through the roof was also checked (Fig. 2-8 and Fig. 2-9) - in case of the need to route our own HF cables. They would be about 10-12 m long.

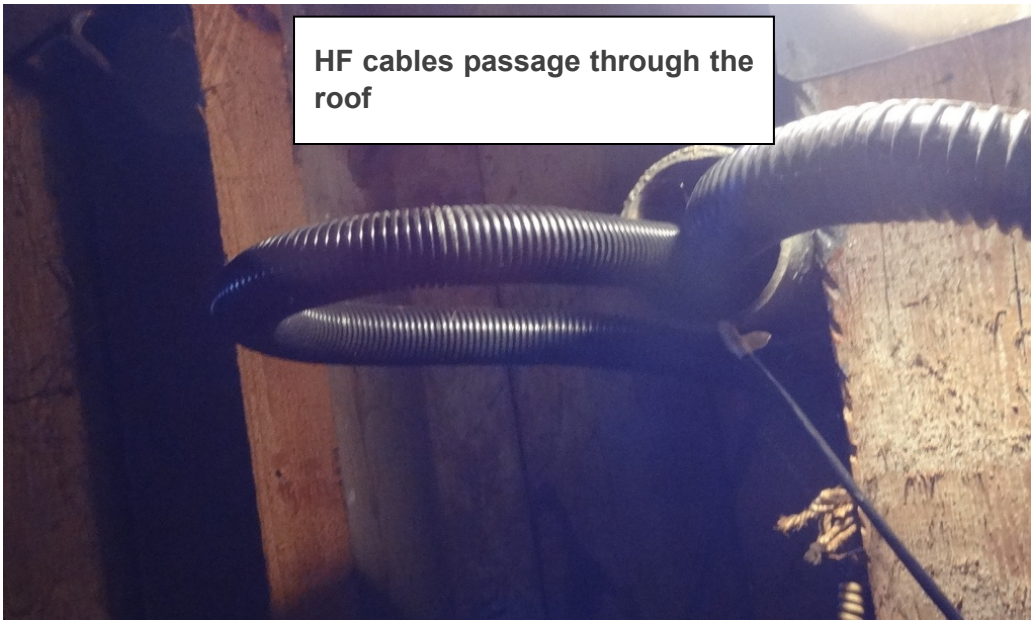

Figure 2-8: View of the entry of antenna cables through the roof with a vertical pipe - bottom view

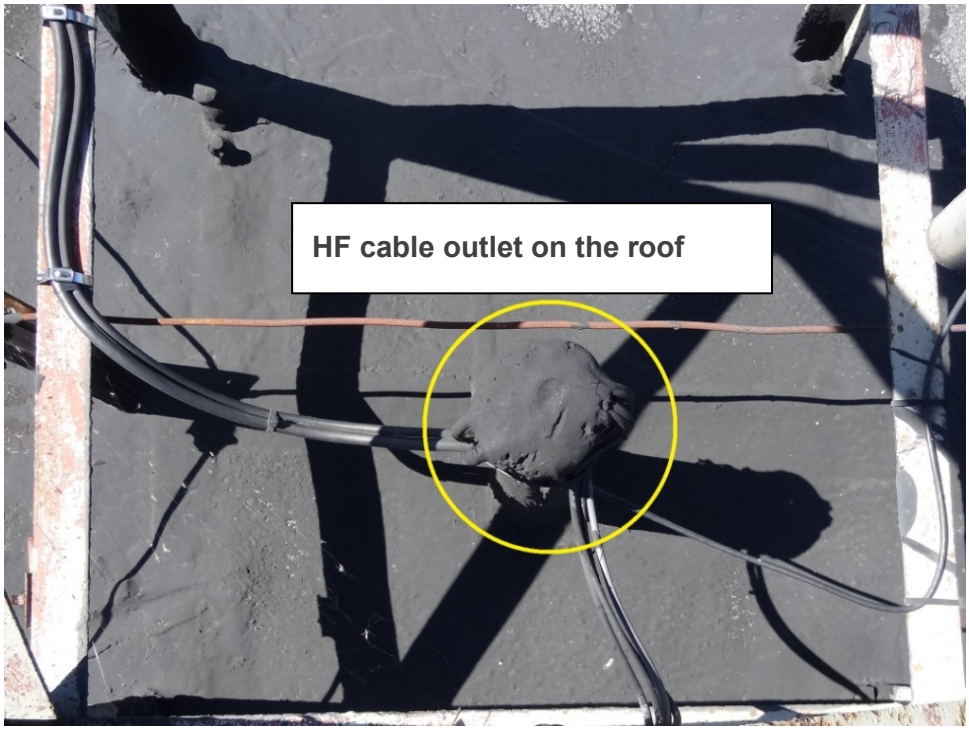

Figure 2-9: View of the antenna cables exit on the roof - top view.

As shown in Fig. 2-6, on the roof there is already a supporting structure for RTK antennas, to which a receiving VDES antenna can be attached - a VHF rod antenna, approx. 1.40 m long. There is also an additional, unused HF cable RG58 without a connector.

In the attic covered with a wooden roof, measurements of the presence of GSM / LTE signal were carried out for the purpose of remote management of the receiver via the Internet.

Good reception of the GNSS satellite signals (GPS, Glonass, Galileo) has also been confirmed there, which will enable the installation of the rubidium time standard GPS antenna in the room, without the need to lead it to the roof.

Outside - on the roof, the spectrum was measured and the intensity of the VDES signal from the station in Gdynia was assessed. For this purpose, a spectrum analyzer with a rod antenna on a geodesic tripod was used.

For the purpose of measuring the height of the VDES antenna mounting, the RTK station was used - see table 2-2. The mounting height of the rod antenna will be approx. 17.0 m above sea level.

Table 2-2: VDES antenna height measurement by Trimble RTK receiver, type BX982

Position	**Latitude**	54˚41’43.69894”N
	Longitude	18˚40’23.55018”E
	Height	45,734 [m]
	Height (orto.)	17,123 [m,EGM96]
	Type	SBAS
	Data	WGS-84
Used satellites	**GPS**	5, 16, 20, 21, 26, 27, 29
Tracked satellites	**GPS**	5, 16, 20, 21, 26, 27, 29
	GLONASS	5, 6, 11, 12, 13, 20, 21, 22
	SBAS	120, 123, 128

Based on the analysis of the existing technical (Tab. 2-1) and organizational conditions, a location in the **Jastarnia Harbor** was selected for the installation of the VDES receiver under the R-Mode Baltic 2 project.

2.2 Technical parameters of the VDES R-Mode 2 stations

The following analysis presents the results of the useful and interfering ranges calculations for the VDES R-Mode 2 Gdynia base station [2-2]. The calculations utilized software developed at the National Institute of Telecommunications in Gdańsk and the digital elevation model of the terrain SRTM 3 Ver. 4 (2008), the vertical and horizontal resolution of which is 3 arc seconds, which for the area of Poland approximately translates into 60x90m. The parameters of the VDES R-Mode 2 Gdynia base station, which is the subject of the analysis, are presented in Table 2-3.

Table 2-3: Technical parameters of the R-Mode Gdynia base station

Transmitting devices	Power amplifier POPEK ELEKTRONIK PEA02-2-50 National Instruments USRP 2945 (platform SDR)
Geographic position:	N 54° 31' 45,36" E 18° 33' 34,48"
Antenna suspension height	28 m a.s.l.
Transmitter power	50 W
Transmitter operating frequency	161,8375 MHz
Antenna	Radmor 32812/1
Antenna characteristics	Omni-directional antenna
Antenna gain	0 dBd (2,15 dBi)
Antenna cable type	H1000
The length of the antenna cable	120 m
Antenna path attenuation	6 dB
ERP power	11 dBW

The calculations of useful and interfering field strengths presented below were made in accordance with the current version of the ITU-R P.1546-6 Recommendation [2-3], using statistical propagation curves for VHF waves. These curves – as a function of distance – give the field strength values, the exceeding of which should be expected with a certain spatial and temporal probability. The values of both these probabilities are selected according to the requirements of the definition and the method of calculating ranges in radiocommunication. The space-time medians, i.e. the E (50.50) curves, illustrate the values exceeded in 50% of locations and 50% of the time and are intended for estimating the intensity of the useful field, while the E (50.10) curves work well in 50% of the locations and 10% of the time - they allow

to calculate the strength of the interfering field. Technical parameters of the transmitter presented in Table 2-3 were used for the analysis and the receiver parameters presented in Table 2-4 were adopted in accordance with Recommendation [2-4].

Table 2-4: Technical parameters of the receiver

Receiver sensitivity	- 107 dBm
The minimum value of the useful field strength	15 dBμV/m
Maximum value of the interfering field strength	14 dBμV/m
Receiving antenna suspension height	4 m a.s.l.

The figures below show the results of propagation analyzes in the form of maps of useful (Fig. 2-10) and interfering (Figs. 2-11) ranges for the R-Mode 2 Gdynia base station.

On the basis of the performed calculations, the maximum range values were determined, which are presented in Table 2-5.

Table 2-5: Maximum useful and interfering ranges of the R-Mode Gdynia base station.

Transmitter power	**Receiving antenna suspension height**	**Maximum range at sea**	
		useful	**interfering**
50 W (ERP 11 dBW)	4 m n.p.m.	45,2 km	54,3 km

Conclusions:

- Based on the analysis of the existing technical and organizational conditions, **the port in Jastarnia** was selected for the installation of the VDES receiver under the R-Mode 2 project.
- **The transmitter is located in the port of Gdynia**, 25 [W] EIRP, the antenna height: 28 m a.m.s.l.
- **The receiver in Jastarnia** - about 20 km away from the transmitter - sea path only and LOS. Receiver antenna height is about 17 m a.m.s.l.
- Both stations are equipped with rubidium disciplined oscillators. The receiver is also equipped with the LNA (NF=0.6 dB) and VHF band-pass 3 dB filter.

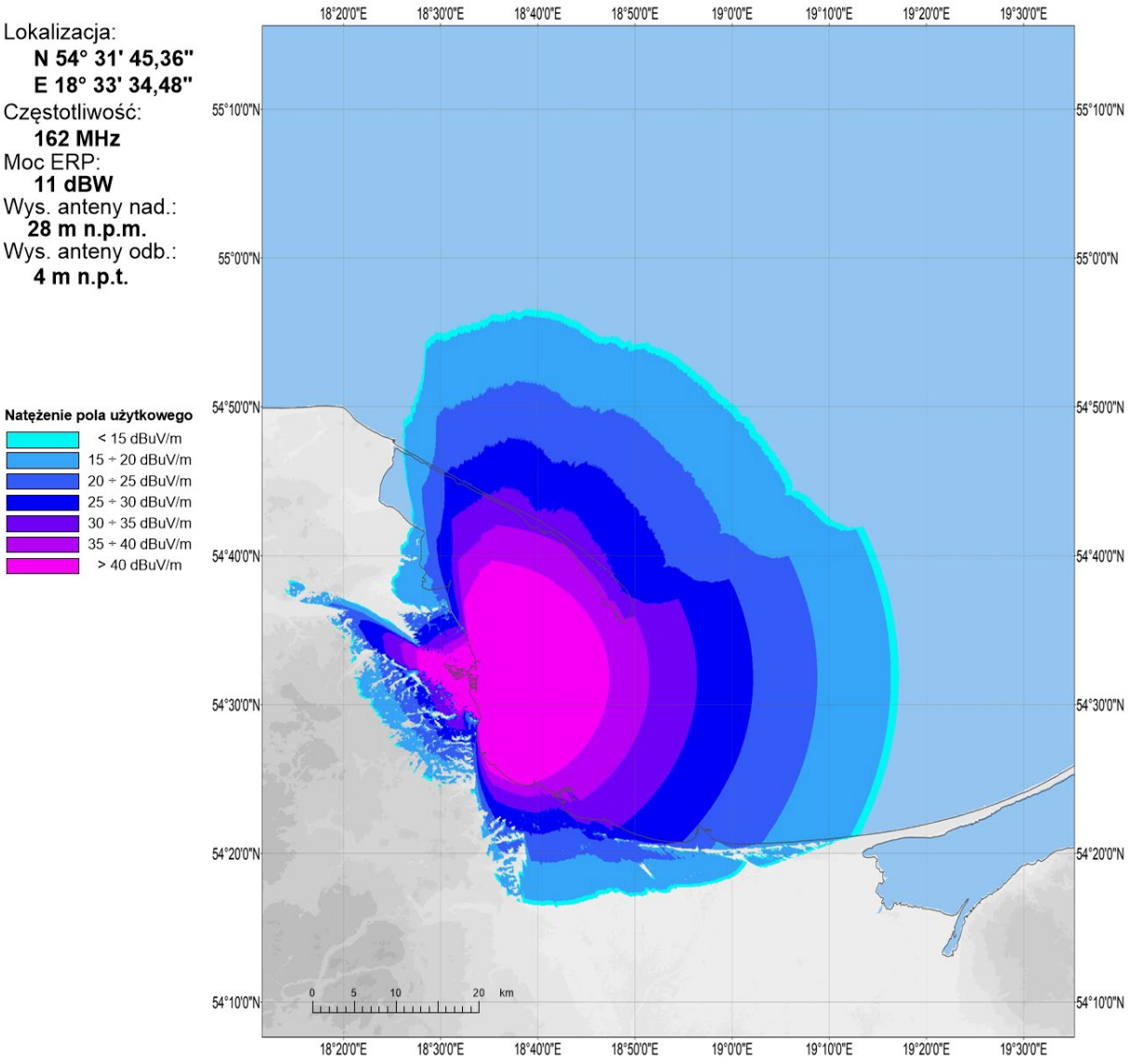

Figure 2-10: Map of the useful range of the R-Mode Gdynia station

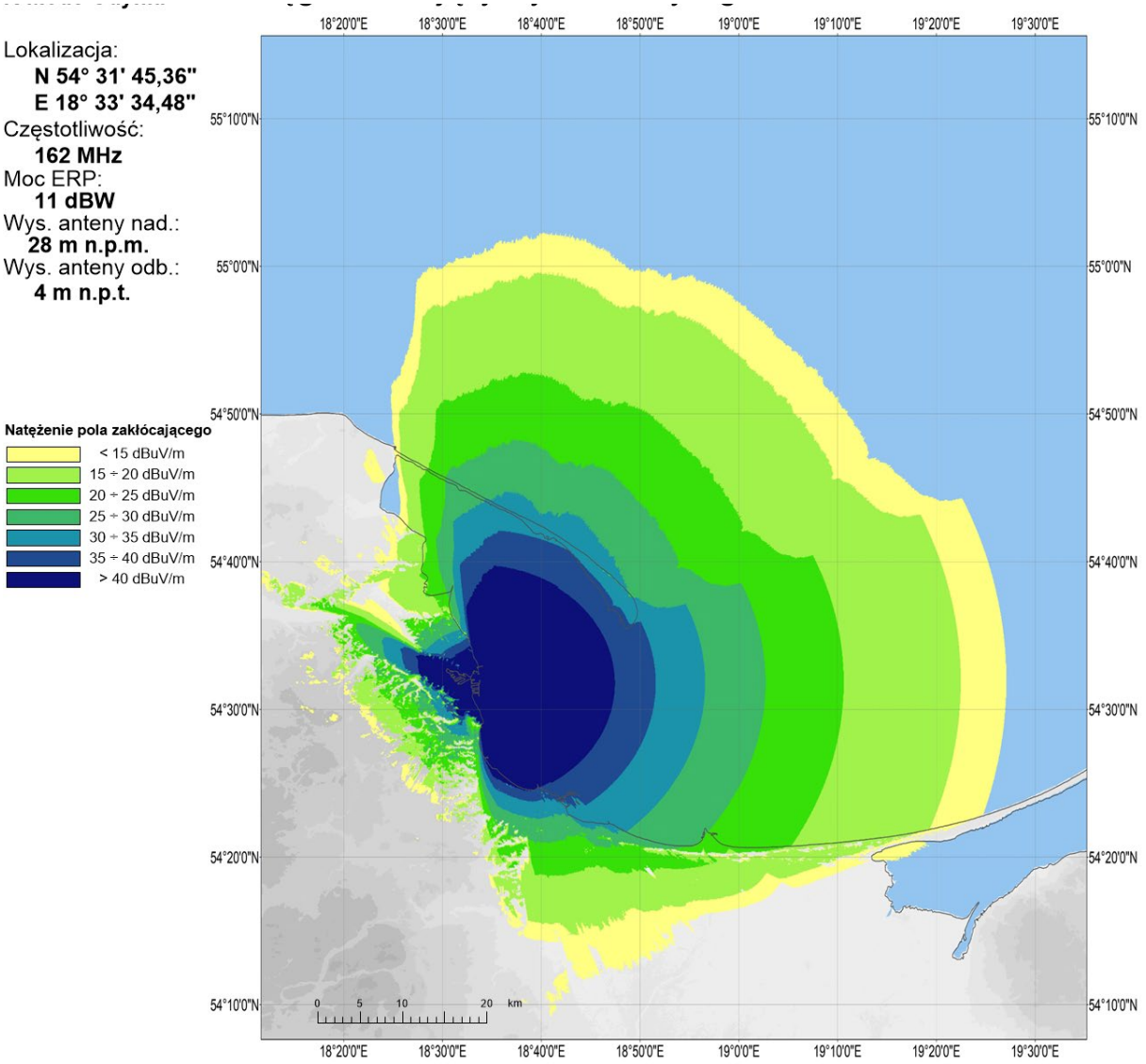

Figure 2-11: Map of the interfering range of the R-Mode Gdynia station

3 R-Mode Baltic 2 measurement campaign

For the purposes of the R-Mode Baltic 2 project, a long-term measurement campaign was conducted. It has been divided into two periods due to problems resulting from the failure of the power amplifier during the measurements. The periods for which the tests were performed are presented below:

- summer measurements for 11 days (19/06/2021 - 29/06/2021),
- autumn measurements for 13 days (25/09/2021 – 18/10/2021).

All collected data were subjected to digital signal processing (from signal correlation and pseudo-ranges to determining the exact position and RMS error).

3.1 Selection of the measurement scenario

In order to finally calculate the receiver's position on the basis of the calculated ranges, a measurement scenario was used where additional base stations were emulated. The coordinates of the emulated stations were chosen in such a way so that their respective distances from the receiver in Jastarnia (fig. 3-1) were exactly the same as the distance between Jastarnia and the "real" transmitting station (fig. 3-2) in the port in Gdynia (it can be seen in fig. 3-3). It is also worth noting that the research took place in the Gulf of Gdańsk in the LOS marine environment. Table 3-1 shows the coordinates of the emulated stations and the coordinates of the "real" transmitter and receiver.

Figure 3-1: Receiving station in Jastarnia

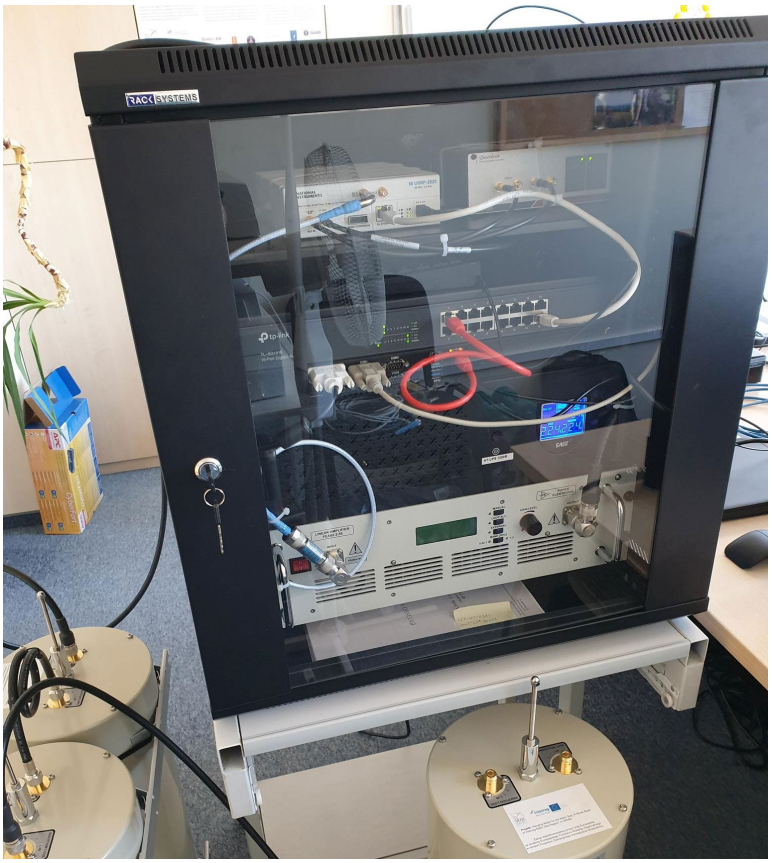

Figure 3-2: Transmitting station in the port of Gdynia [3-1]

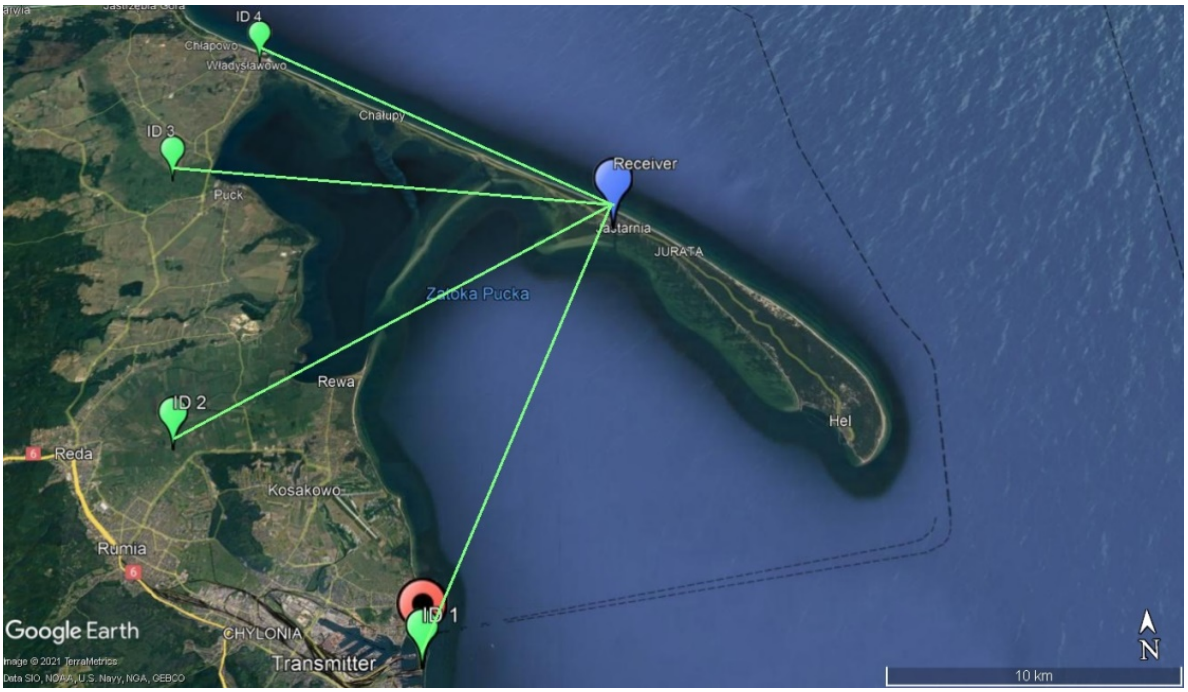

Figure 3-3: Measurement scenario for four emulated broadcasting stations

Table 3-1: Coordinates of the emulated stations as well as the transmitter and receiver

Station	Latitude [N]	Longitude [E]
transmitter station in Gdynia	54.529286	18.559539
receiver station in Jastarnia	54.6954586	18.673196
emulated station 1	54.5292887	18.5595547
emulated station 2	54.6057741	18.4064813
emulated station 3	54.7261218	18.3690009
emulated station 4	54.7925510	18.4137167

In the above measurement scenario, the following structure of the transmitted message was used (fig. 3-4). In this case, the correlation sequence consisted of the Gold and alternative sequences (fig. 3-5) [3-2]. This was to obtain better correlation properties and thus – to obtain a better position accuracy.

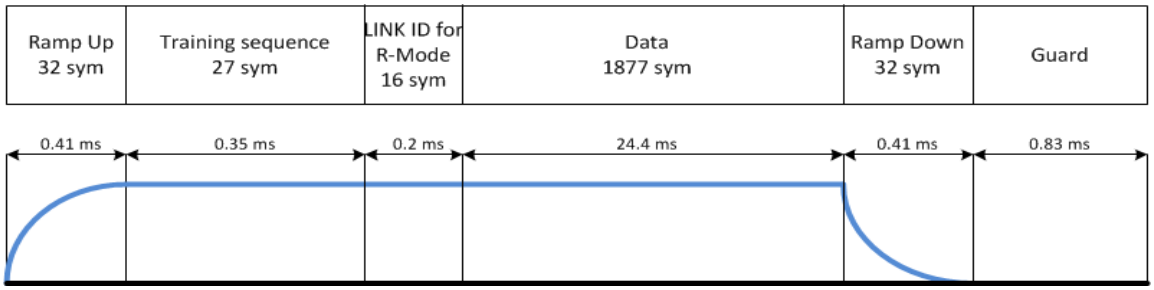

Figure 3-4: Frame structure VDES

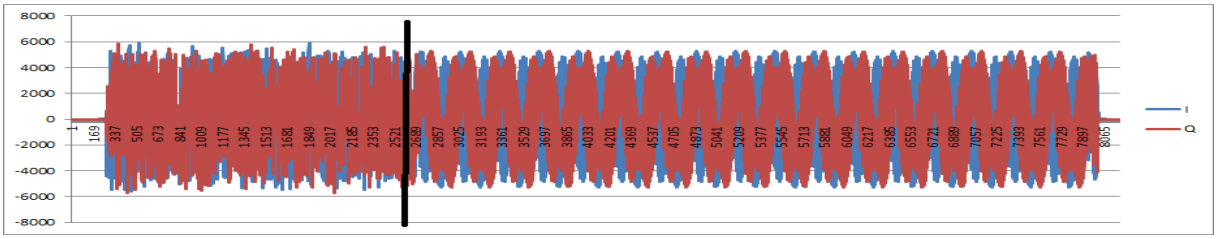

Figure 3-5: R-Mode ranging signal

The diagrams of the VDES transmitting and receiving blocks are presented in Figures 3-6 and 3-7, respectively. The transmitting and receiving sides of the R-Mode 2 VDES system have been modified on the basis of the previous project's outcome, which is described in detail in the articles [3-3,3-4].

Both testbeds were based on the following hardware components:

- Industrial PC,
- SDR Radio Module (Software Defined Radio), type National Instruments NI USRP2954 [3-5],
- INPUT filter type PROCOM BPF 2/1-250 (receiver side) or PROCOM BPF 2/2-250 (transmitter side) [3-6],
- Power Amplifier, POPEK ELEKTRONIK PEA02-2-50 – transmitter side,
- Low Noise input amplifier type WanTcomWLLA0005A – receiver side,
- GNSS reference receiver type U-Blox EVK-M8T,
- VHF omni-directional transmitting antenna with 0 dB gain, mounted at the 20 m msl tower in the Gdynia Port,
- The receiving VHF antenna installed on the roof of the harbour master office in the port of Jastarnia (12m msl).

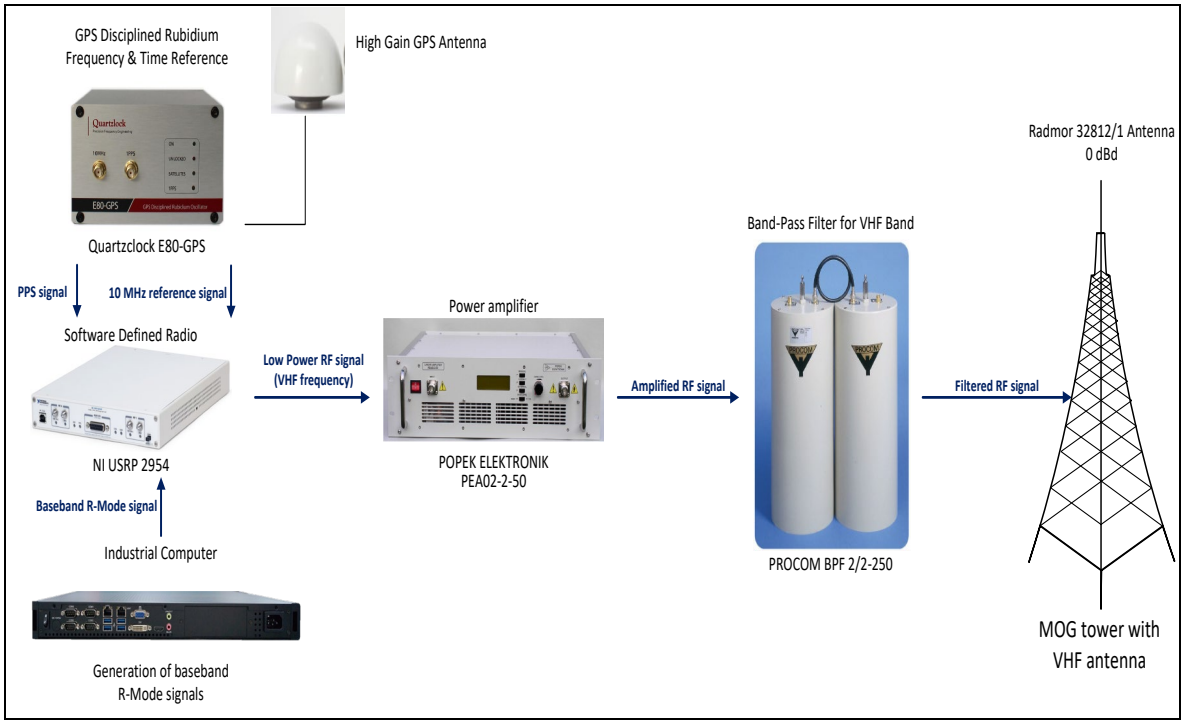

Figure 3-6: VDES transmitter block diagram (Gdynia Port)

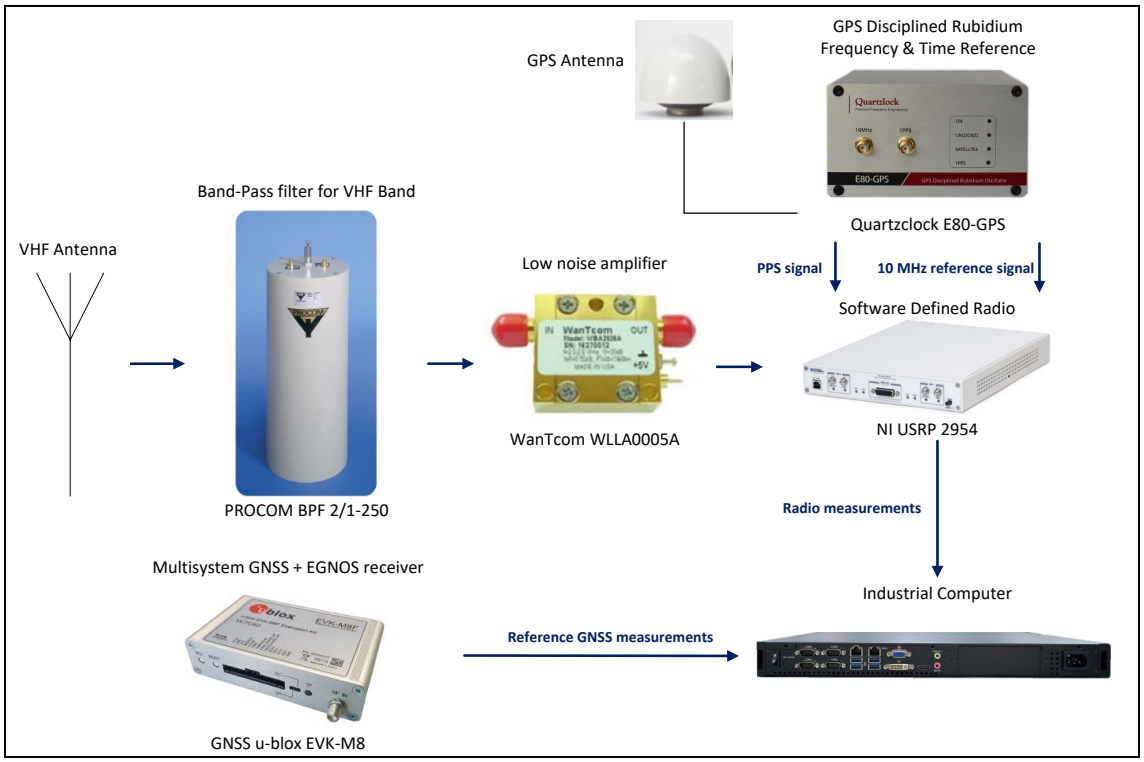

Figure 3-7: VDES receiver block diagram (Jastarnia Harbor)

Conclusions:

- The station in Jastarnia receives signals from 4 **emulated / virtual** stations from the Gdynia station,
- The distance between the stations is about 20 km - purely sea path. We achieved here about 10 m of positioning accuracy,
- We intend to receive signals for 5 minutes each hour for at least one month,
- We transmit once per 3 seconds so for each five-minute period we have 100 measurements for each virtual station.

3.2 Collected data in the measurement campaign

In the measurement campaign conducted in the R-Mode Baltic 2 project, data was collected in two periods: during summer and during autumn. All data was saved on hard drives and then digitally processed. The table below shows a summary of the data collected during the summer campaign (tab 3-2).

Table 3-2: Measurement data collected in summer

DAY	range of hours of collected data	Hours Collected
19.06	**all day**	**24**
20.06	**all day**	**24**

21.06	**all day**	**24**
22.06	**all day**	**24**
23.06	**all day**	**24**
24.06	**all day**	**24**
25.06	**all day**	**24**
26.06	**all day**	**24**
27.06	**all day**	**24**
28.06	**all day**	**24**
29.06	**all day**	**24**

As can be seen in the table 3-2 above, we managed to collect the full set of data for each measurement day. Unfortunately, further measurements were interrupted due to a failure of the power amplifier. The next measurements were continued in the fall and the table 3-3 below includes a list of collected data:

Table 3-3: Measurement data collected in autumn

DAY	range of hours of collected data	Hours Collected
25.09	0:00-8:00	8
28.09	18:00 – 24:00	6
29.09	7:00 – 24:00	17
30.09	**all day**	**24**
01.10	0:00 – 16:00	16
11.10	17:00 - 24:00	7
12.10	5:00 – 21:00	16
13.10	14:00 – 24:00	10
14.10	**all day**	**24**
15.10	**all day**	**24**
16.10	**all day**	**24**
17.10	**all day**	**24**
18.10	0:00 – 10:00	10

During the data recording in the autumn period, problems were encountered with the industrial computer, which restarted automatically due to a failure. The consequence of this is

the collection of incomplete data for some days. Despite the encountered difficulties, the analysis of the collected data was carried out. Table 3-4 provides a summary of the collected test samples.

Table 3-4: Measurement data collected

Summary	
Number of collected hours of measurements	474
Number of days of measurements	24
Number of complete measurement days	16

In the following chapters, the process of analyzing the collected data will be shown. The analysis of static measurements will be presented, mainly in relation to the obtained RMS values - for range cases and cases with position determination.

4 VDES R-Mode 2 static "long-term" ranging results

In this chapter, we will present the analysis of data collected during the summer and autumn campaigns (as described in the chapter above). The figure 4-1 shows the general concept of collecting data from four emulated broadcast stations. As part of the static long-term measurements, all samples were recorded (Fig. 4-2) and saved in binary files using the USRP receiver (Fig. 4-3). During the R-Mode Baltic 2 project, the software of the transmitting and receiving part of the USRP platform was expanded compared to the version used in R-Mode Baltic 1. The software implemented in the LabView environment was adapted to the needs of long-term measurements performed remotely between the transmitting station installed in Gdynia and the receiving station located in Jastarnia. On the transmitting side, the message sending process and the transmission schedule were optimized, while on the receiving side, the measurement data recording process and the data reception schedule were optimized.

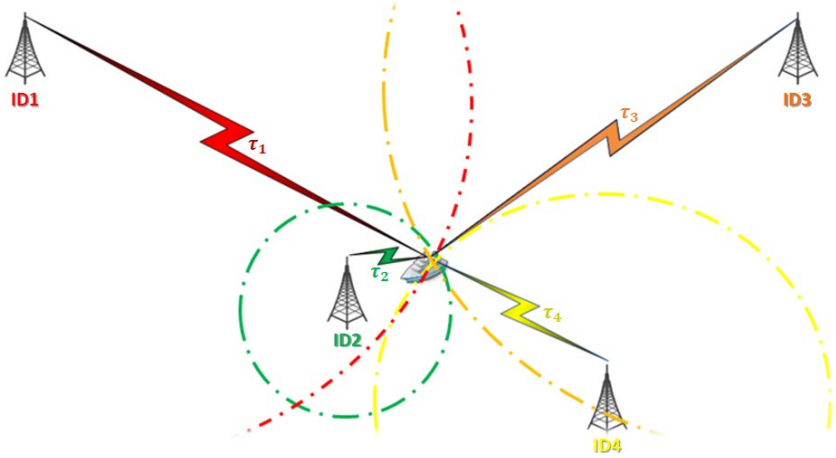

Figure 4-1: Concept of collecting data from four emulated broadcasting stations

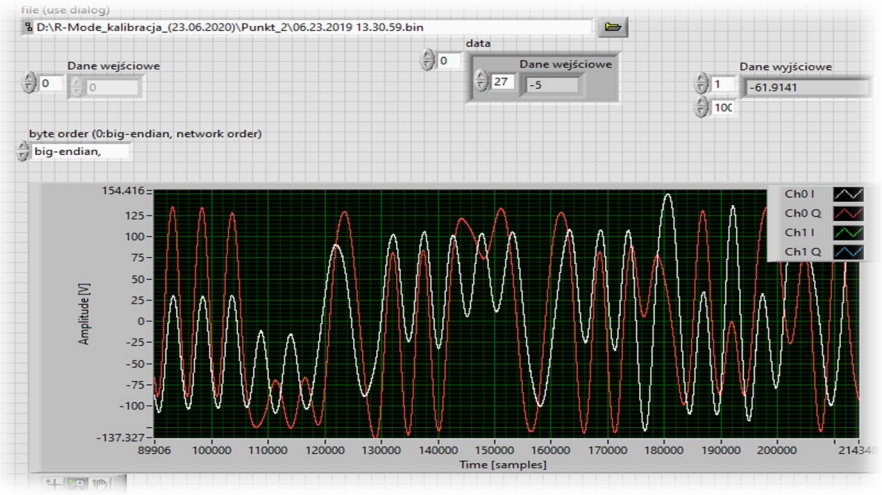

Figure 4-2: Measurement data samples recording

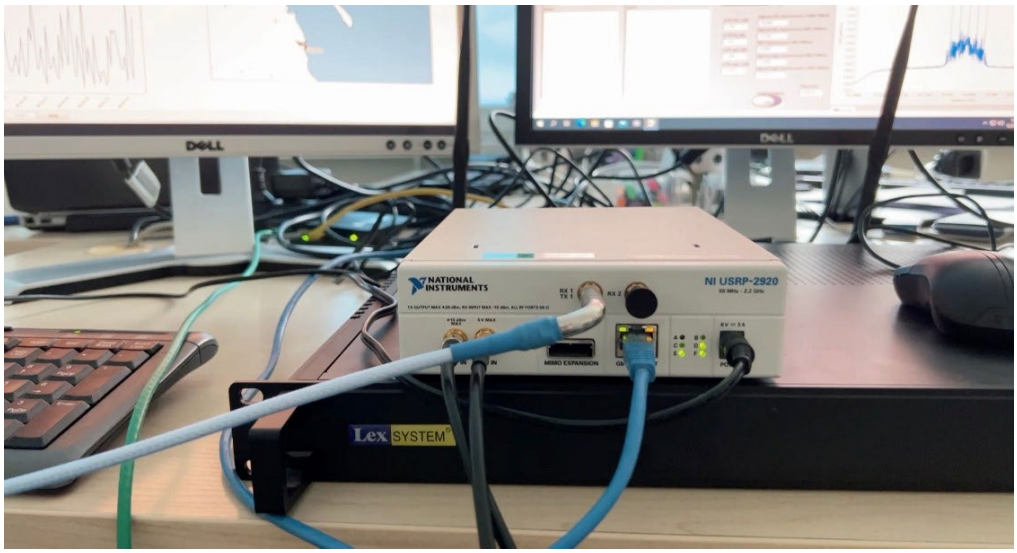

Figure 4-3: USRP platform

The samples for four slots, saved in binary form, were sent to the input of the signal correlation application. On the basis of the processed and correlated signal, the required pseudoranges were obtained (Fig 4-4). For the R-Mode Baltic 2 project, the software for calculating ranges based on the correlation function [4-1] has been modified (Fig. 4-5). The application for the correlation of VDES signals (written in C ++) in order to determine the distance between the transmitting and receiving antennas - has been extended with an additional module for the analysis of data collected during long-term stationary measurements. As part of the implemented functionalities, the application made it possible to calculate the RMS pseudo-distance for the entire measurement period / for selected days / for selected hours / for selected times of the day, thanks to which the obtained results could be correlated with the prevailing weather conditions during the measurements. The application has also been extended with the capability of analyzing the RMS accumulation in long-term measurements.

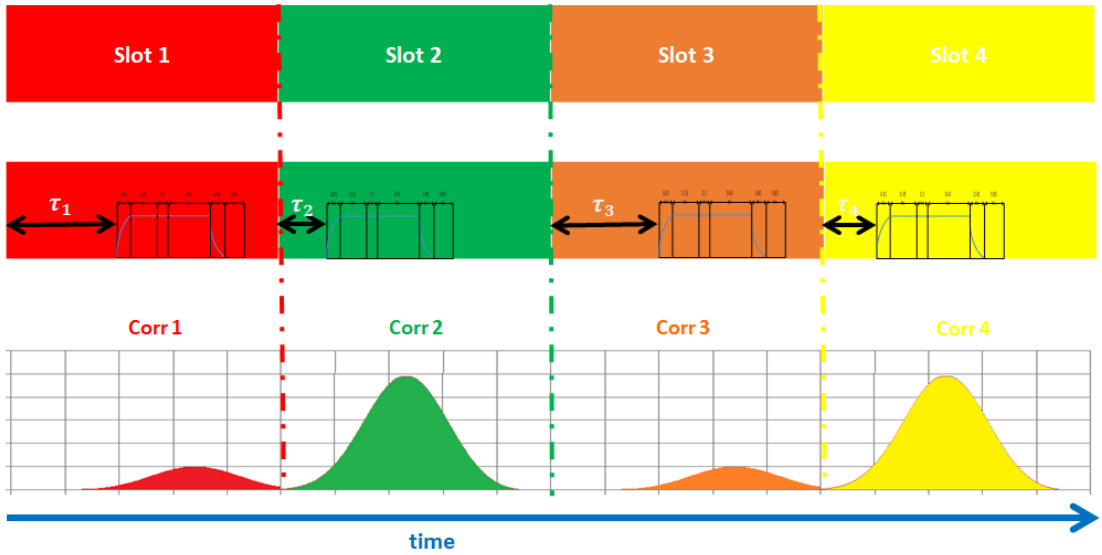

Figure 4-4: Recorded sample slots and corresponding correlation functions

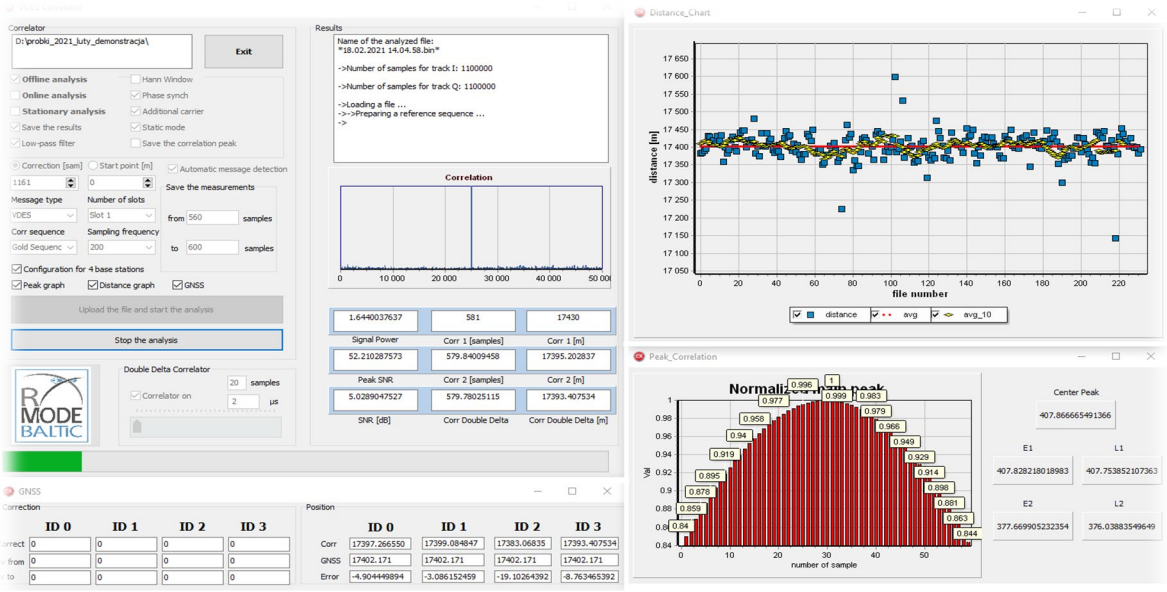

Figure 4-5: Signal correlation application - ranging

All the recorded data, which was processed by the signal correlation application, was subjected to detailed analysis. The obtained pseudo-ranges were analyzed as follows:

- Analysis of RMS changes depending on the measuring time (day/night),
- Analysis of the power and quality of correlation of received signals,
- Dependence of the obtained RMS in the measurement campaign on the prevailing meteorological conditions,
- The phenomenon of tropospheric ducts in measurements.

In the next step, such an analysis was then used to determine the exact position of the receiver.

4.1 Analysis of RMS fluctuations depending on the measurement time (day/night)

The analysis of the results was based primarily on the collected and processed measurements that were recorded for 5 minutes every hour (Fig. 4-6). We transmitted once per 3 seconds so for each five-minute period we recorded 100 measurements for each virtual station.

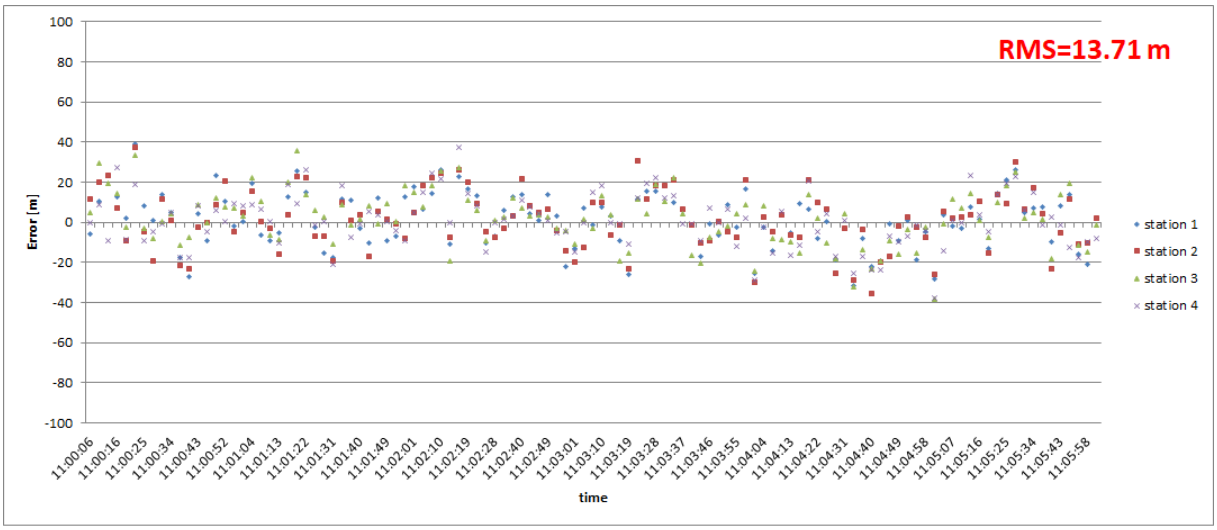

Figure 4-6: The results obtained from 5-minute segments of measurements

On the basis of all collected data, the RMS analysis was first performed for the summer period for each measurement day (Fig. 4-7). The obtained results show, first of all, the RMS for two cases: when the mean error from the measurements (a) was subtracted every day and (b) was subtracted just once – on the first day of the measurements.

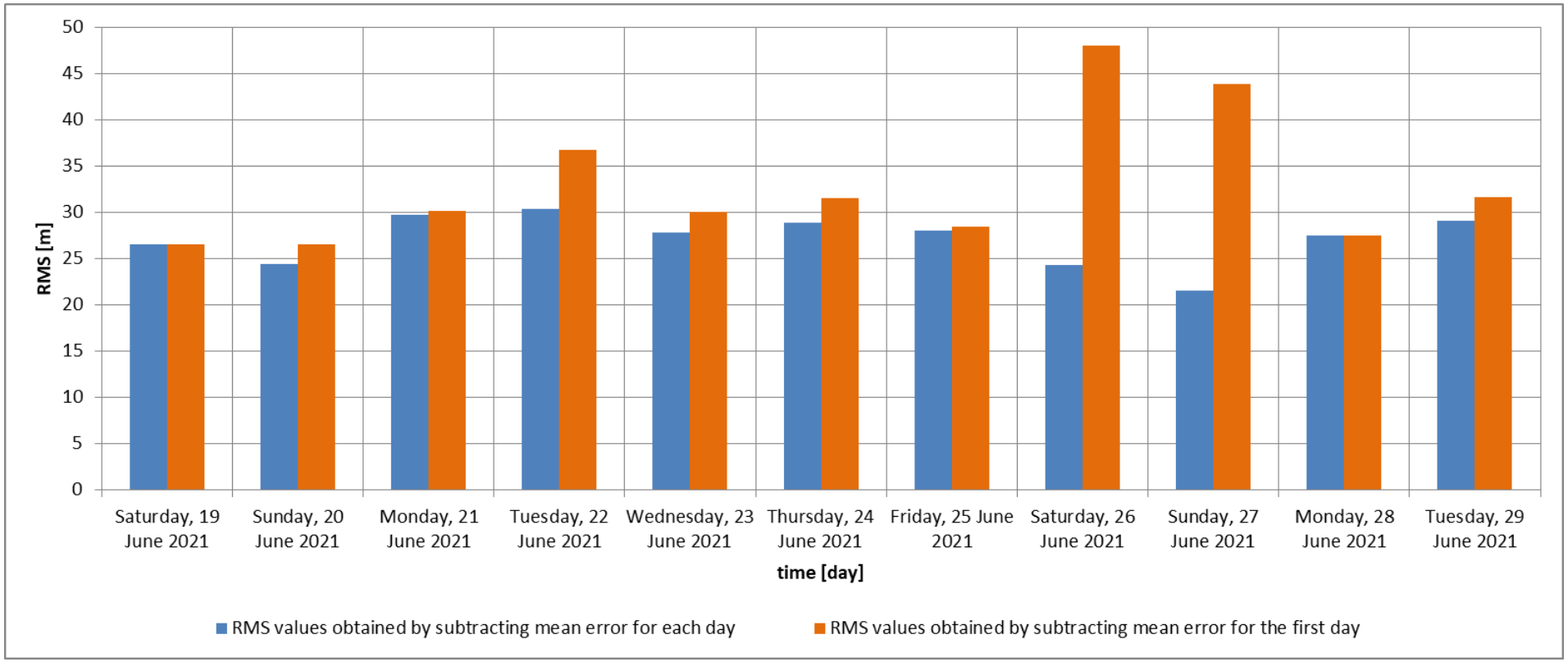

Figure 4-7: Results for measurements that lasted 11 days - the obtained RMS for each day during the summer campaign

The above graph, representing the summer period, is based on 30,000 measurements. With the daily reset of the mean error, it can be seen that the accuracy of the pseudo range determined compared to the reading from the GNSS receiver was about 20 meters. The average RMS value did not exceed 30 meters. On the other hand, when the average error was reset only on the first day of measurements, it can be noticed that the accuracy of the determined pseudo ranges deteriorated only on two measurement days and amounted to about 45 meters. Thanks to the above list, it can be seen that the mean error did not accumulate over time, which proves that the measurements were carried out correctly.

The next analysis concentrated on the RMS errors depending on the time of the day with zeroing the mean error only during the first day of measurements. The results can be seen in the figure 4-8.

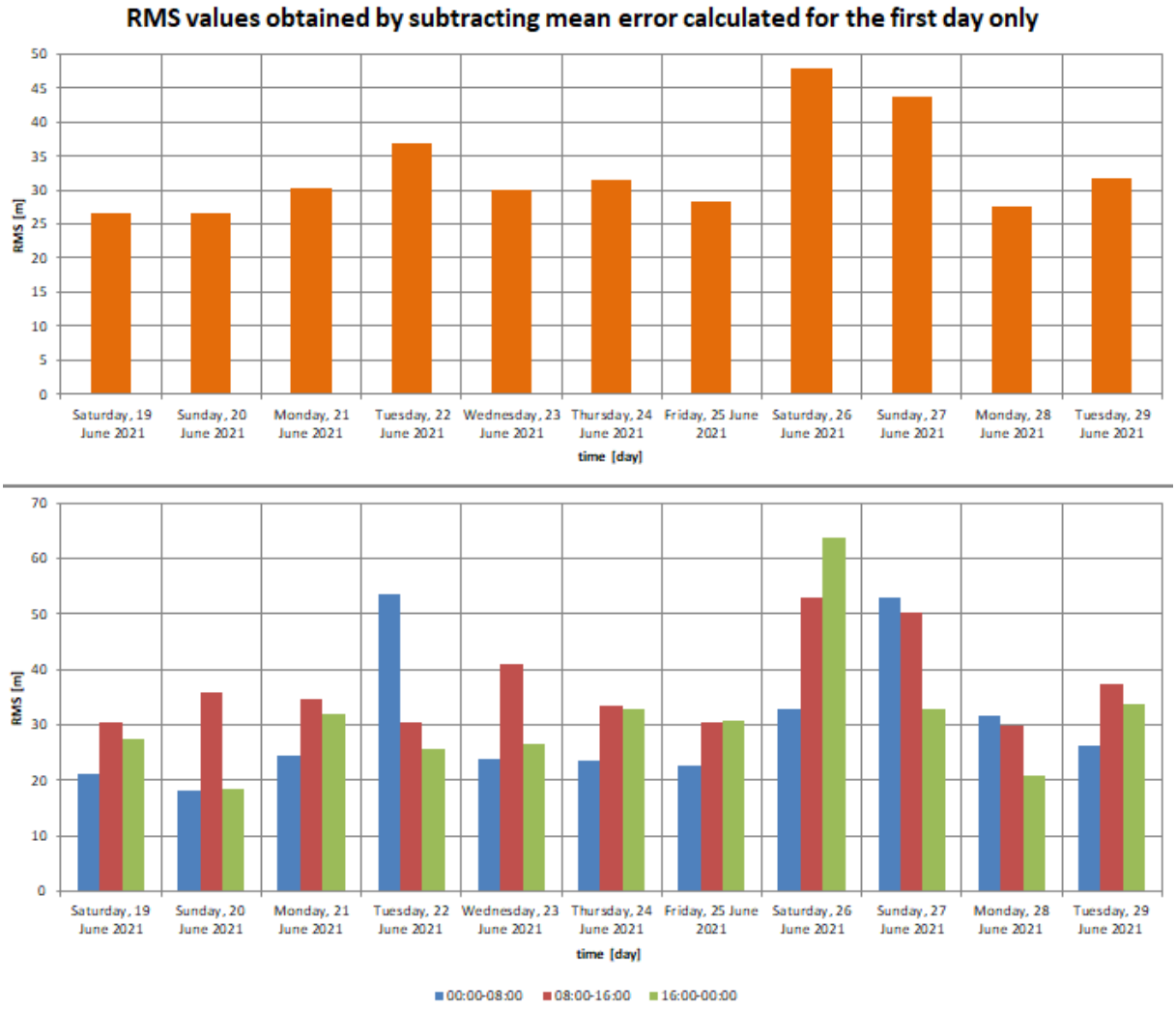

Figure 4-8: RMS for different times of day for summer measurements (subtracting mean error calculated for the first day only)

The above graph shows that at some periods during the day, it was possible to observe the increase of the RMS error. It can also be seen that in most cases, the RMS during the night hours was lower than in the afternoon. For the complete picture, a similar analysis was also carried out – only this time the mean error was reset every measurement day (Fig 4-9).

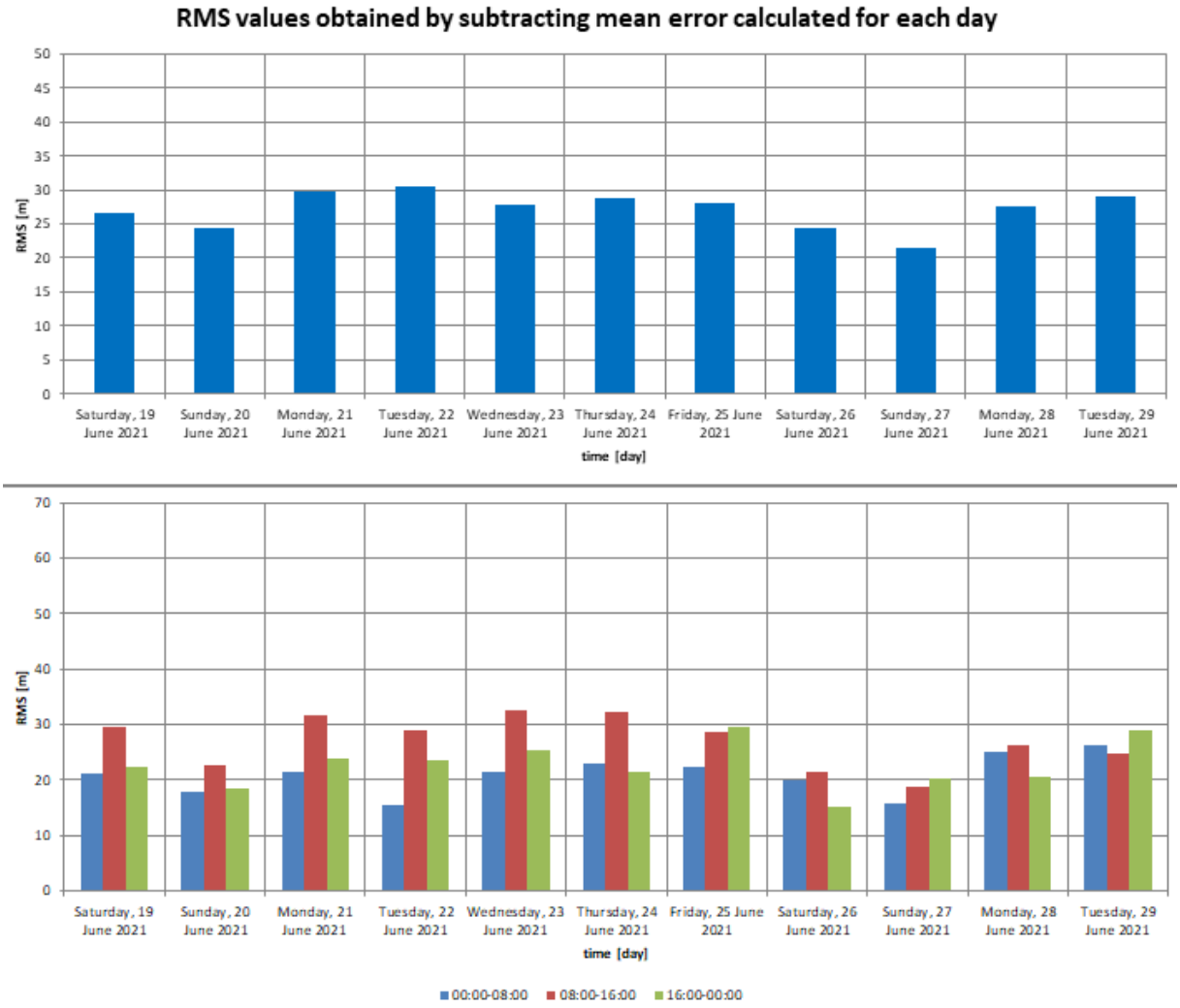

Figure 4-9: RMS for different times of day for summer measurements (subtracting mean error calculated for each day)

In this case, it was also confirmed that the RMS at night is lower than that of the daytime. First of all, it may be related to the prevailing meteorological conditions, which will be analyzed in the following subsections. At this stage, we can see that the RMS is hovering around 20 meters. The achieved RMS pseudoranges will be crucial in finding out how this parameter affects the accuracy of the receiver's position. The next analysis will concern the RMS determined for each hour (Fig. 4-10).

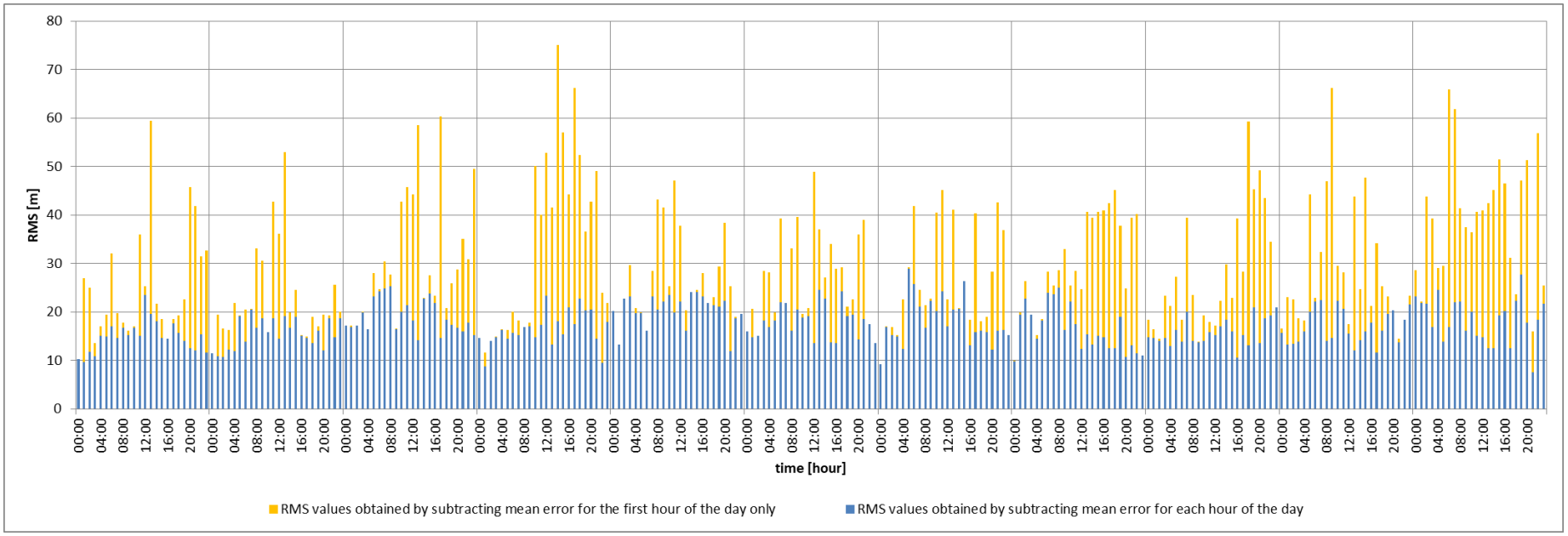

Figure 4-10: Determined RMS for each measuring hour for summer data

The above analysis shows that for the mean error subtracted every hour, the RMS values are in the range of 10-20 m. From what can be seen, the RMS in this case has a stable tendency. On the other hand, when the average error is reset every 24 hours, we can see how the RMS increases significantly in the afternoon. Cases up to 70 meters can be observed here. This may be influenced by meteorological conditions. In order to take a closer look at such a tendency, an analysis of general errors during the measurements was also performed, including the RMS analysis, where the average error was subtracted only at the beginning of the measurements. The results are shown in the figure 4-11.

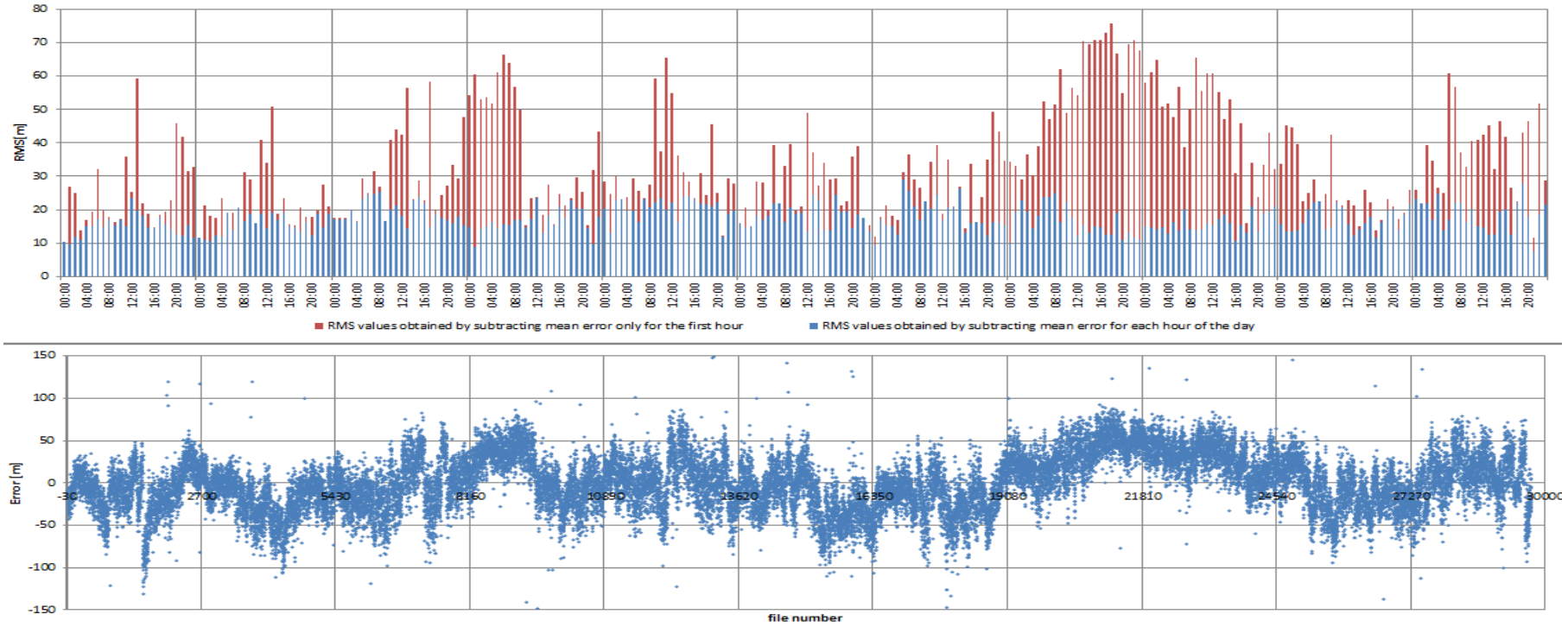

Figure 4-11: Determined RMS for each measuring hour for summer data and measurement errors

As can be seen above, the measurement errors are within the range of +/- 100 meters. On the other hand, the average RMS error for each hour fluctuates around 20 meters. The graph also includes RMS errors for which the average error was subtracted only at the beginning of the measurements. The highest errors for the 26.06.2021 and 27.06.2021 are best seen. It could be caused by various weather phenomena, but also e.g. be a result of the duct phenomenon, which will be examined in the following subsections. To take a closer look at the cases where the RMS increases significantly, the figures (Fig. 4-12, 4-13, 4-14, 4-15, 4-16) and tables (Tab. 4-1, 4-2, 4-3, 4-4, 4-5) below present the RMS analyzes for each day:

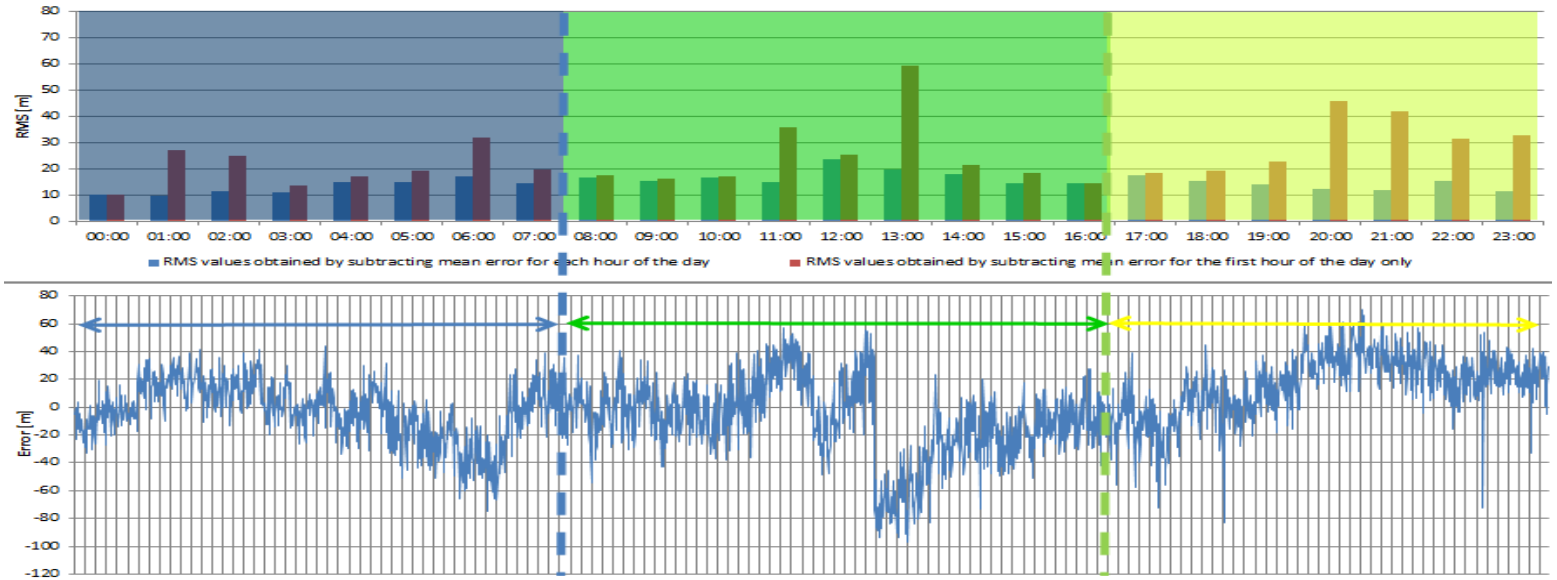

Figure 4-12: Detailed analysis of the RMS observed for one day depending on the consideration of the mean error - 19.06.2021

Table 4-1: RMS summary for given periods of the day - 19.06.2021

	Time [h]		
	00:00 – 8:00	***08:00 -16:00***	***16:00 – 00:00***
Avg RMS (mean error subtracted for every hour)	13.03	17.48	14.18
Avg RMS (mean error subtracted only for the first hour)	20.21	26.66	28.42

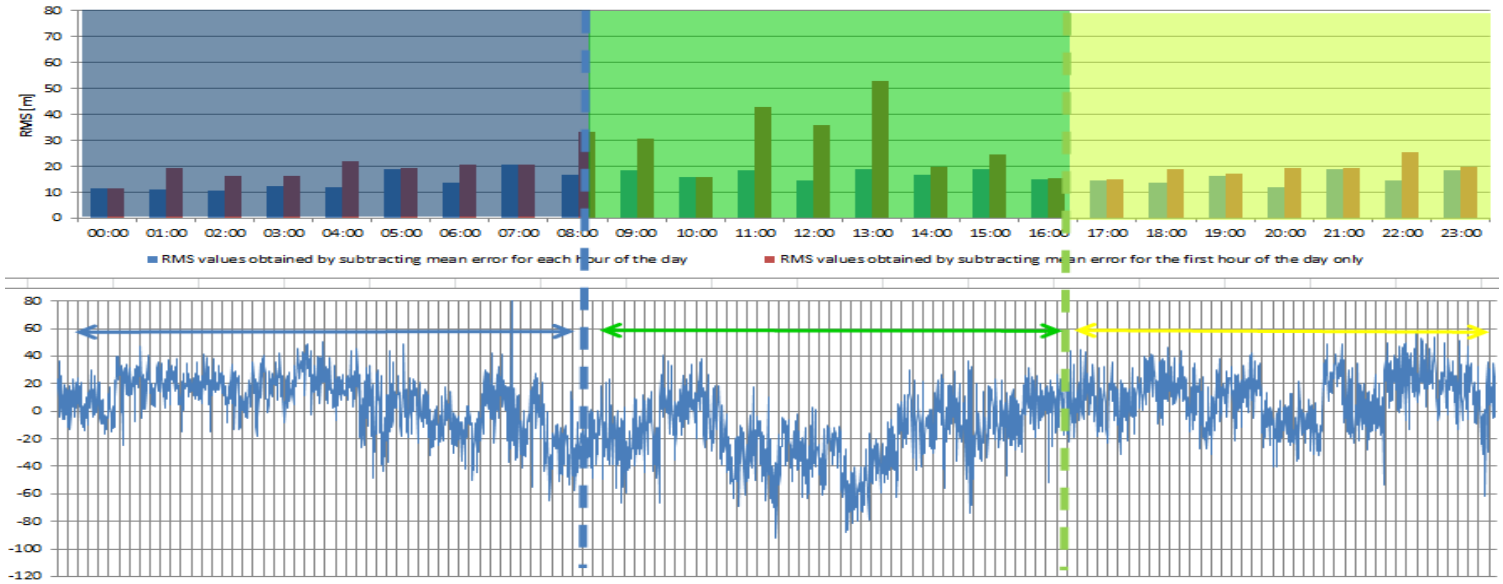

Figure 4-13: Detailed analysis of the RMS observed for one day depending on the consideration of the mean error - 20.06.2021

Table 4-2: RMS summary for given periods of the day - 20.06.2021

	Time [h]		
	00:00 – 8:00	***08:00 -16:00***	***16:00 – 00:00***
Avg RMS (mean error subtracted for every hour)	13.84	17.41	15.49
Avg RMS (mean error subtracted only for the first hour)	18.24	31.99	18.83

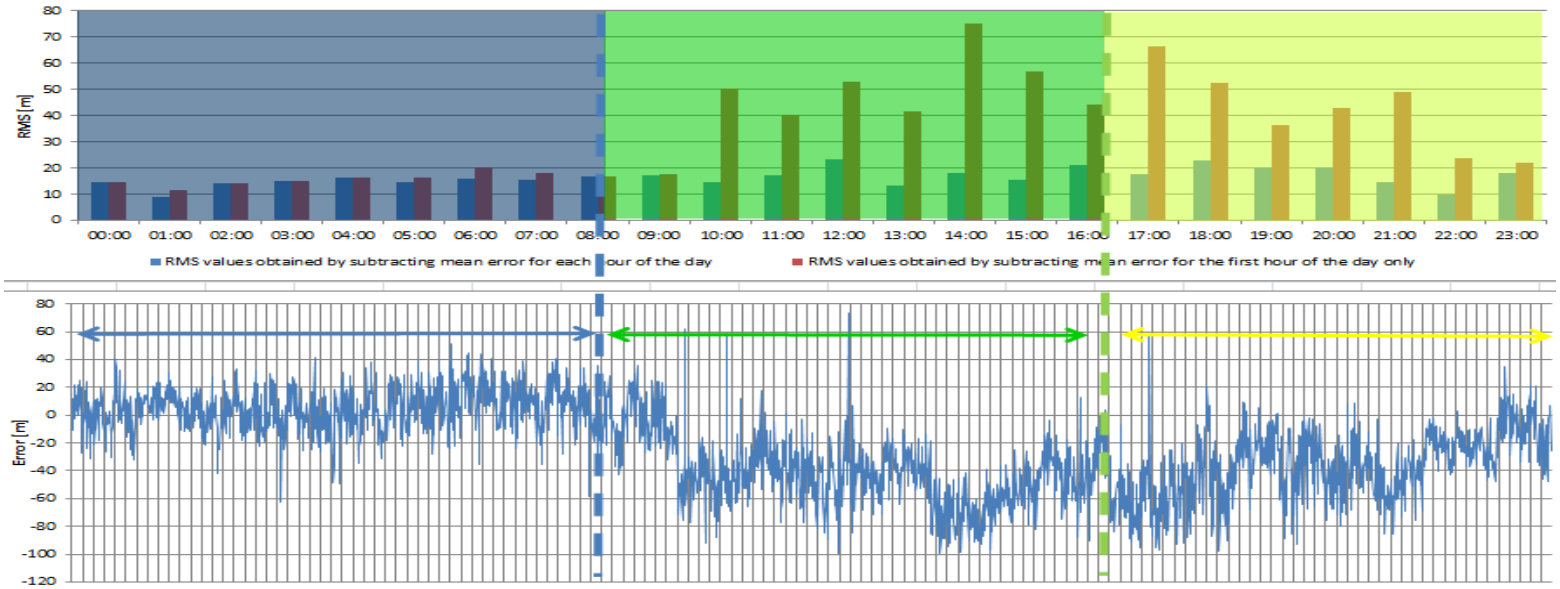

Figure 4-14: Detailed analysis of the RMS observed for one day depending on the consideration of the mean error - 22.06.2021

Table 4-3: RMS summary for given periods of the day - 22.06.2021

	Time [h]		
	00:00 – 8:00	***08:00 -16:00***	***16:00 – 00:00***
Avg RMS (mean error subtracted for every hour)	14.26	17.02	18.02
Avg RMS (mean error subtracted only for the first hour)	15.81	43.92	42.12

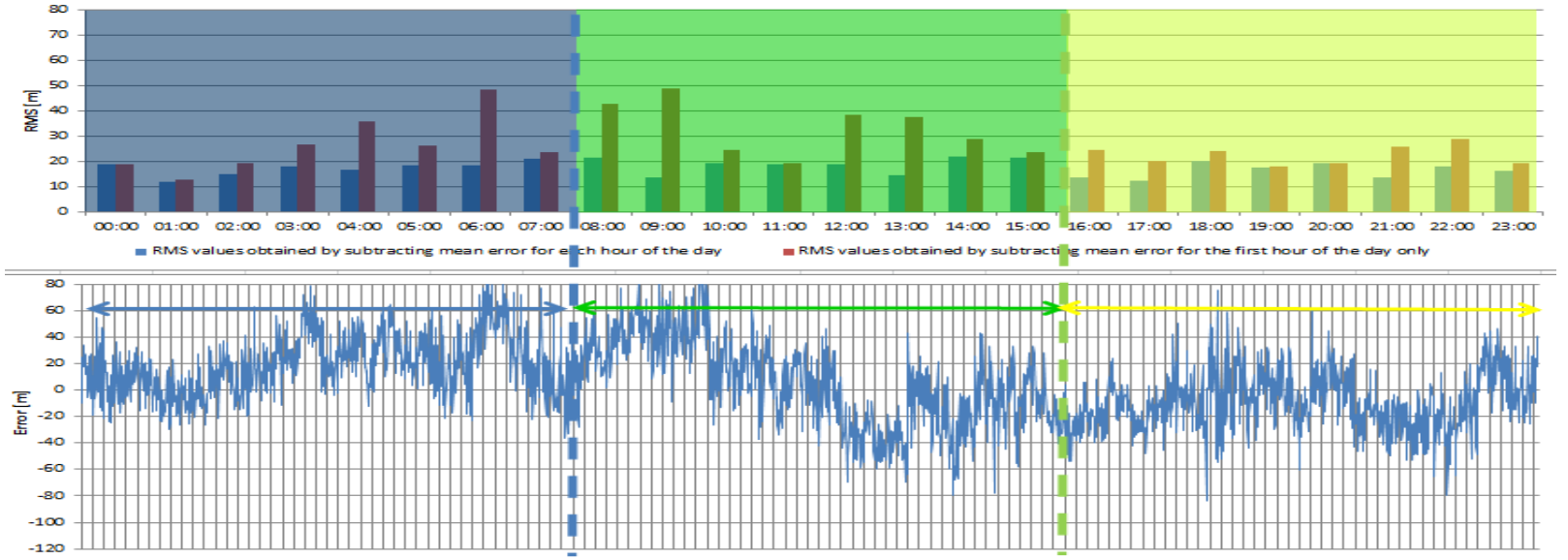

Figure 4-15: Detailed analysis of the RMS observed for one day depending on the consideration of the mean error - 24.06.2021

Table 4-4: RMS summary for given periods of the day - 24.06.2021

	Time [h]		
	00:00 – 8:00	***08:00 -16:00***	***16:00 – 00:00***
Avg RMS (mean error subtracted for every hour)	16.48	18.38	17.65
Avg RMS (mean error subtracted only for the first hour)	23.57	35.64	23.78

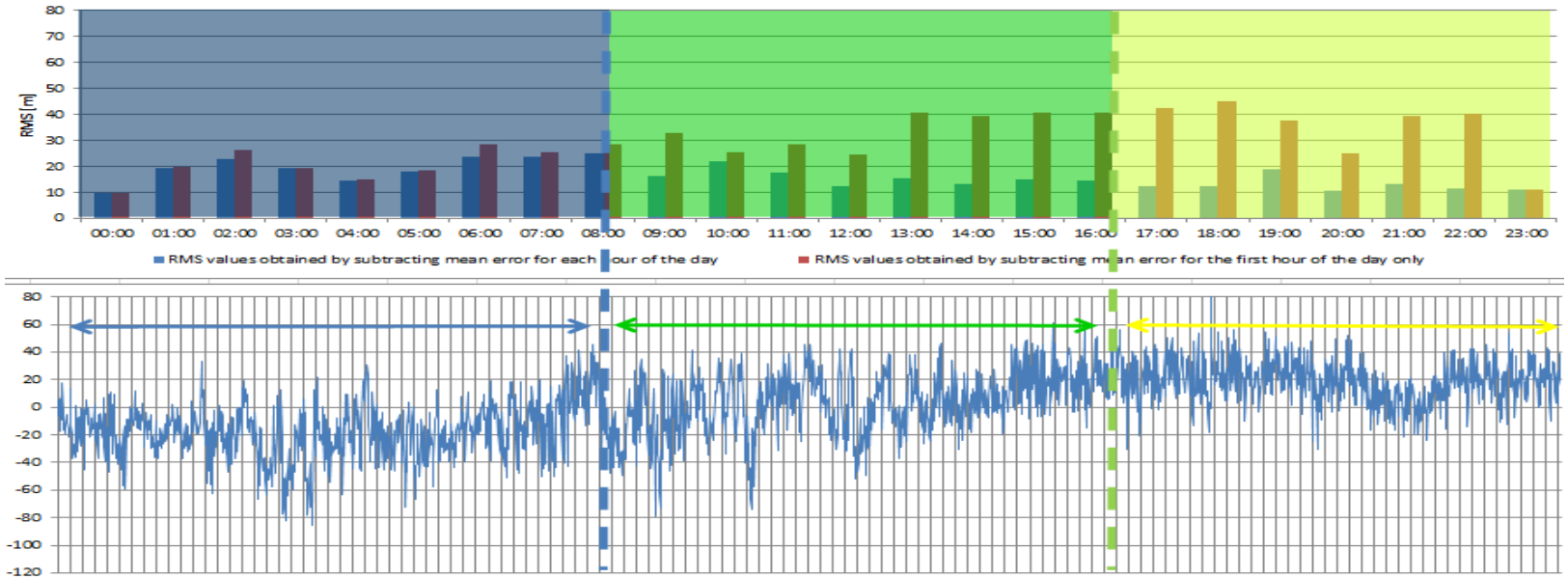

Figure 4-16: Detailed analysis of the RMS observed for one day depending on the consideration of the mean error - 26.06.2021

Table 4-5: RMS summary for given periods of the day - 26.06.2021

	Time [h]		
	00:00 – 8:00	***08:00 -16:00***	***16:00 – 00:00***
Avg RMS (mean error subtracted for every hour)	18.97	17.14	13.17
Avg RMS (mean error subtracted only for the first hour)	20.41	32.62	35.26

As shown in the above graphs, the analysis was divided into three time parts:

- 00:00-08:00,
- 08:00-16:00,
- 16:00-00:00.

For each of these periods, the RMS analysis was performed and the tables show the average RMS in the given time interval. In most cases, it can be seen that the measurements were most stable between 00:00 - 08:00. In that period, the RMS values were also the lowest and the measurements - the most accurate. By taking into account only the RMS results for which the average error was reset every hour, we can see that the RMS was in the range from 10 meters to 20 meters. On the other hand, when the average error was reset only in the first hour of measurements, it can be seen that in the majority of cases, the RMS increased in the afternoon. The reasons for that can be found in the meteorological conditions, which are analyzed in the following subsections.

For further research, the results for the autumn period were analyzed and compared with the results obtained during the summer campaign. Thanks to this, it was possible to see the tendency of the RMS value change depending on the different time of the measurements. The figure 4-17 below shows the RMS for each measurement day during both the summer and autumn campaign.

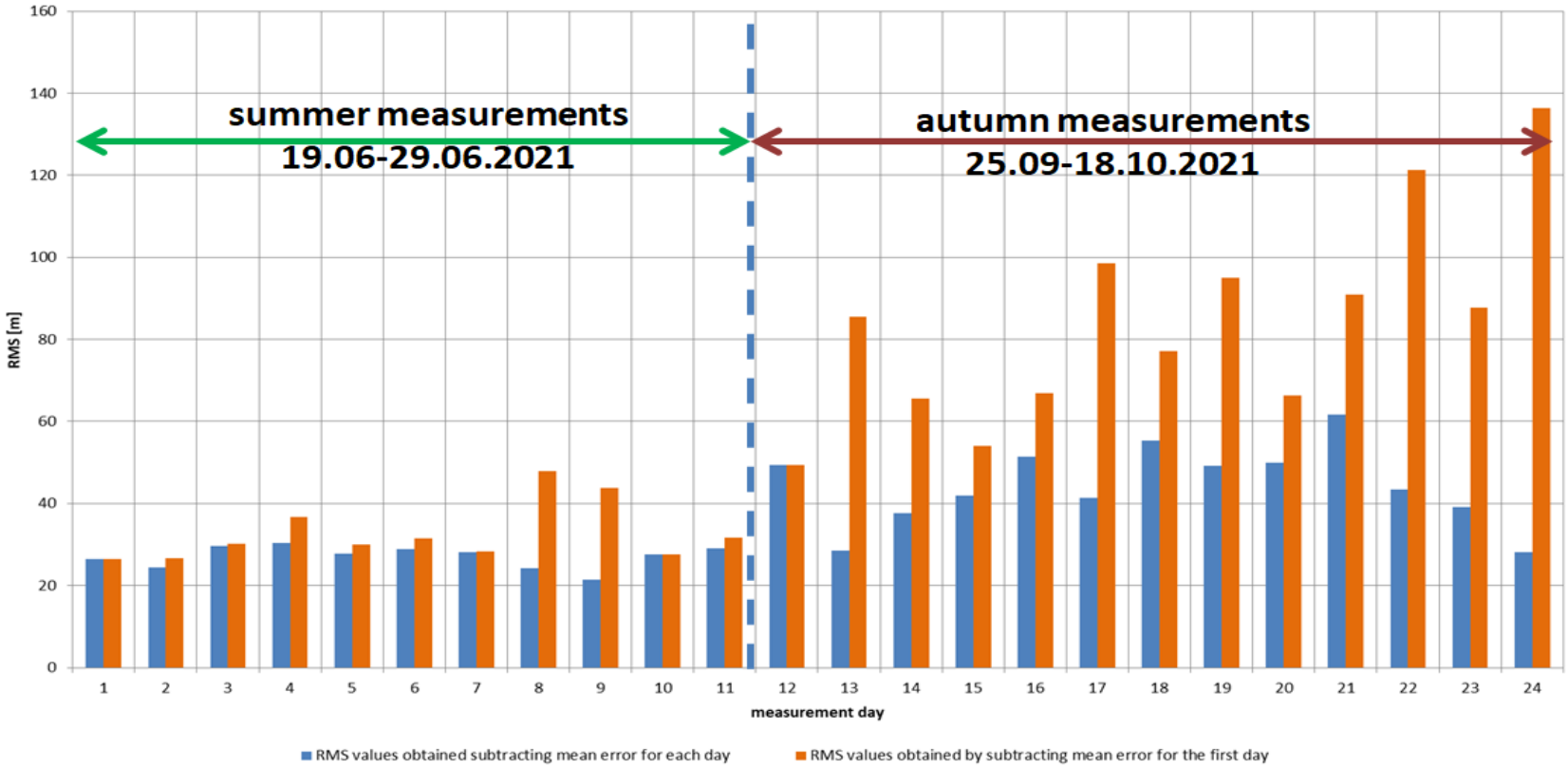

Figure 4-17: Results for measurements - the RMS obtained for each day during the summer and autumn campaign

The above chart 4-17 presents a summary of the obtained RMS for summer and autumn measurements. It can be easily noticed that the accuracy of the pseudo-ranges obtained in the autumn is much worse than in the summer. In autumn, the average RMS, in case where the mean error was subtracted every day, was around 40 meters, while in case where the average error was subtracted only at the beginning of the measurements, the RMS oscillated around 100 meters. These are much worse results compared to the summer campaign. In order to trace such large differences in measurements, the next chart 4-18 presents the measurement errors with respect to the GNSS receiver for summer and autumn measurements.

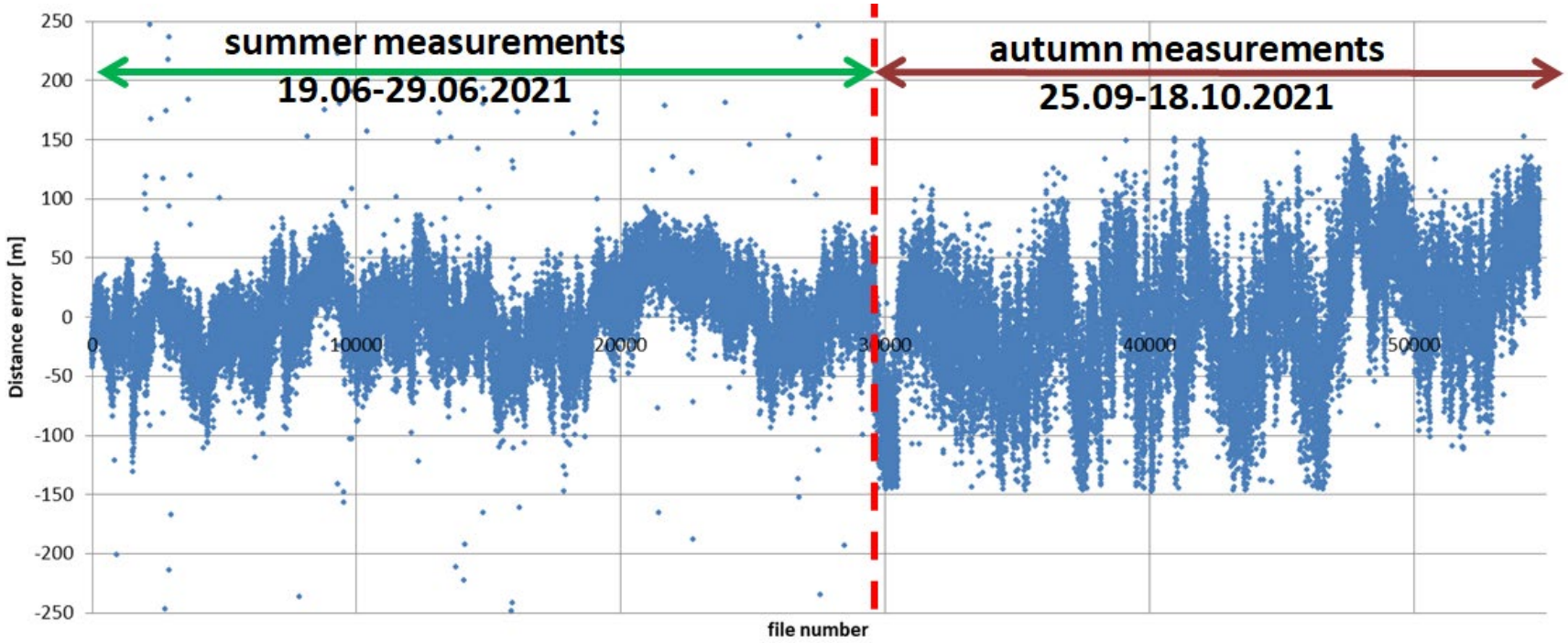

Figure 4-18: Measurement errors with respect to the GNSS receiver for summer and autumn measurements

For summer measurements, the error resulting from the difference in distance determined by the GNSS receiver and the correlation application is smaller than for autumn measurements. For the autumn measurements, it can be seen that these discrepancies are much more significant and more abrupt.

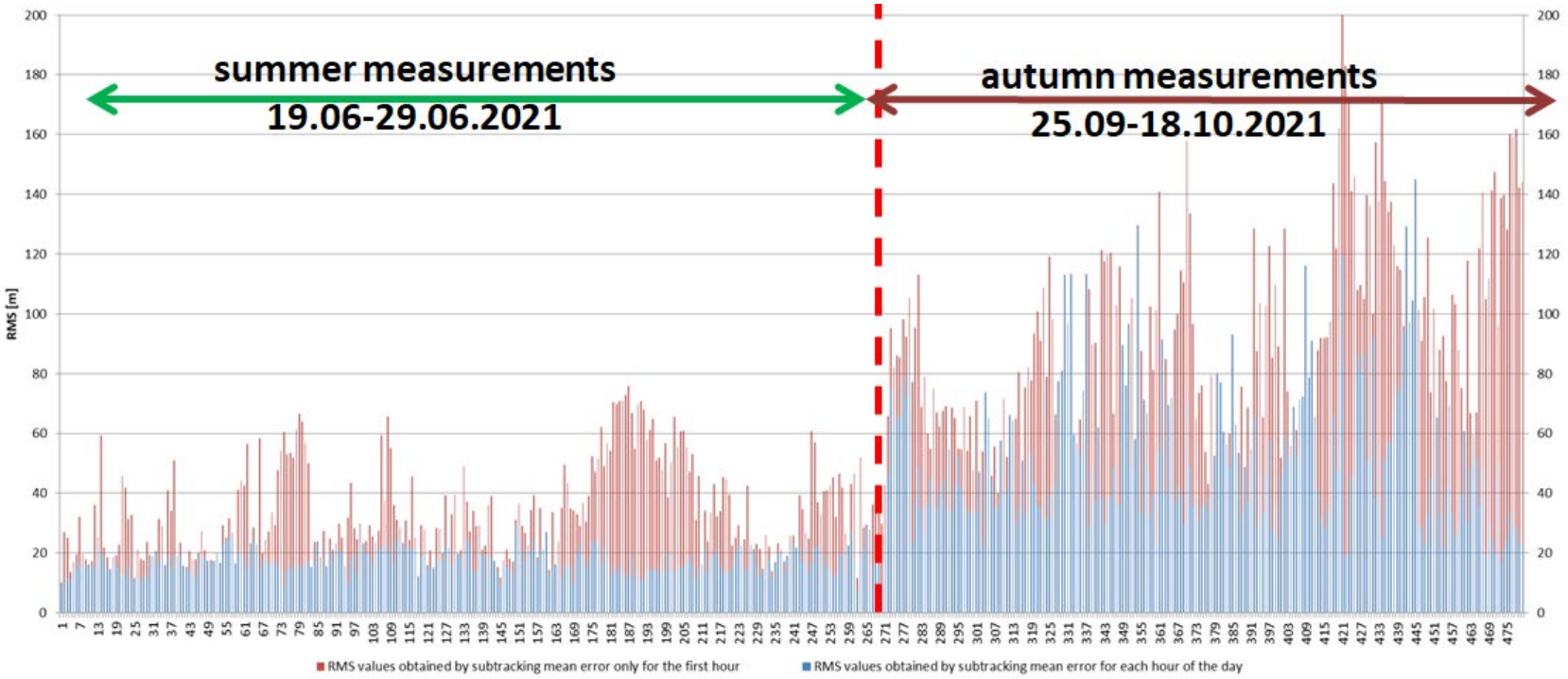

Figure 4-19: Measurement errors with regard to the GNSS receiver for summer and autumn measurements

The above chart 4-19 shows very clearly the RMS's disproportion between the two measurement periods. Were it not for the technical problems with the power amplifier, these changes could have been traced in a much longer scale. The increase of the RMS values observed in the fall season could also be related to weather conditions, which will be analyzed in the next sections.

4.2 Analysis of the power and quality of correlation of received signals

In order to compare the results for the two measurement periods, the characteristics of the received signal power vs. time was plotted. We can see some small (fig. 4-20) discrepancies, but they are caused by the replacement of the power amplifier during the measurement period between the summer and autumn campaign. Throughout the respective measurement campaigns, the received signal was stable and no anomalies were noted.

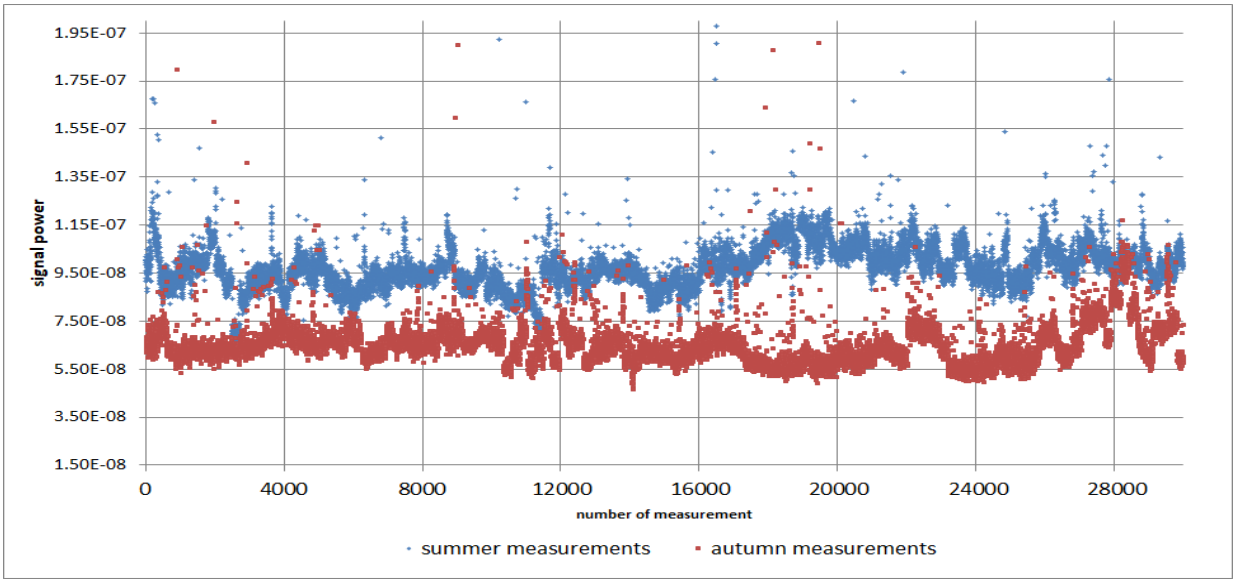

Figure 4-20: Comparison of the received signals strength for the summer and autumn campaigns

Fig. 4-21 shows the received signal level represented by the SNR vs. time characteristics.

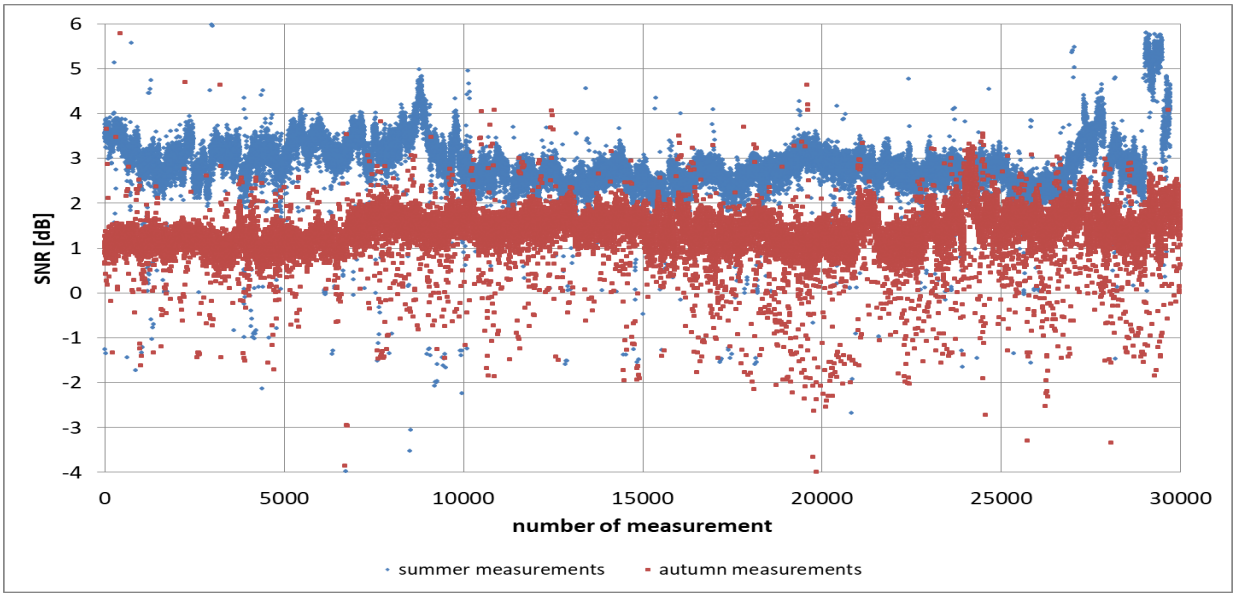

Figure 4-21: Comparison of the SNRs obtained during summer and autumn measurements

The received signals were also analyzed in terms of quality. For each of the signals, a correlation function with a reference signal was generated. The ratio of the main correlation peak to the side lobes was checked. The better the quality of the given signal, the better the correlation coefficient (fig. 4-22).

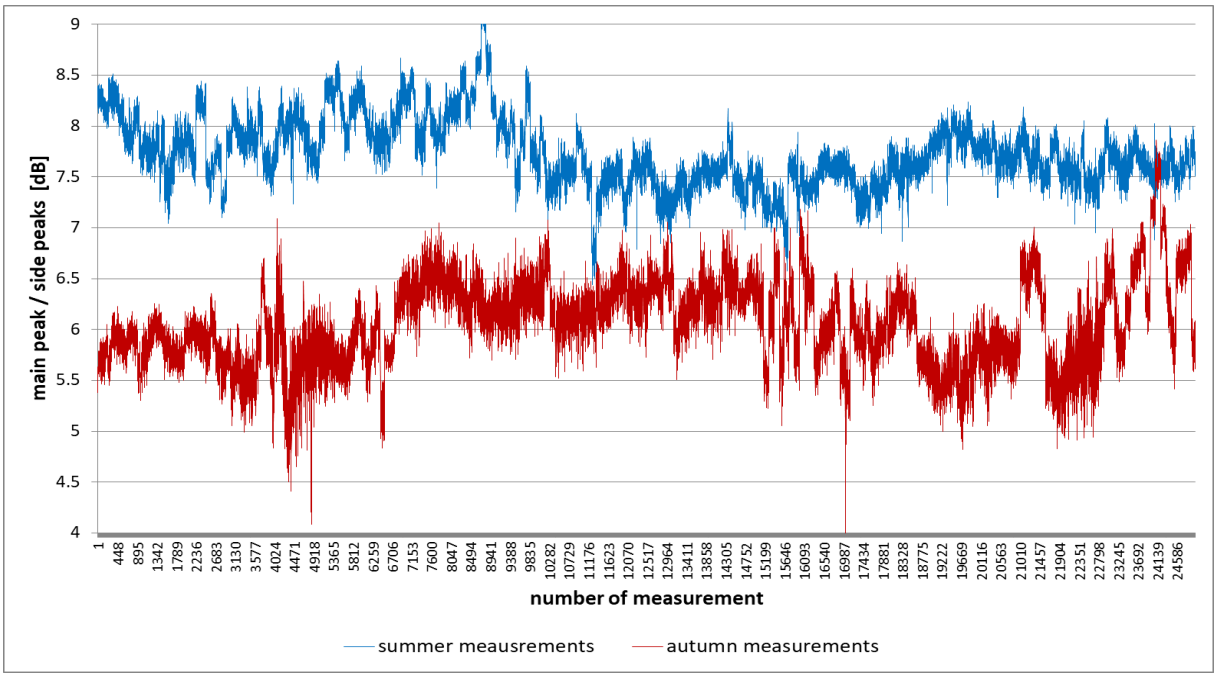

Figure 4-22: Correlation quality for summer and autumn measurements

The correlation quality in this case was better during the summer measurements. The differences between the received power values compared to the autumn campaign were small but to some extent it could also affect the accuracy of the pseudo ranges.

4.3 The relation between the RMS and the prevailing meteorological conditions

On the basis of all the processed data, it was possible to obtain numerous characteristics of the pseudo-ranges' RMS values. In order to interpret these results better, it was decided to compare them with the meteorological conditions prevailing at the moment when the given signal was being received. This helped to evaluate the extent to which the obtained RMS depended, inter alia, on air temperature, humidity, cloudiness or atmospheric pressure (fig. 4-23).

In this case, too, the analysis for the summer measurements was done first, followed by the analysis for all the collected measurements.

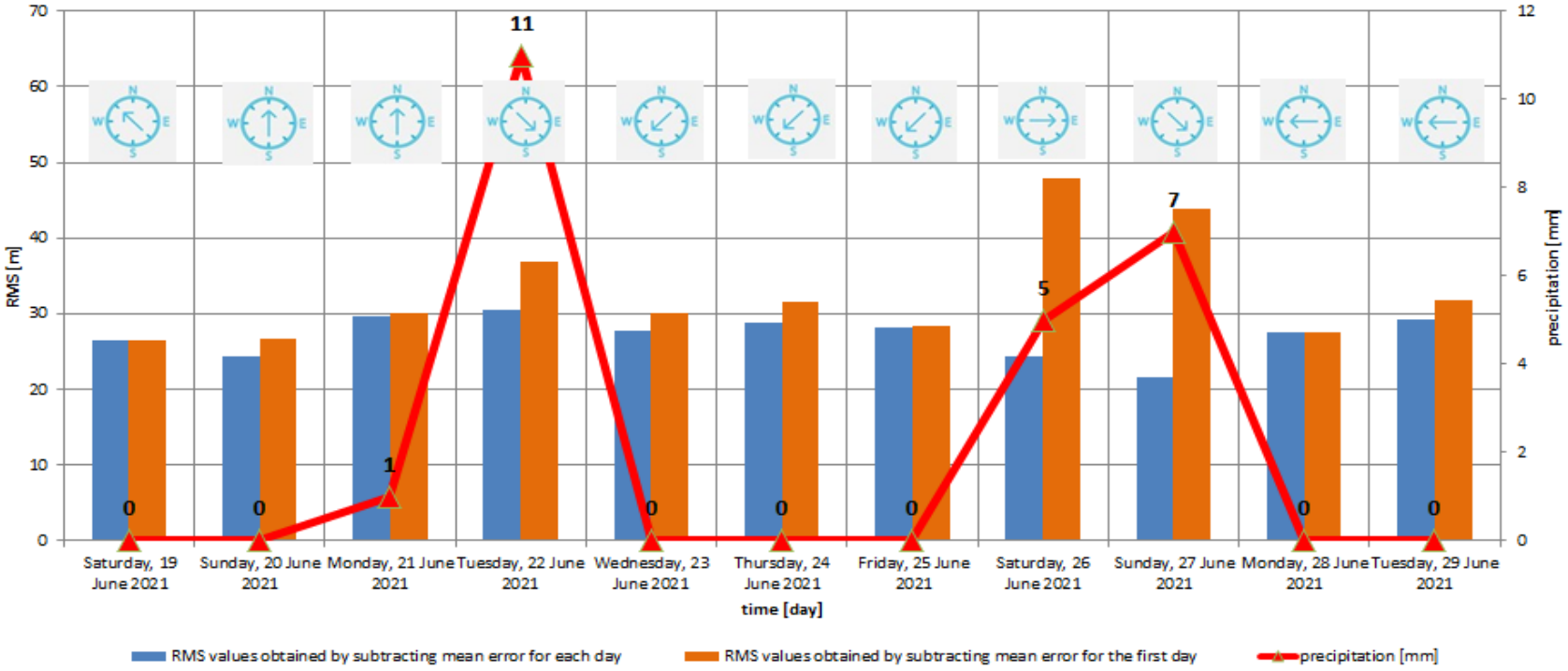

Figure 4-23: The obtained RMS values per day during the summer campaign (including meteorological data)

First, an RMS analysis was made for each day during the summer measurements, which was correlated with the weather conditions prevailing at the time. Initially, it was verified whether wind direction had any influence on the RMS fluctuations. Such a relationship was not observed. It was then checked whether the rainfall could affect the RMS figures. It turned out that on the days when it rained, the RMS for the mean error subtracted at the beginning of the measurements was noticeably higher than during the rest of the measurements. This means that it is possible that rainfall caused a variation in the calculated RMS [4-2]. The next chart shows the RMS for each time of the day with a summary of rainfall (fig. 4-24):

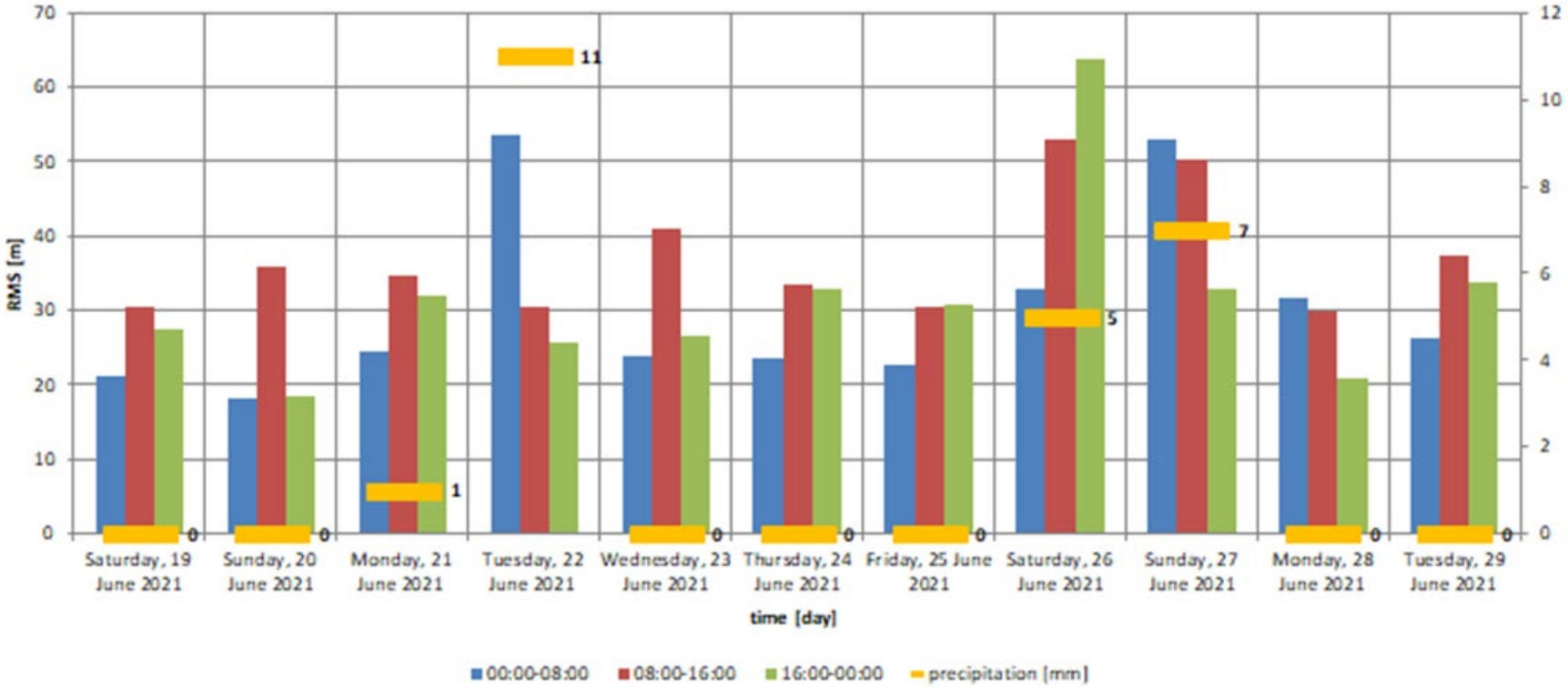

Figure 4-24: RMS for different times of day for summer measurements (subtracting mean error calculated for the first day only, including meteorological data)

The increase in the RMS error in a given period of the day could have been caused by the rainfall that occurred at that time. Unfortunately, we did not have access to such detailed weather history, so it is not possible to draw such a conclusion. A similar observation can be made for the figure 4-25. There, the RMS has been plotted for each measuring hour during the summer.

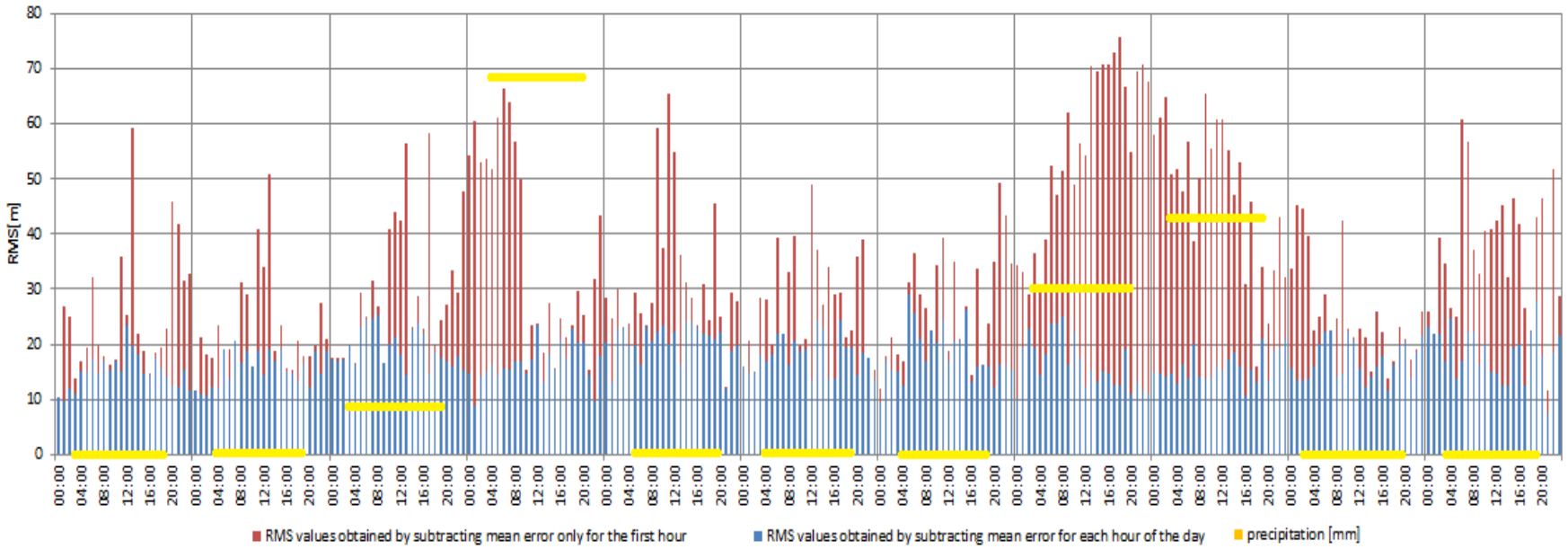

Figure 4-25: RMS values for each hour during the summer campaign, including meteorological data

With the rainfall levels marked, the graph shows that the RMS for each hour (if the mean error is subtracted only in the first hour of measurement) is greater during rainfall. In such cases (i.e. during rain), the RMS rises to as much as 70 meters, while it is otherwise kept at 20 meters. To take a closer look at this relationship, two measurement days were carefully analyzed with respect to the prevailing weather conditions (4-26, 4-27, 4-28, 4-29).

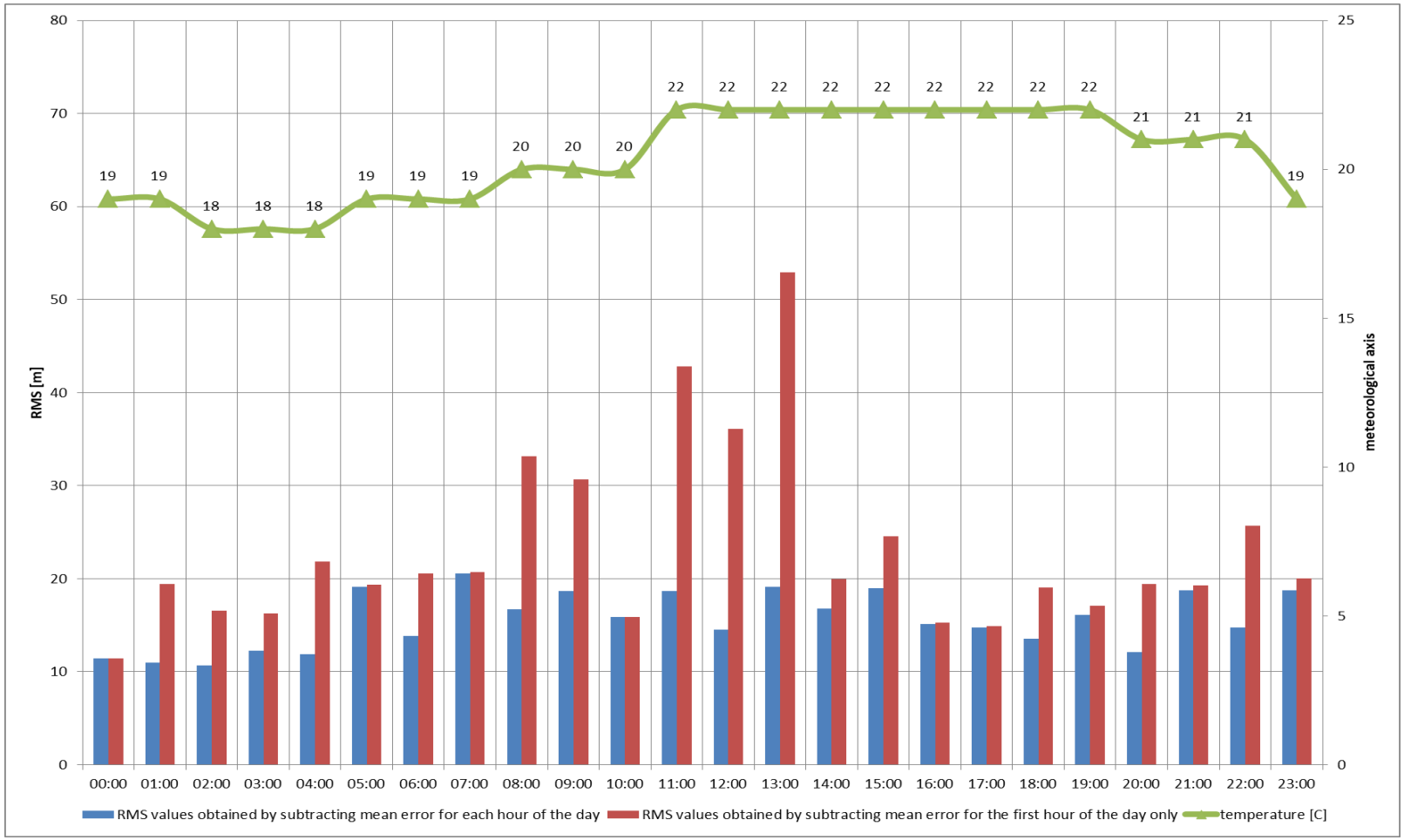

Figure 4-26: Analysis of the observed RMS depending on the meteorological conditions (20.06.2021) 1/2

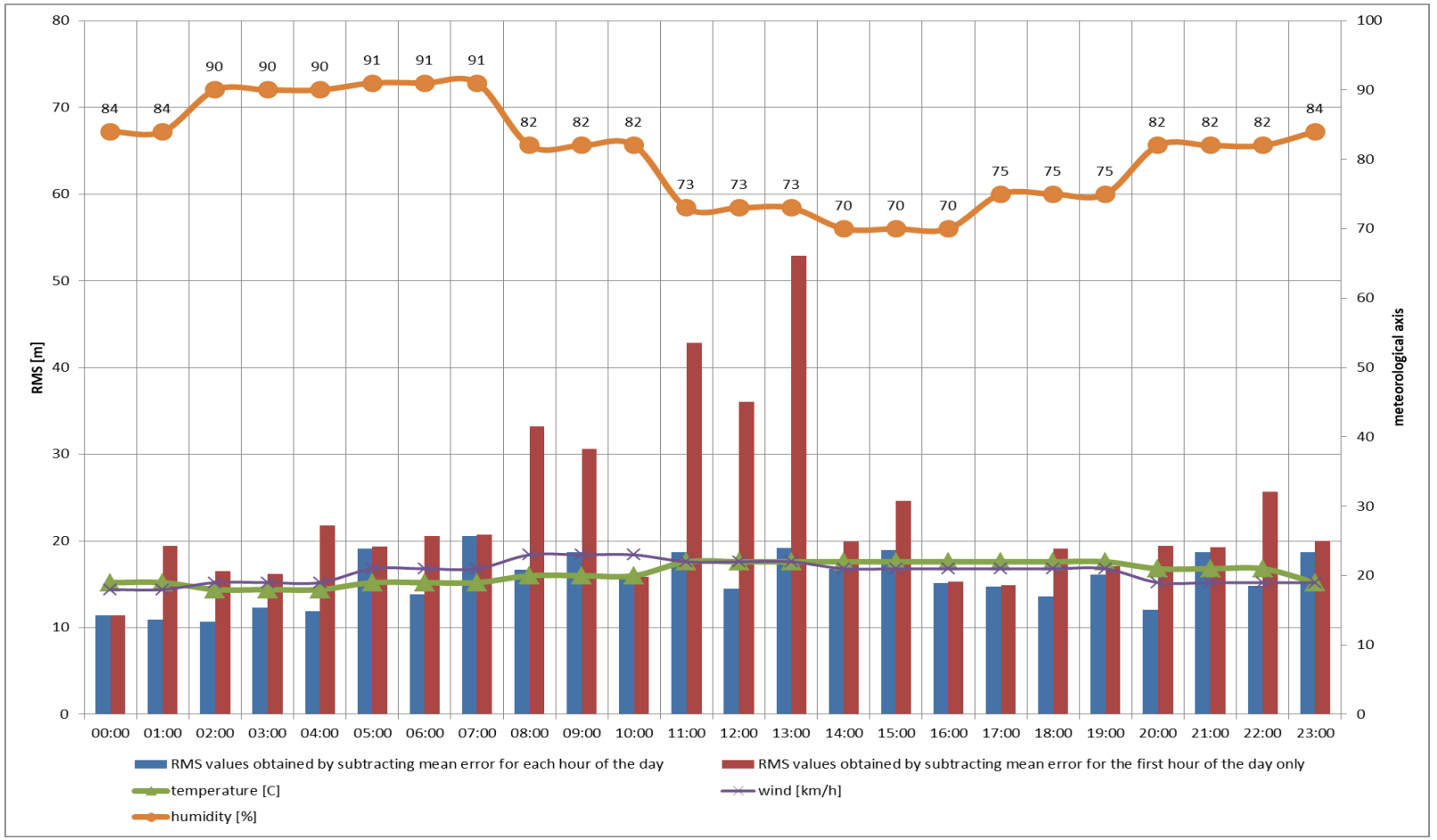

Figure 4-27: Analysis of the observed RMS depending on the meteorological conditions (20.06.2021) 2/2

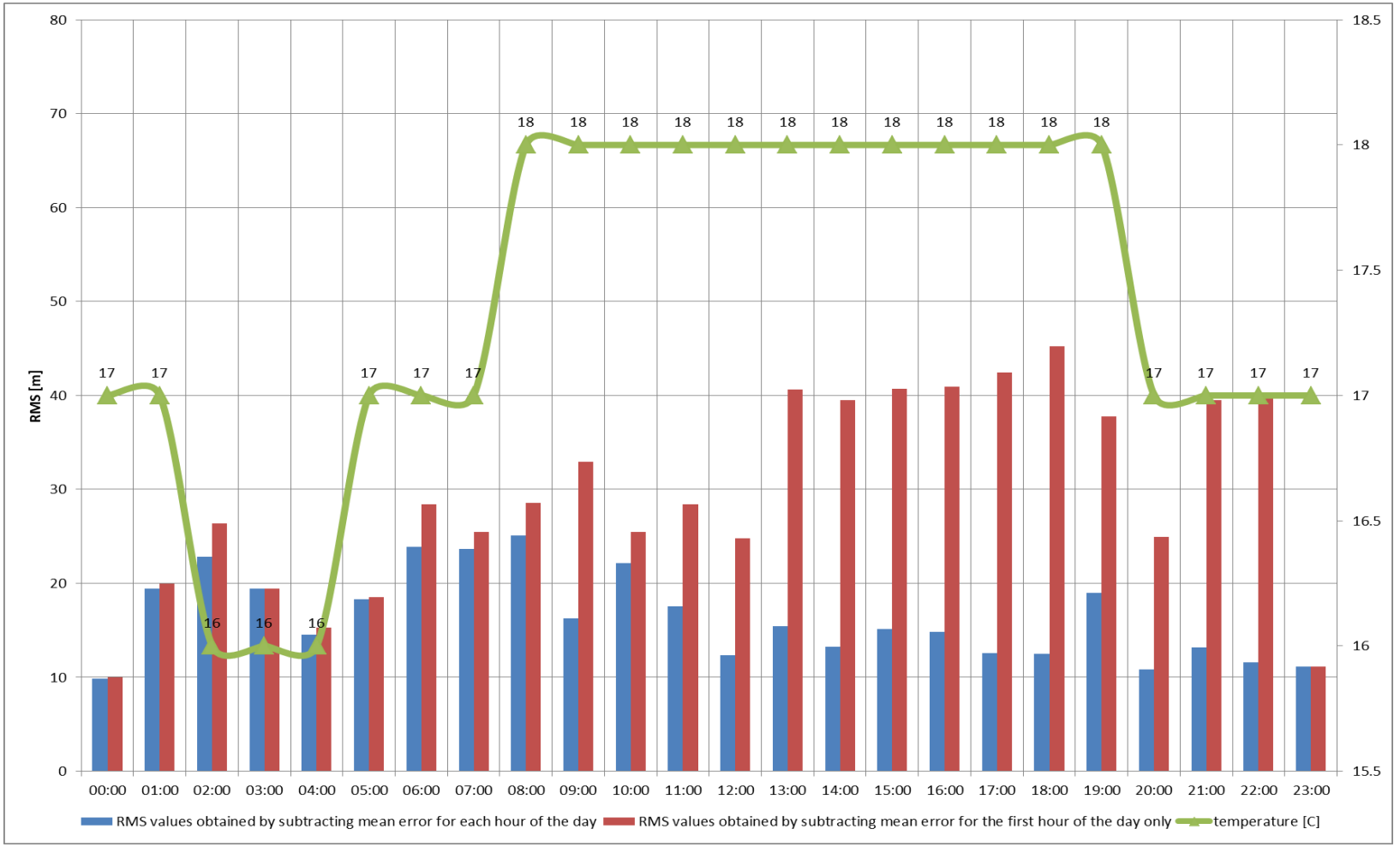

Figure 4-28: Analysis of the observed RMS depending on the meteorological conditions (26.06.2021) 1/2

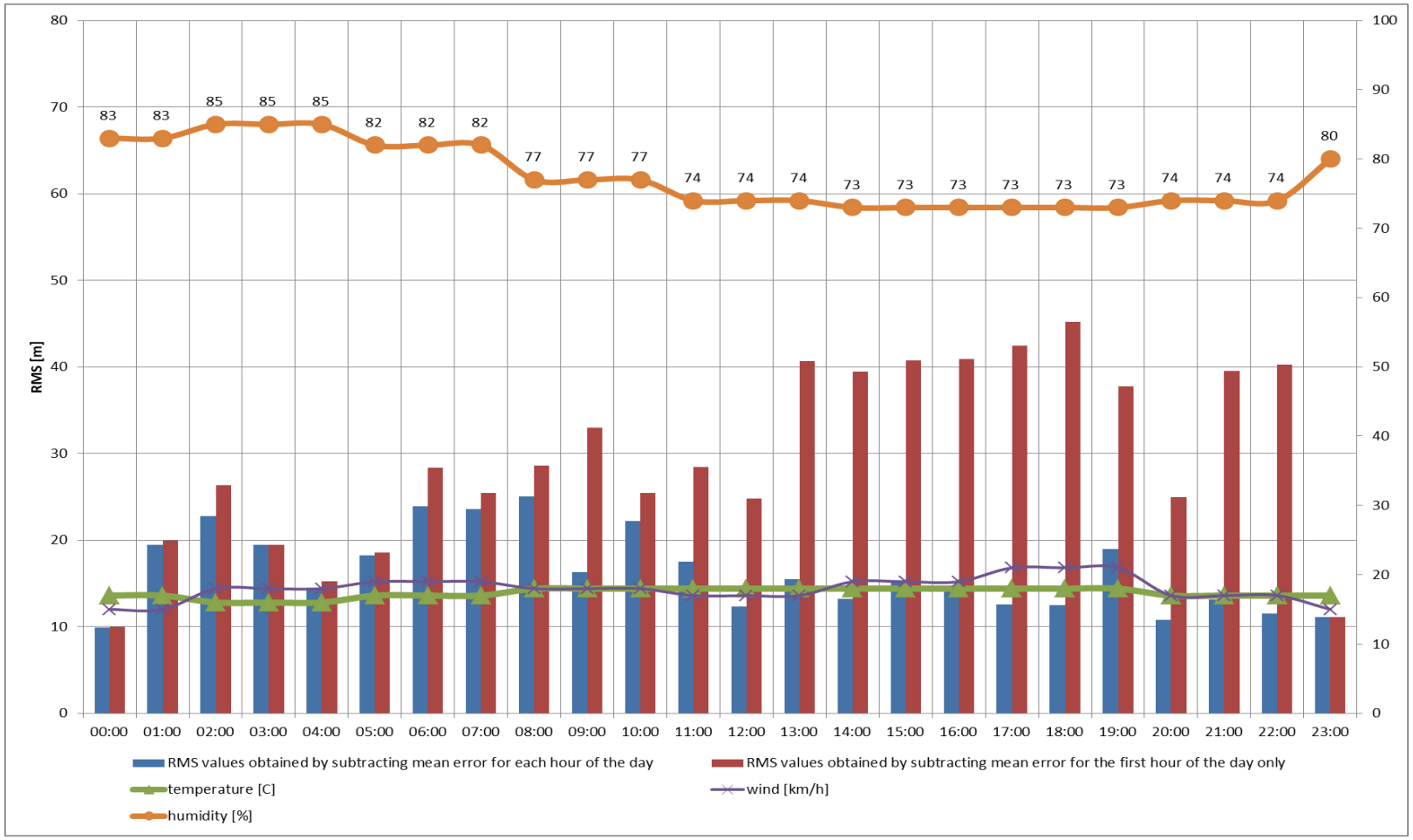

Figure 4-29: Analysis of the observed RMS depending on the meteorological conditions (26.06.2021) 2/2

Two isolated measurement days (20 June and 26 June 2021) were analyzed in detail to observe the periodic build-up of the RMS error over the course of the day and to establish its cause. First, the ambient temperature for the first analysed day is plotted in Figure 4-26. It was clearly shown that it had no effect on the RMS changes during that day. In fig. 4-27, the humidity, temperature and wind force are shown. Here, we can observe a correlation between humidity and RMS, but to confirm that more graphs of this type should be reviewed. On the other hand, the detailed analyzes for 26.06 2021 showed that RMS could depend on the occurrence of the tropospheric duct phenomenon on that day. This case was analyzed in a separate subsection. Additionally, the graphs 4-30, 4-31, 4-32, 4-33, 4-34, 4-35, 4-36, 4-37 show how the RMS values during the autumn measurements were affected by the following meteorological conditions:

- wind,
- clouds,
- humidity,
- temperature,
- rainfall.

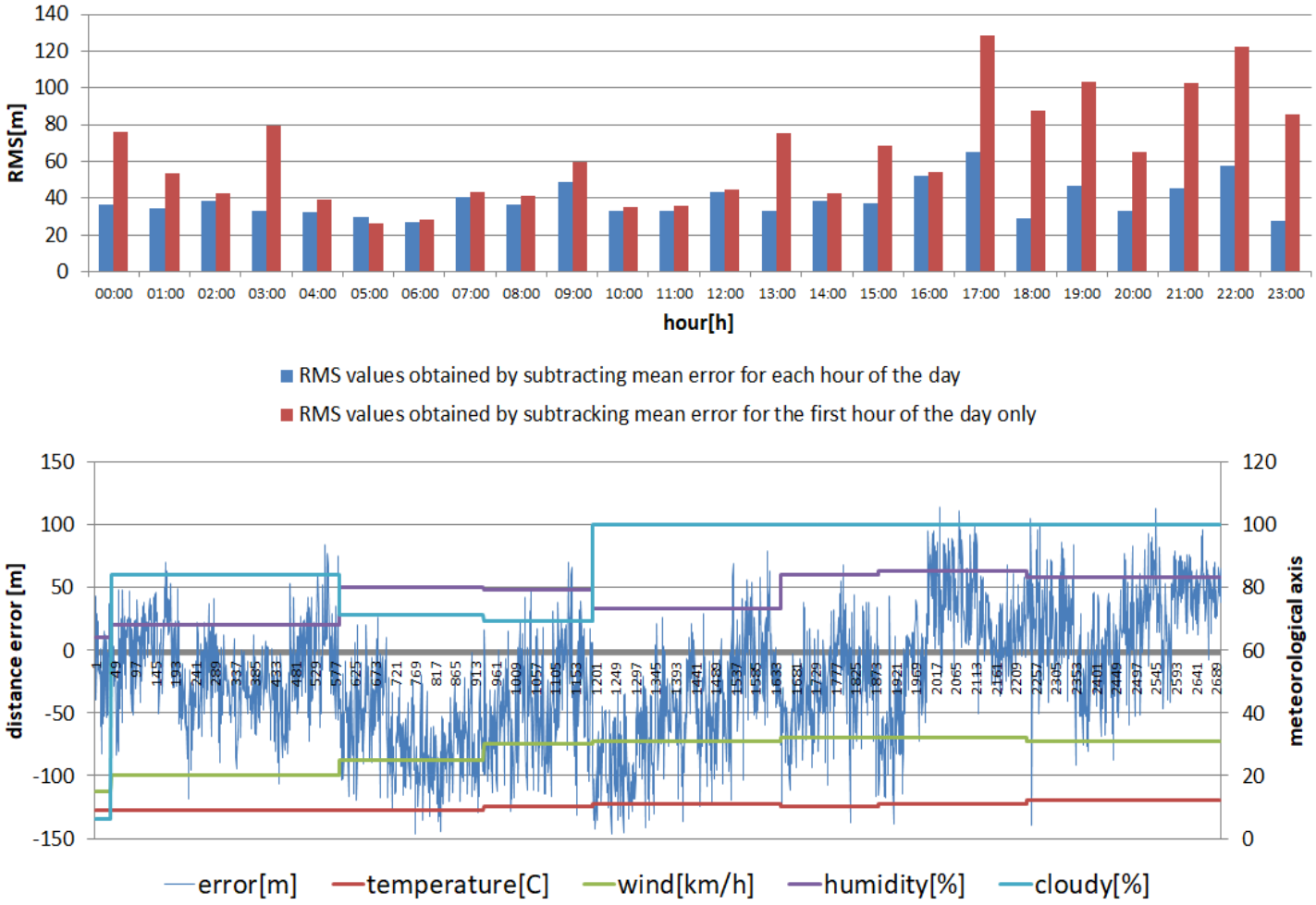

Figure 4-30: Detailed analysis of the RMS (upper graph) and distance error characteristic for various meteorological factors (bottom graph) - 14.10.2021 (1/2)

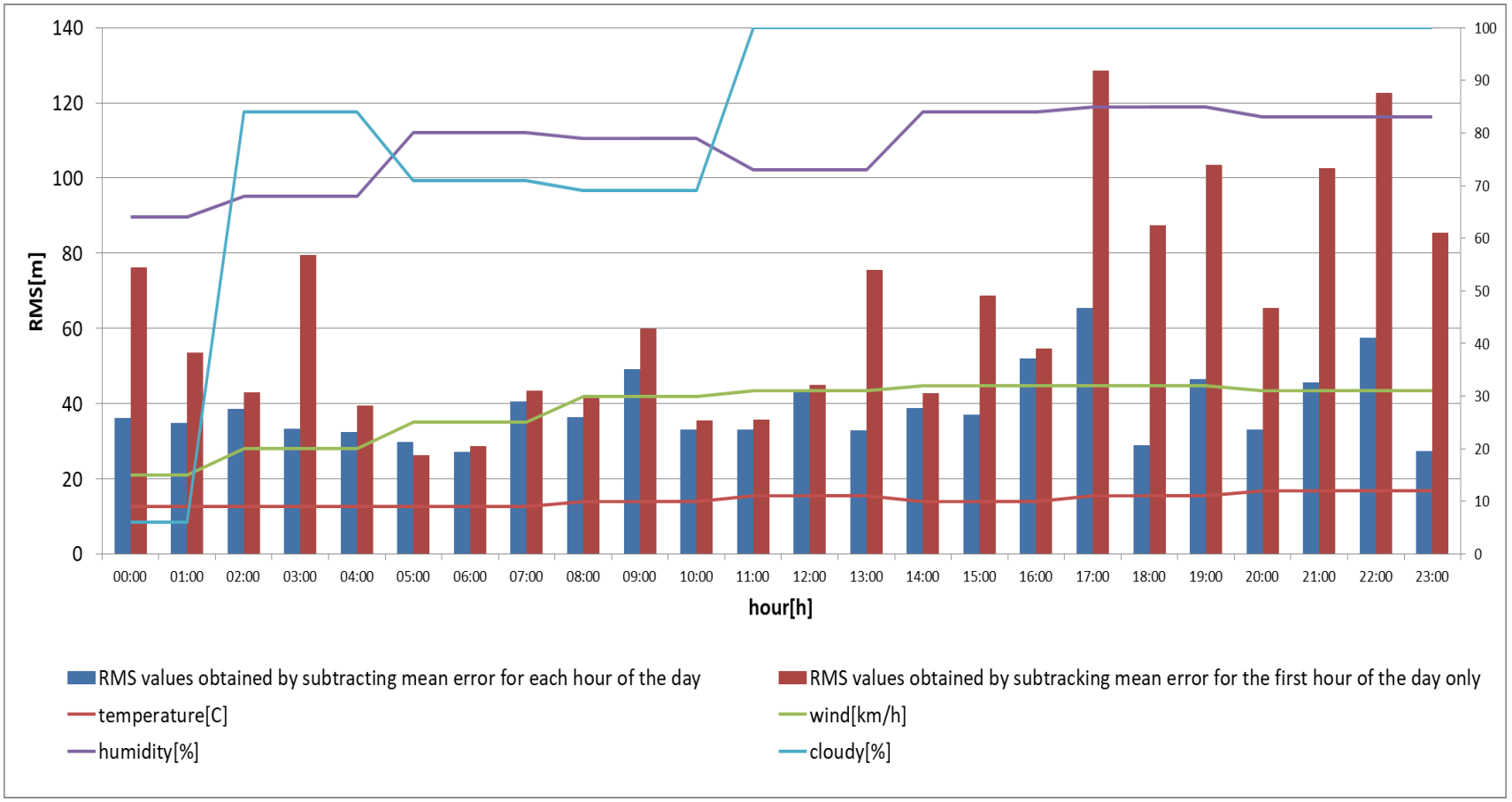

Figure 4-31: Detailed analysis of the RMS (upper graph) and distance error characteristic for various meteorological factors (bottom graph) 14.10.2021 (2/2)

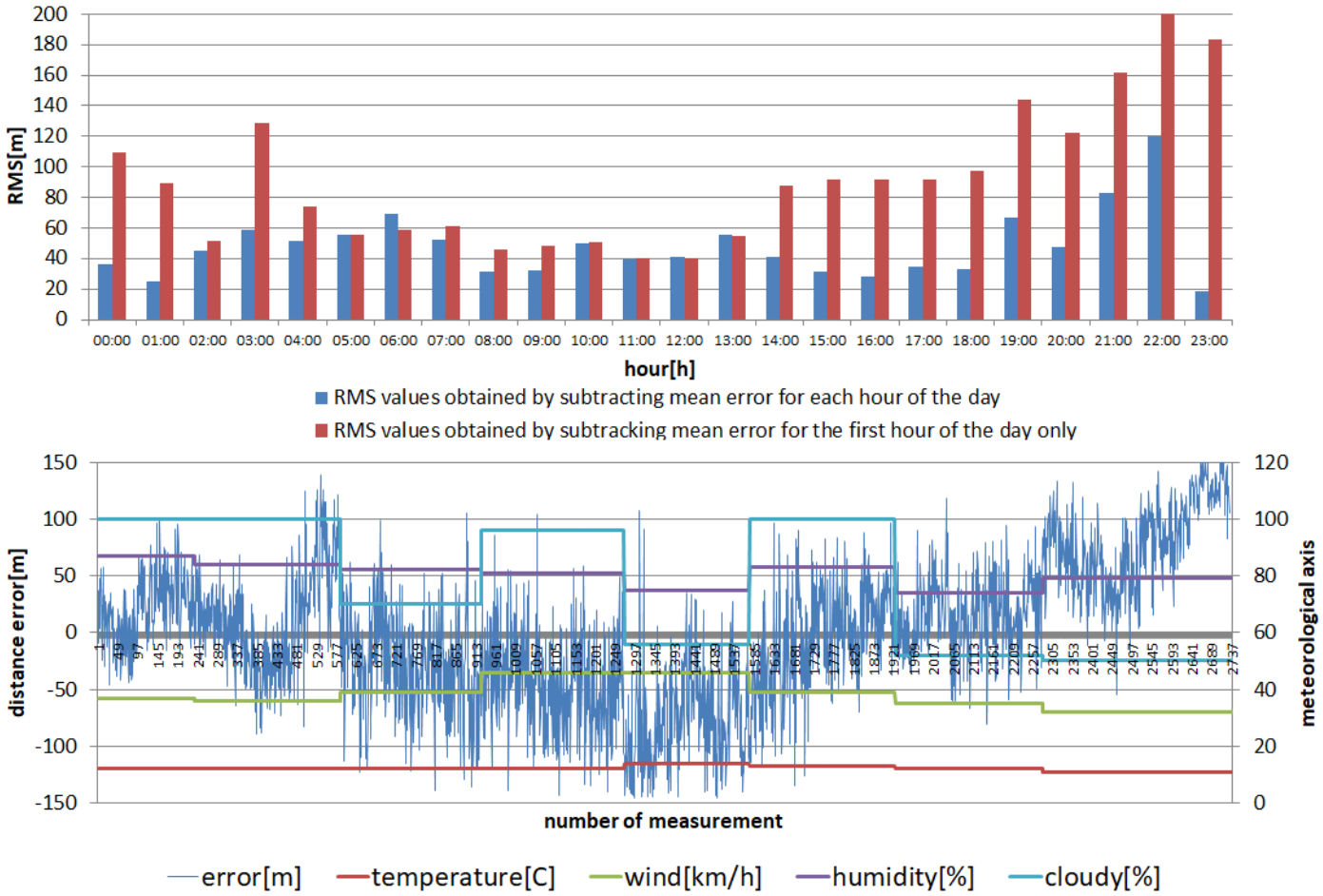

Figure 4-32: Detailed analysis of the RMS (upper graph) and distance error characteristic for various meteorological factors (bottom graph) 15.10.2021 (1/2)

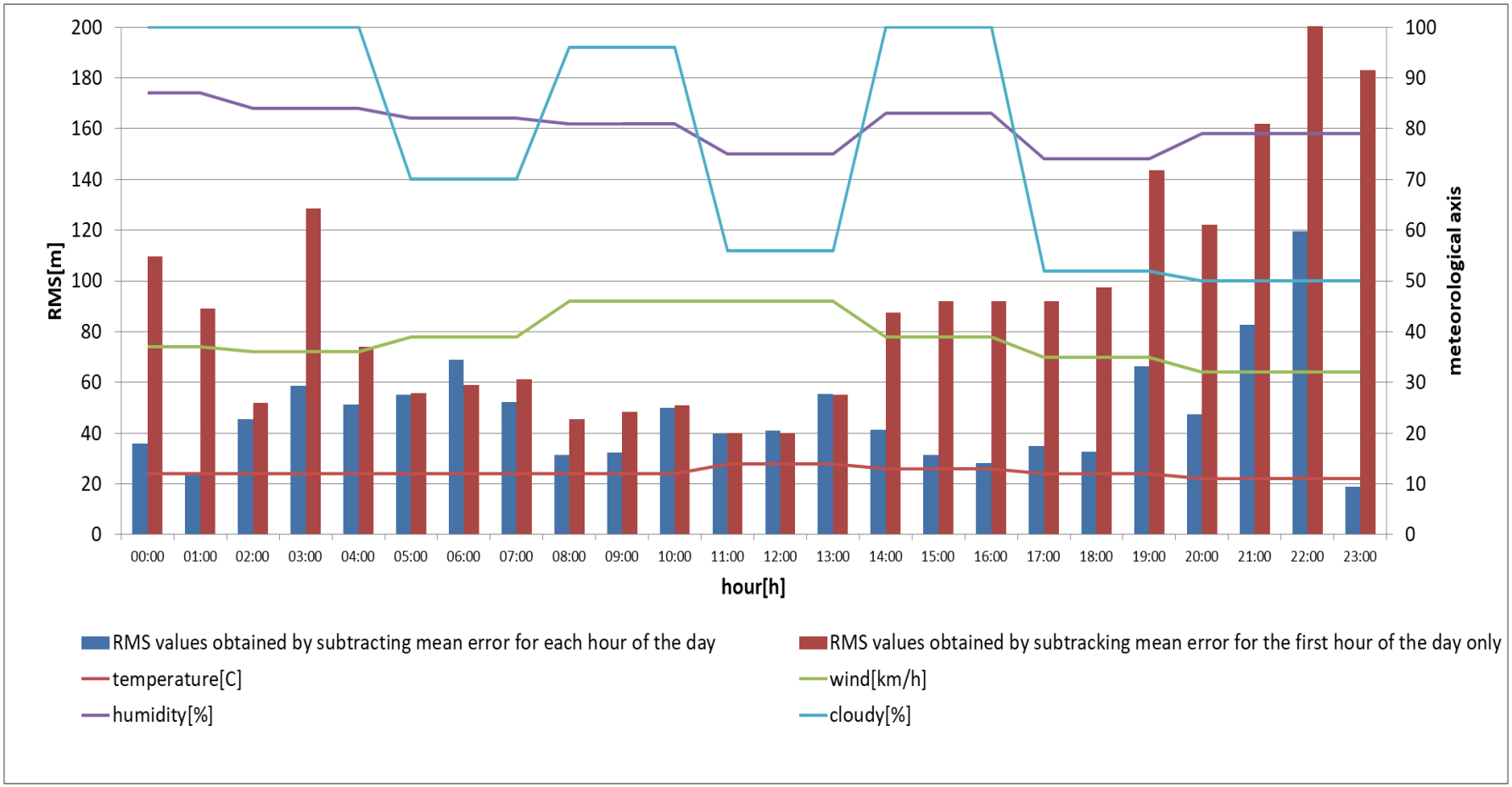

Figure 4-33: Detailed analysis of the RMS (upper graph) and distance error characteristic for various meteorological factors (bottom graph) 15.10.2021 (2/2)

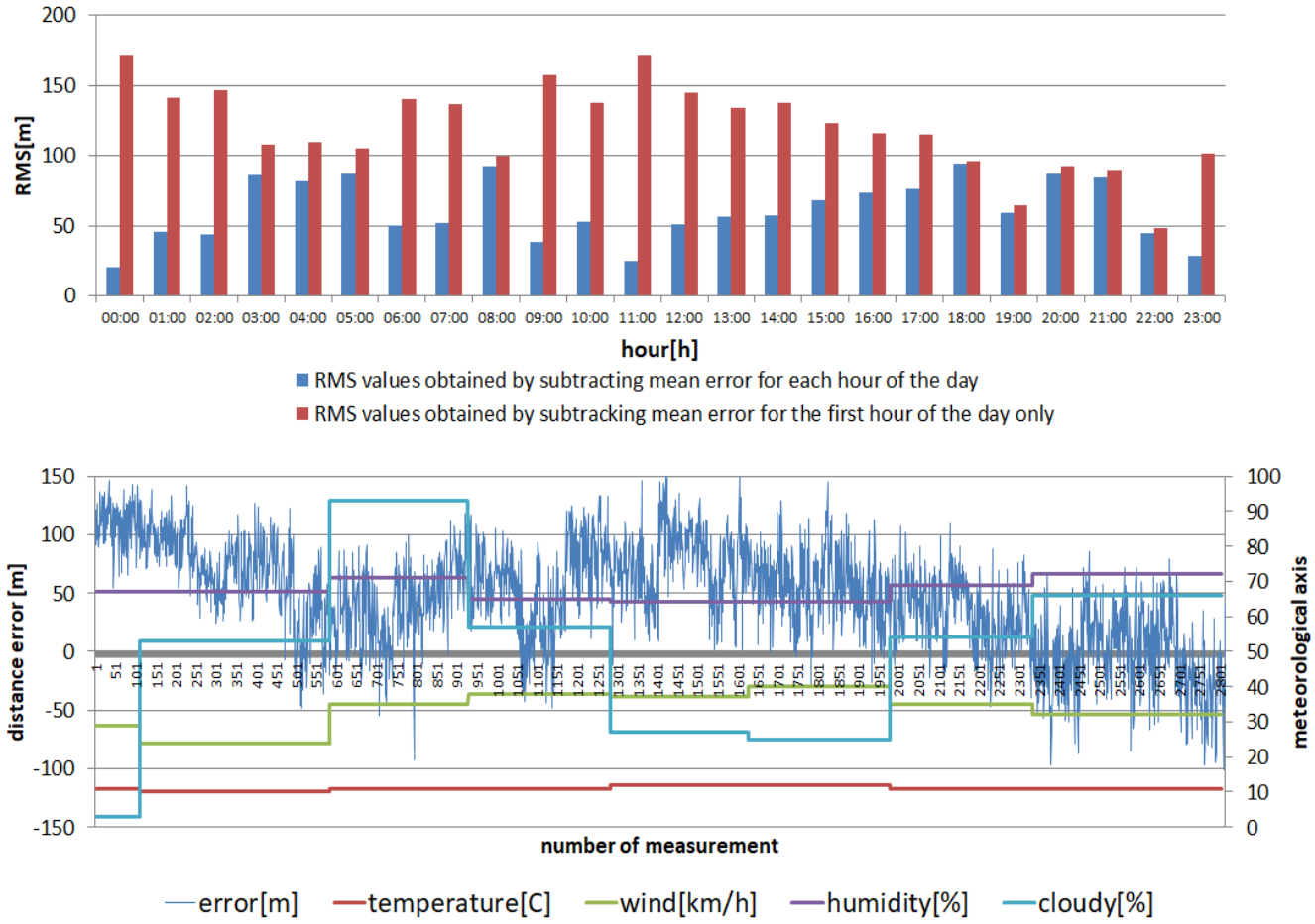

Figure 4-34: Detailed analysis of the RMS (upper graph) and distance error characteristic for various meteorological factors (bottom graph) 16.10.2021 (1/2)

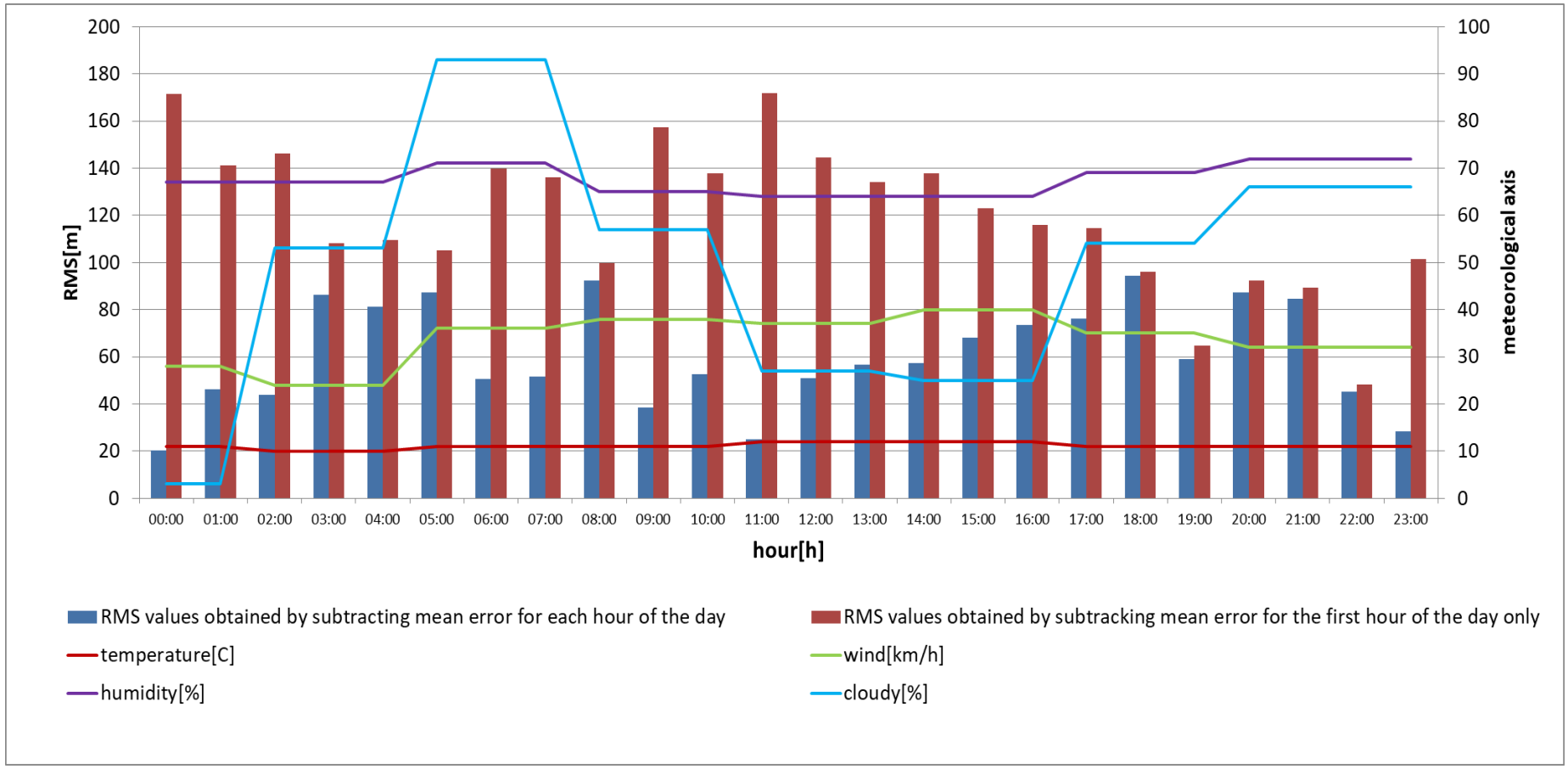

Figure 4-35: Detailed analysis of the RMS (upper graph) and distance error characteristic for various meteorological factors (bottom graph) 16.10.2021 (2/2)

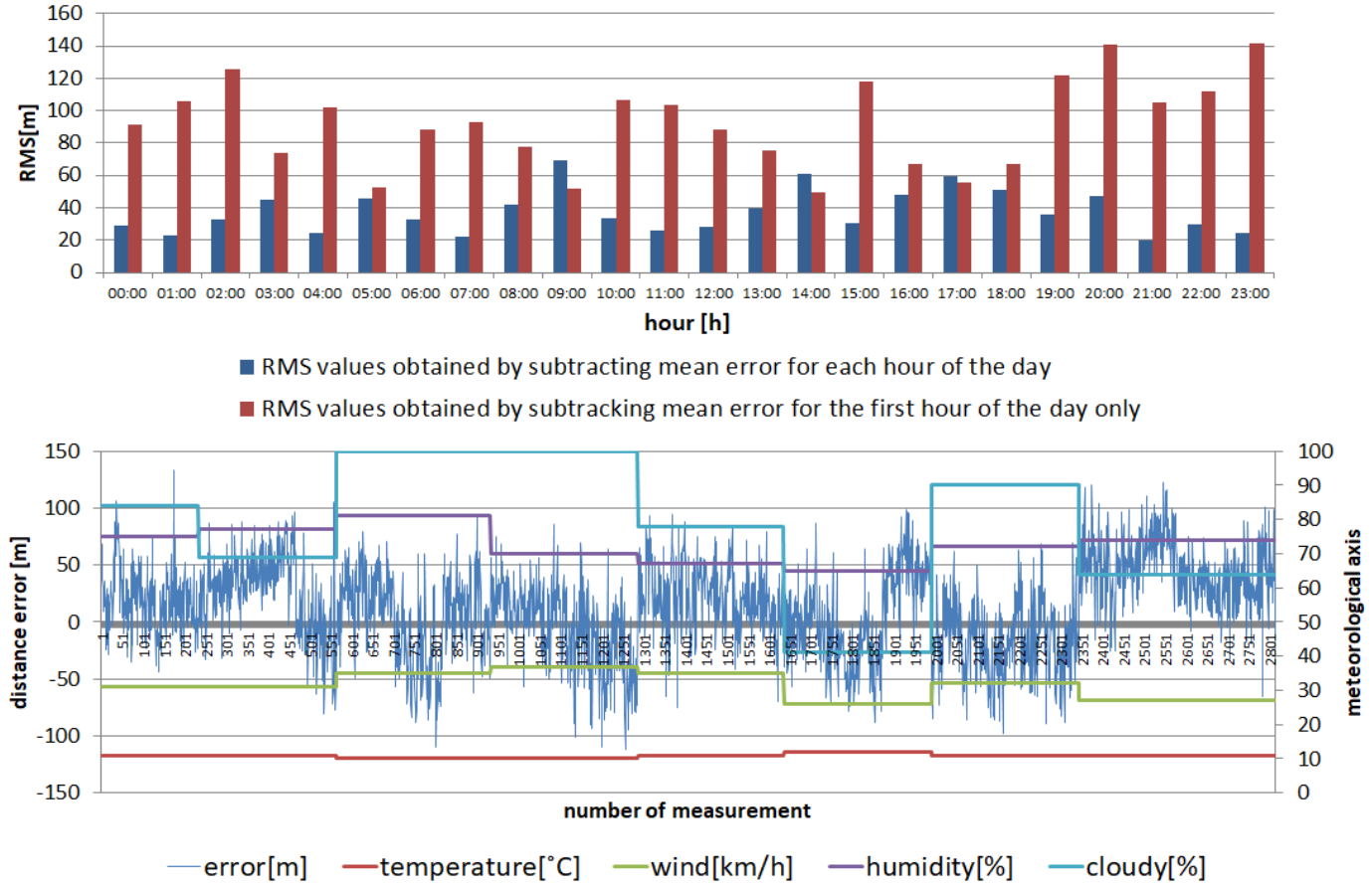

Figure 4-36: Detailed analysis of the RMS (upper graph) and distance error characteristic for various meteorological factors (bottom graph) 17.10.2021 (1/2)

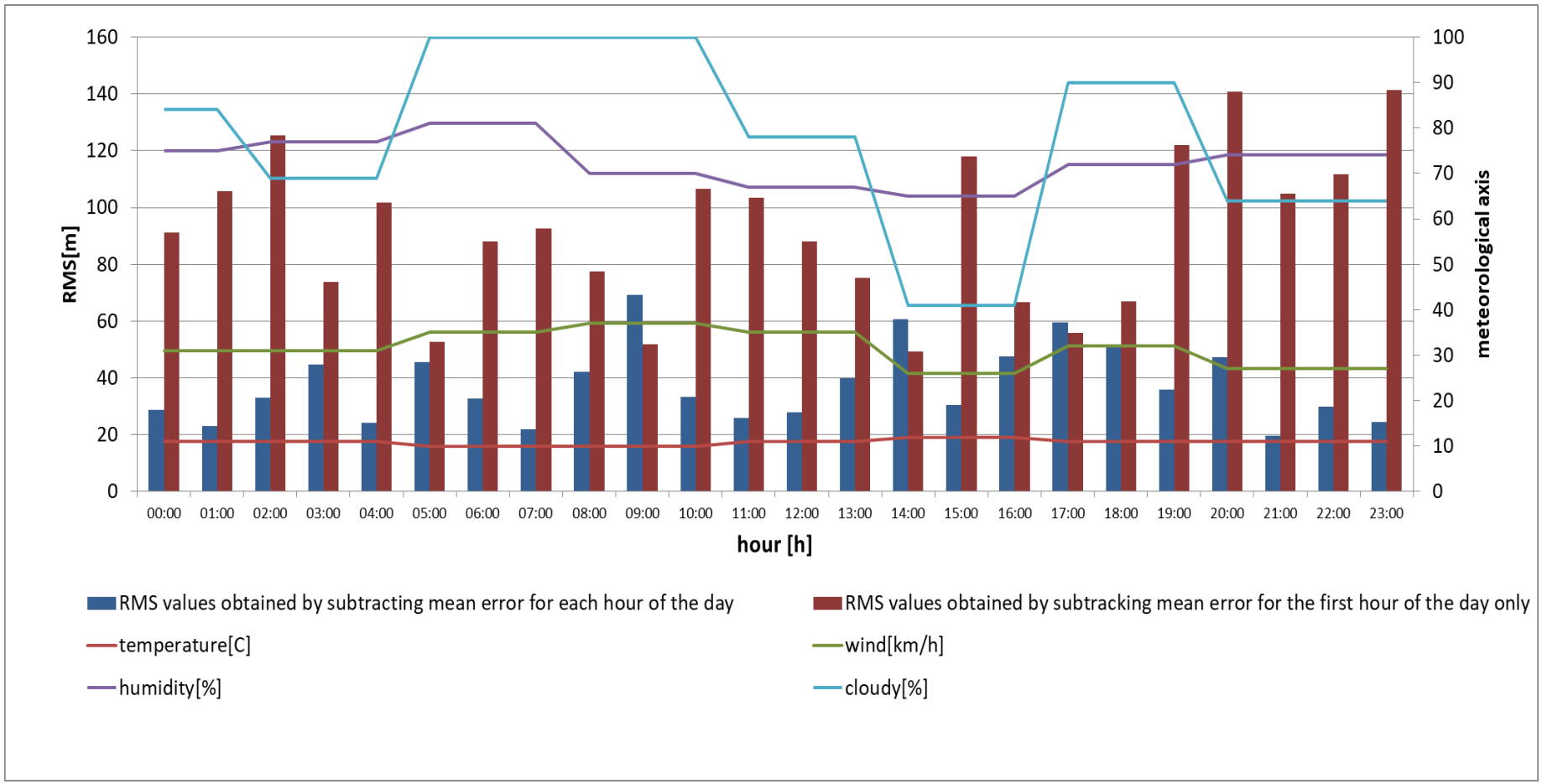

Figure 4-37: Detailed analysis of the RMS (upper graph) and distance error characteristic for various meteorological factors (bottom graph) 17.10.2021 (2/2)

All results from the autumn measurement campaign feature much worse results of RMS compared to the summer campaign. As we can see, the meteorological conditions did not have a major impact on the fluctuations of the RMS value. In order to have a complete picture of the RMS changes, long-term monitoring studies would need to be carried out to determine what exactly the RMS changes depend on. In the summer measurements, it could be noticed that the rainfall had a large impact on the RMS changes. However, in the autumn measurement period, no precipitation occurred.

4.4 The phenomenon of tropospheric ducts in measurements

Signal propagation in radio channel is a phenomenon that is influenced by many factors. Primarily, it depends on the properties of the wave itself, i.e. its length and polarization, as well as on the conditions of the environment in which the wave propagates. By "environmental conditions" we mean the topography and the type of its coverage - radio waves propagate differently in areas covered with water, in forests, in urban areas or in open areas. The phenomenon that substantially shapes the signal in radio channel is multipath transmission. Multipath means that the signal – through diffraction, refraction, scattering and reflection – reaches the receiver as a sum of composite signals with different delays, phases and amplitudes [4-3]. Additionally, in the vicinity of the receiver, each of the components is dispersed into another N components. If the receiver is in motion, the carrier frequency of each scattering component is shifted by Doppler pulsation. Figure 4-38 shows the impact of multipath propagation on the shape of the correlation function.

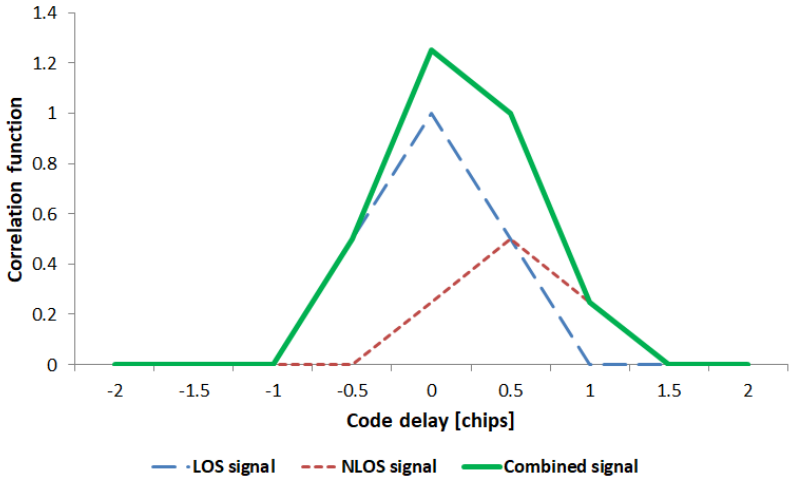

Figure 4-38: Influence of the multipath phenomenon on the shape of the correlation function [4-4]

The delay of the multi-path signal depends on the additional distance traveled by the reflected signal, which is longer than that of the direct signal. During the measurement campaign organized by the National Institute of Telecommunications, the transmitter was installed in the port of Gdynia, where, for the initial short-range measurements, the multipath effect was caused by neighboring silos or buildings. On the other hand, for measurements in the open sea, the signal could also find its way to the receiver through reflections from maritime infrastructure - ships, ports or breakwaters. The presence of land (Hel Peninsula) on the transmitting-receiving line had its impact on the reflected signals reaching the

receiver. A phenomenon that is also conducive to the occurrence of multi-path at sea was the tropospheric waveguide channel - the duct (Fig. 4-39) [4-5]. This is a type of radio propagation that tends to occur during periods of stable, anti-storm weather.

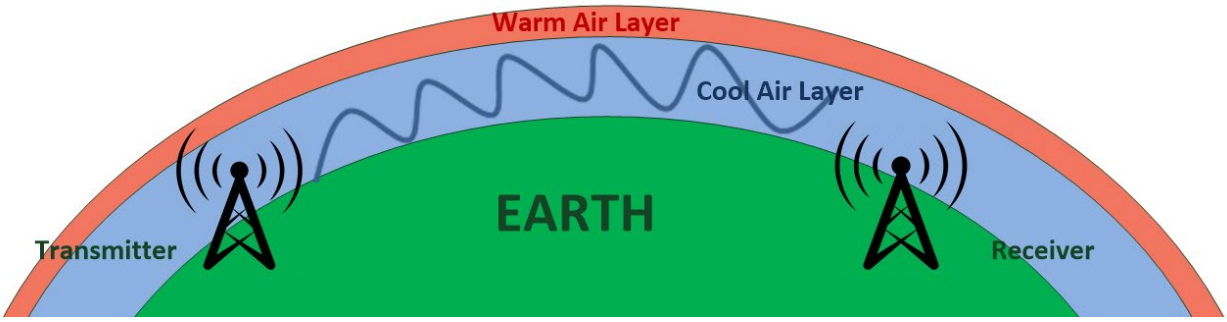

Figure 4-39: The phenomenon of tropospheric ducts

In the propagation phenomenon shown in fig. 4-39, when the signal encounters an increase in temperature instead of its drop (known as temperature inversion), a higher refractive index of the atmosphere will cause the signal to bend. Especially favorable conditions for the formation of tropospheric ducts occur mainly in the second half of the year [4-6]. The autumn migrations of high-pressure systems, a large supply of moisture in the atmosphere and daily temperature fluctuations have a beneficial effect in this case. Tropospheric ducts affect all frequencies, and the signals amplified in this way tend to travel up to 1300 km. The day on which the duct phenomenon occurred is marked in the following picture (fig. 4-40):

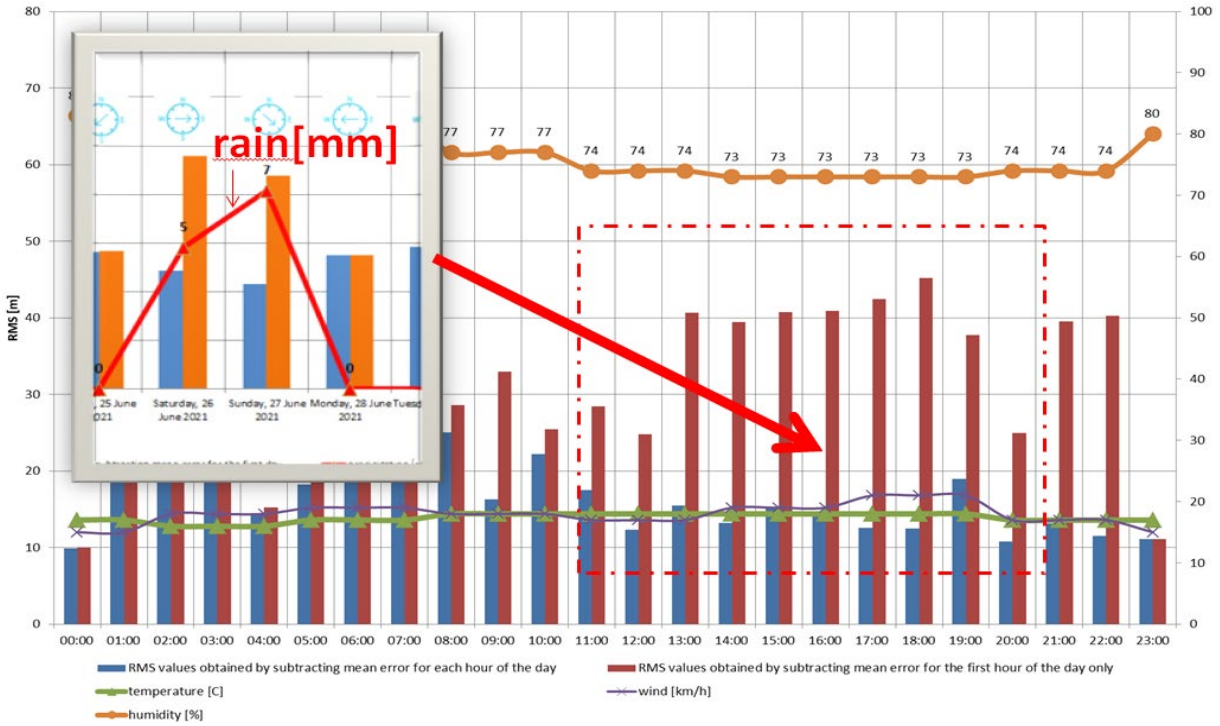

Figure 4-40: The phenomenon of tropospheric ducts - 26.06.2021

On the other hand, the figures 4-41, 4-42 show the attenuation of signals that occurred during the summer measurements (yellow line) and it can be seen that at the time of the occurrence of the tropospheric ducts phenomenon, the attenuation was greater.

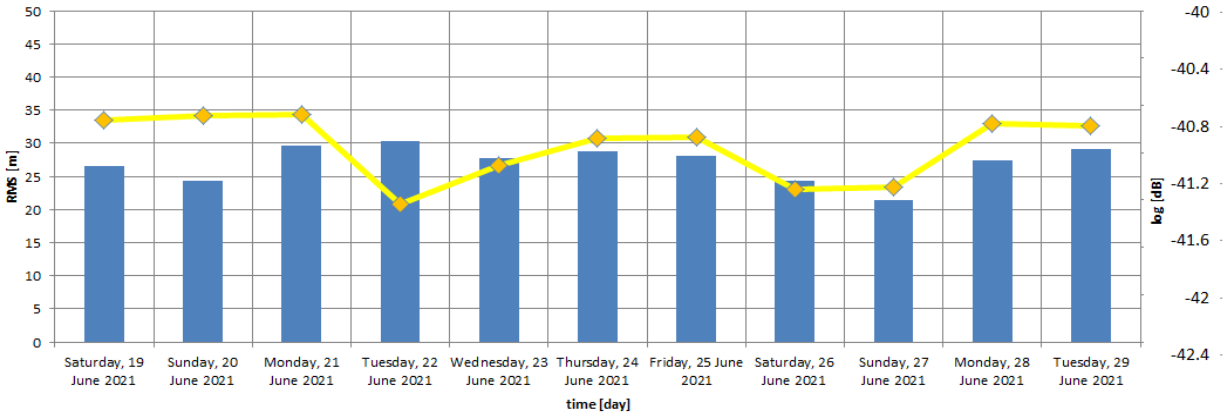

Figure 4-41: Signal attenuation (yellow line) and RMS (blue bars) for each day in the summer campaign

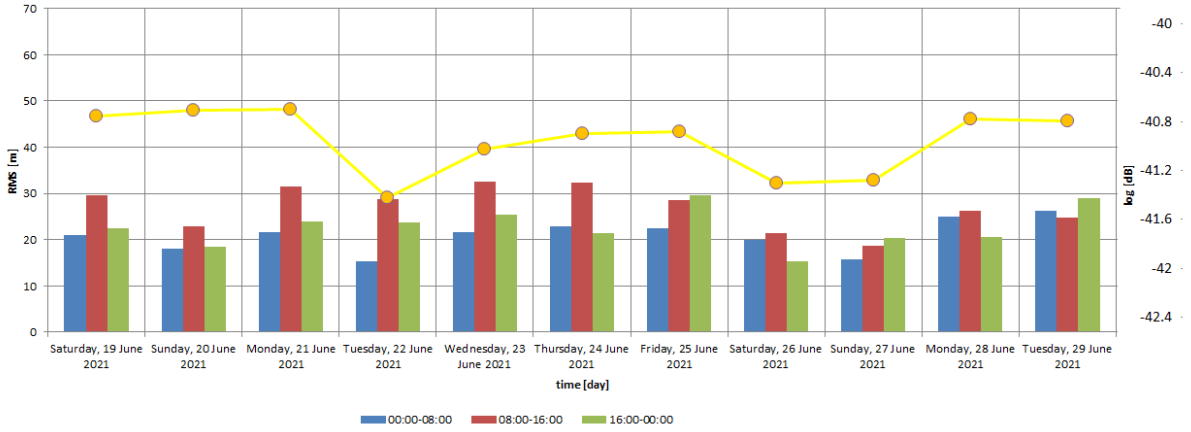

Figure 4-42: Signal average attenuation (yellow line) and RMS (color bars) for each day in the summer campaign

As we can see in the above graphs, when the attenuation was -41 dB, the RMS of the cumulative distance error increased significantly. Such a case is especially visible on the measurement day of June 26, 2021. On that day, rainfall occurred resulting in this phenomenon.

5 VDES R-Mode Baltic 2 static "long-term" positioning results

Based on the range measurements presented in Chapter 4, the position of the receiver was calculated using the TOA method. The position was determined for each set of four distance measurements. The arrangement of the reference stations is shown in Figure 5-1. There is a real reference station in Gdynia, whereas the location of the other stations is virtual. They were emulated, as described in chapter 4. The receiver has been installed in Jastarnia. For the scenario analyzed in this chapter (distribution of reference stations in relation to the receiving terminal), the HDOP coefficient is 3.39.

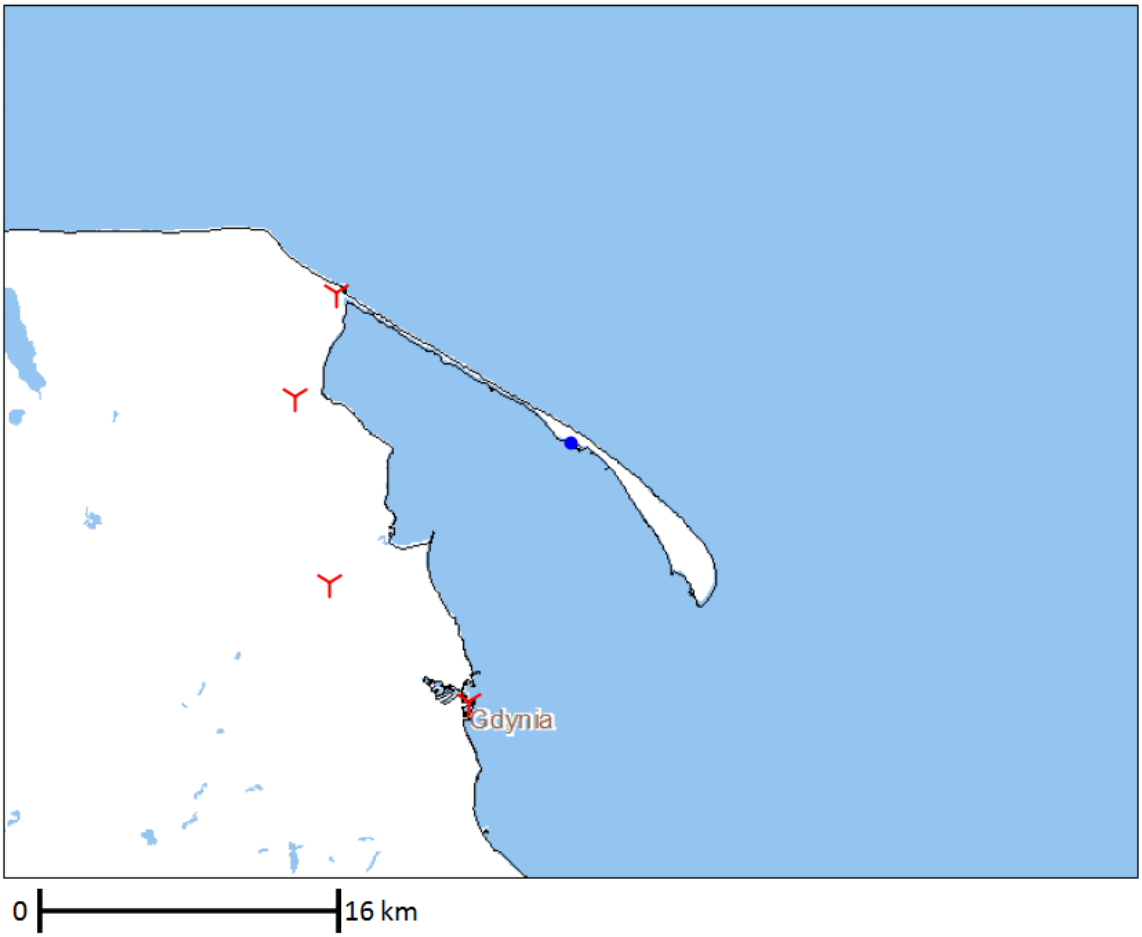

Figure 5-1: Geometry of the reference stations' location for long term static analysis

The location calculations were made using the software developed as part of the R-Mode Baltic project, which is still being improved with new functionalities. The calculation method is described in detail in the design documentation [1-3, 1-4]. It includes the determination of the clock bias value of the receiving terminal and its compensation. The position was determined for the range measurements without subtracting the mean error for each day.

5.1 Comparison of the positioning accuracy depending on RMS changes with the measurement time (day/night)

As described in Chapter 3, there were two measurement campaigns: summer and autumn. The summer campaign was carried out without breaks in measurements, therefore it is analysed in more detail in this chapter.

For each computed position, an error was determined representing the shift between the actual position of the receiver and the computed one. Positioning accuracy was assessed based on the RMS value of position errors.

Figure 5-2 shows the RMS positioning errors for each day of the summer measurement campaign. The positioning error values with the distribution geometry used are similar to the distance measurement errors.

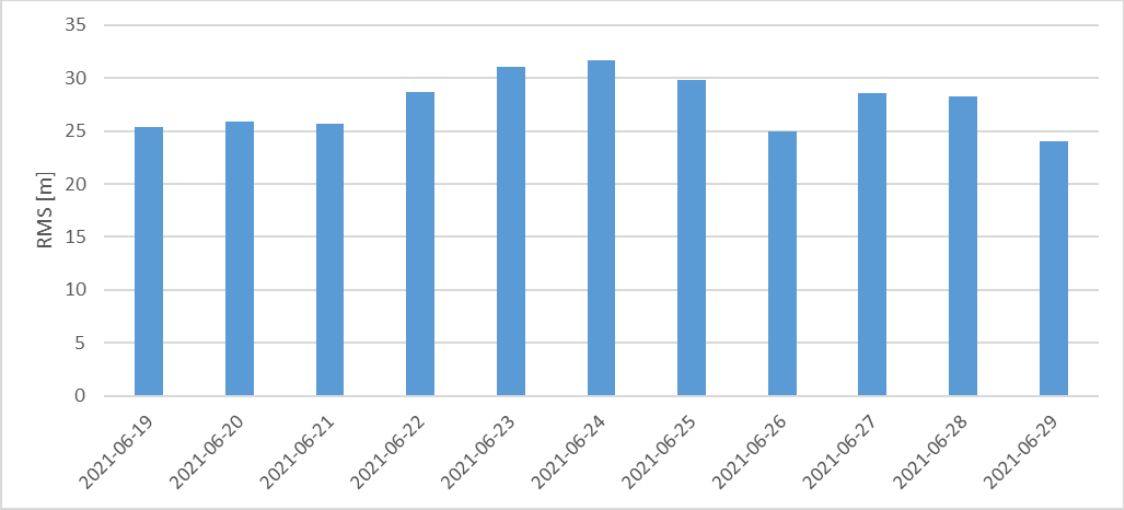

Figure 5-2: Summer campaign – RMS positioning errors for each day

Figure 5-3 shows the RMS positioning errors for each measurement day during the summer and autumn measurement campaigns. A significant increase of the RMS values is visible in the second half of this graph, it results from much larger errors in range measurements obtained in the autumn.

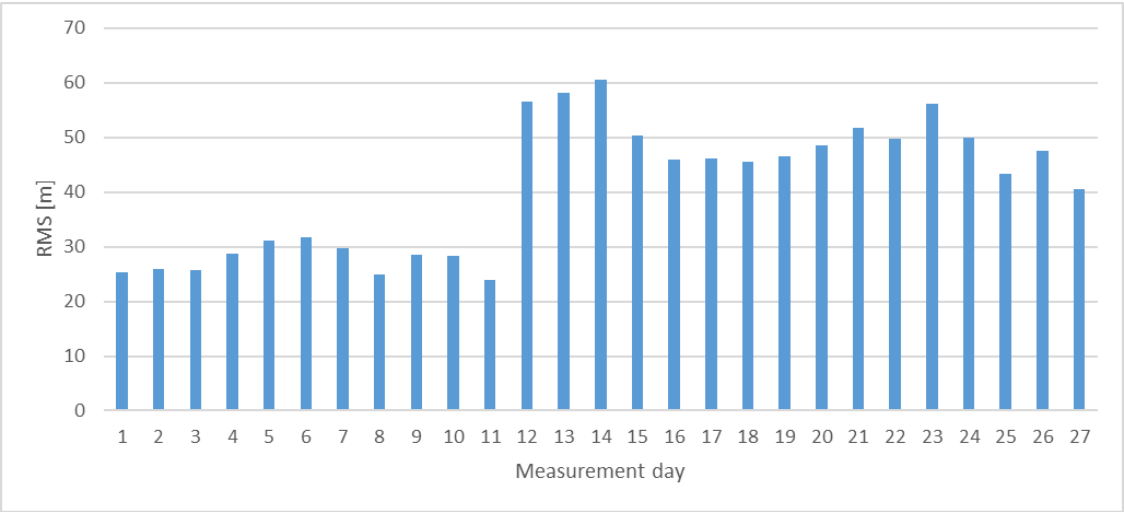

Figure 5-3: Summer and autumn campaign – RMS positioning errors for each day

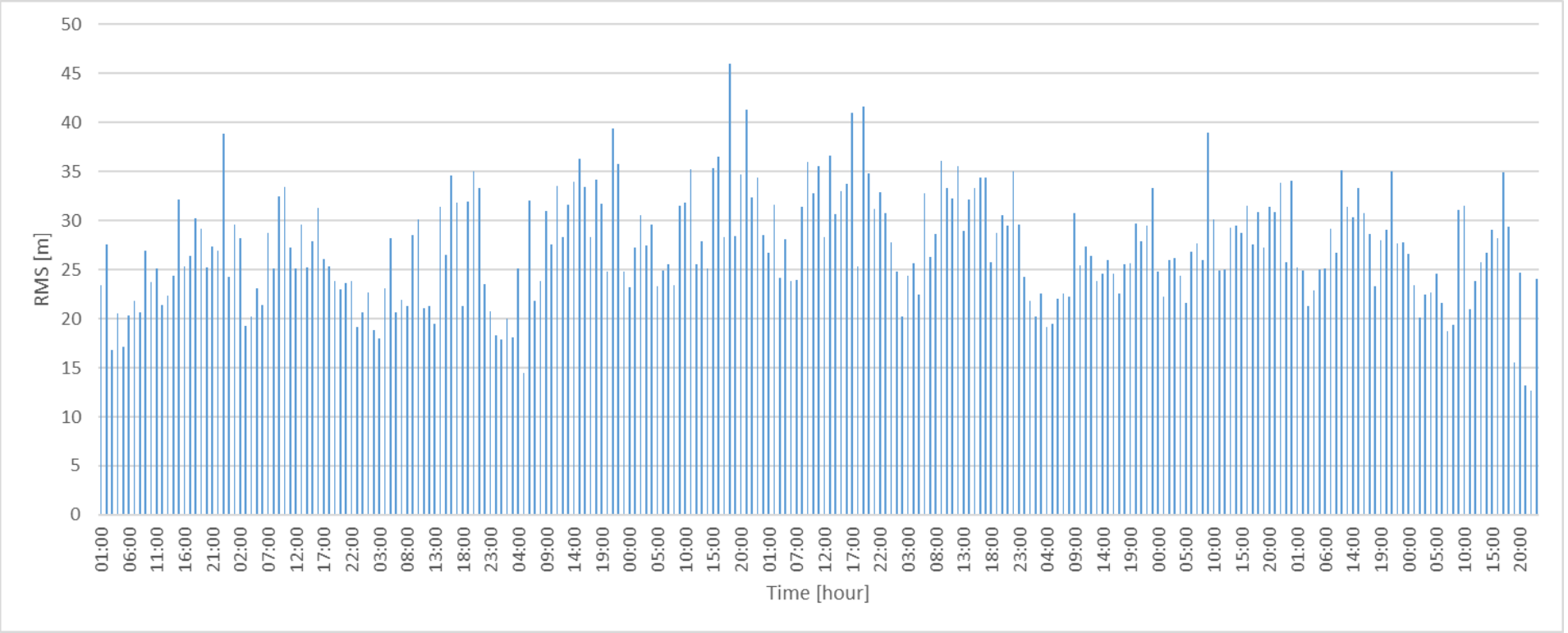

Figure 5-4: Summer campaign – RMS positioning errors for each hour

Figure 5-4 shows the RMS values for each hour of the summer measurement campaign. There is a certain periodicity in the chart - positioning errors at night are lower than during the day.

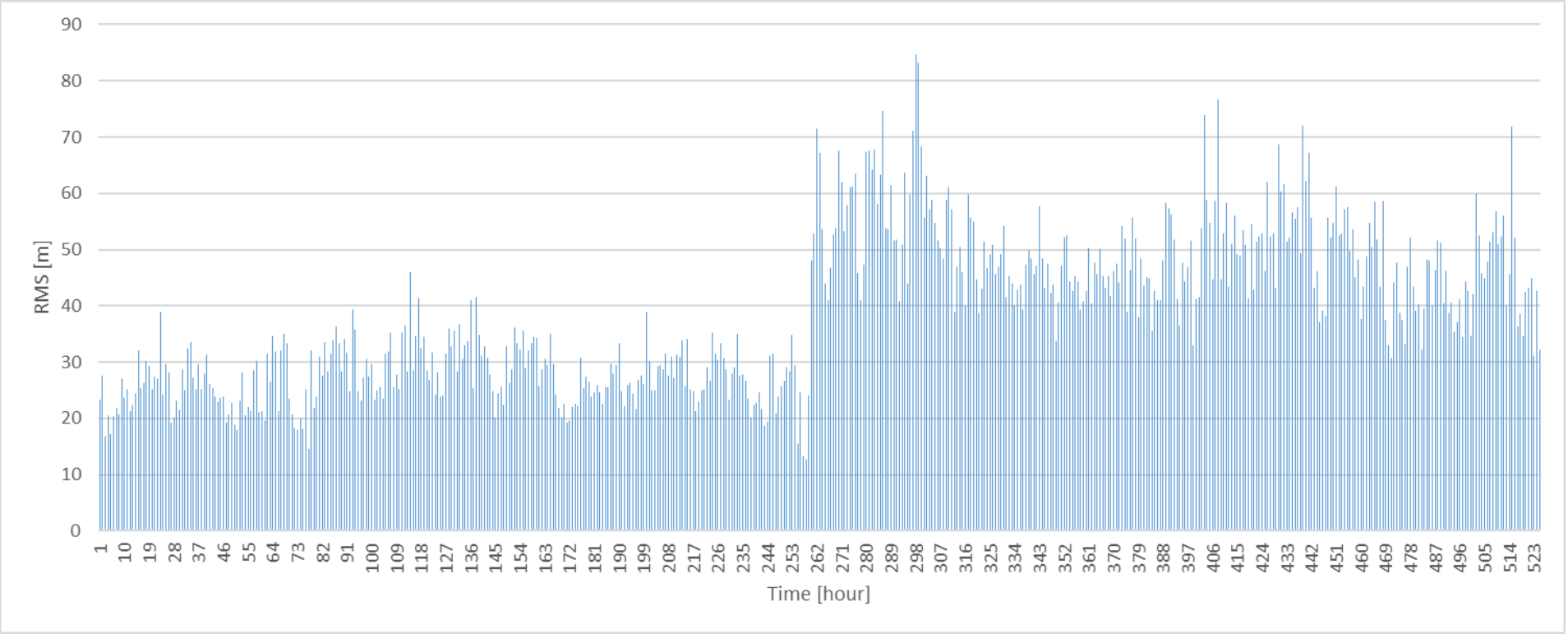

Figure 5-5: Summer and autumn campaign – RMS positioning errors for each hour

Figure 5-5 contains an hourly RMS chart for the data obtained from both measurement campaigns. The autumn results are burdened with a clearly higher positioning errors than those observed in the summer. The periodicity of the values obtained is less visible, but still noticeable.

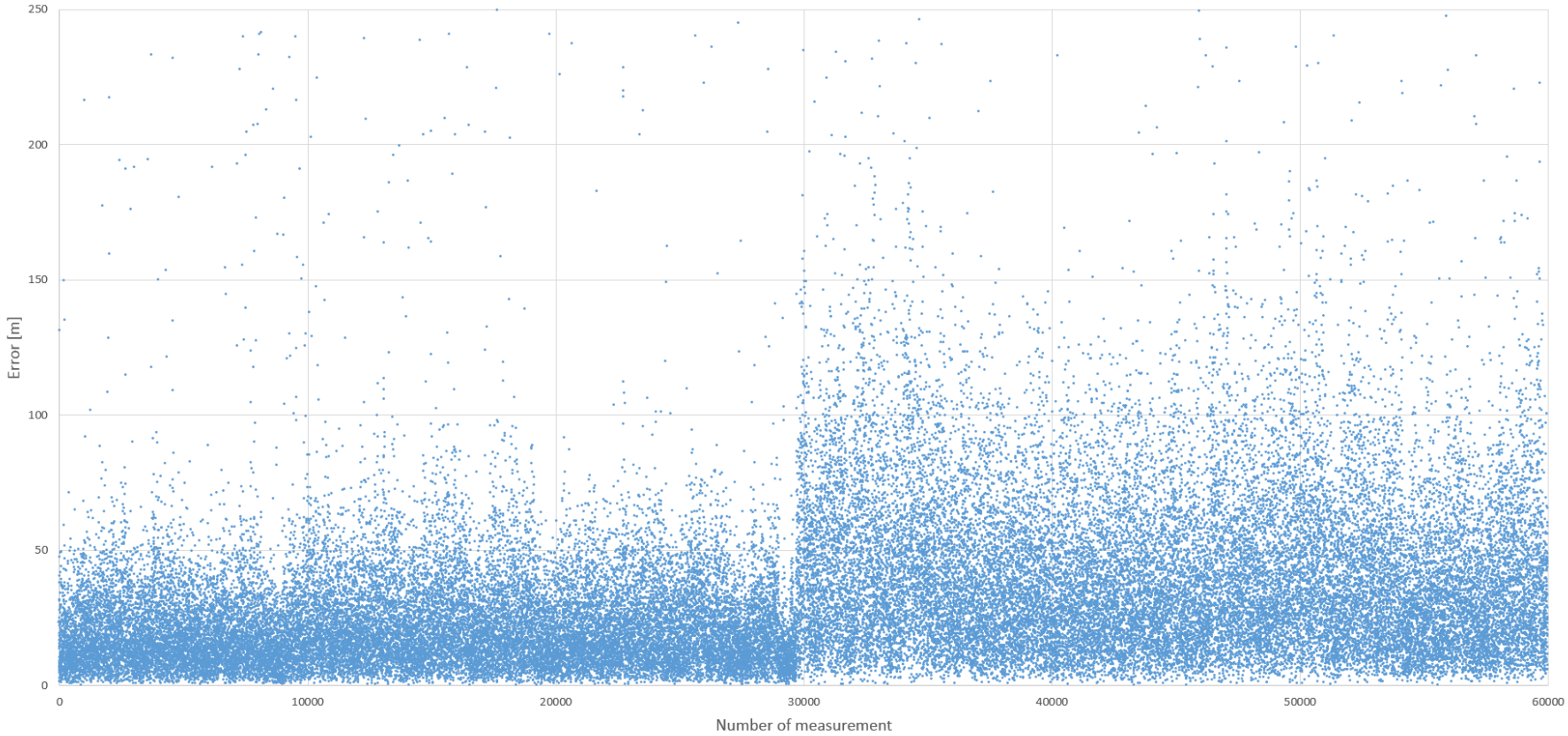

Figure 5-6: Summer and autumn campaign – positioning errors

Figure 5-6 shows the distribution of positioning errors obtained on the basis of both measurement campaigns. Gross errors were not included in the chart.

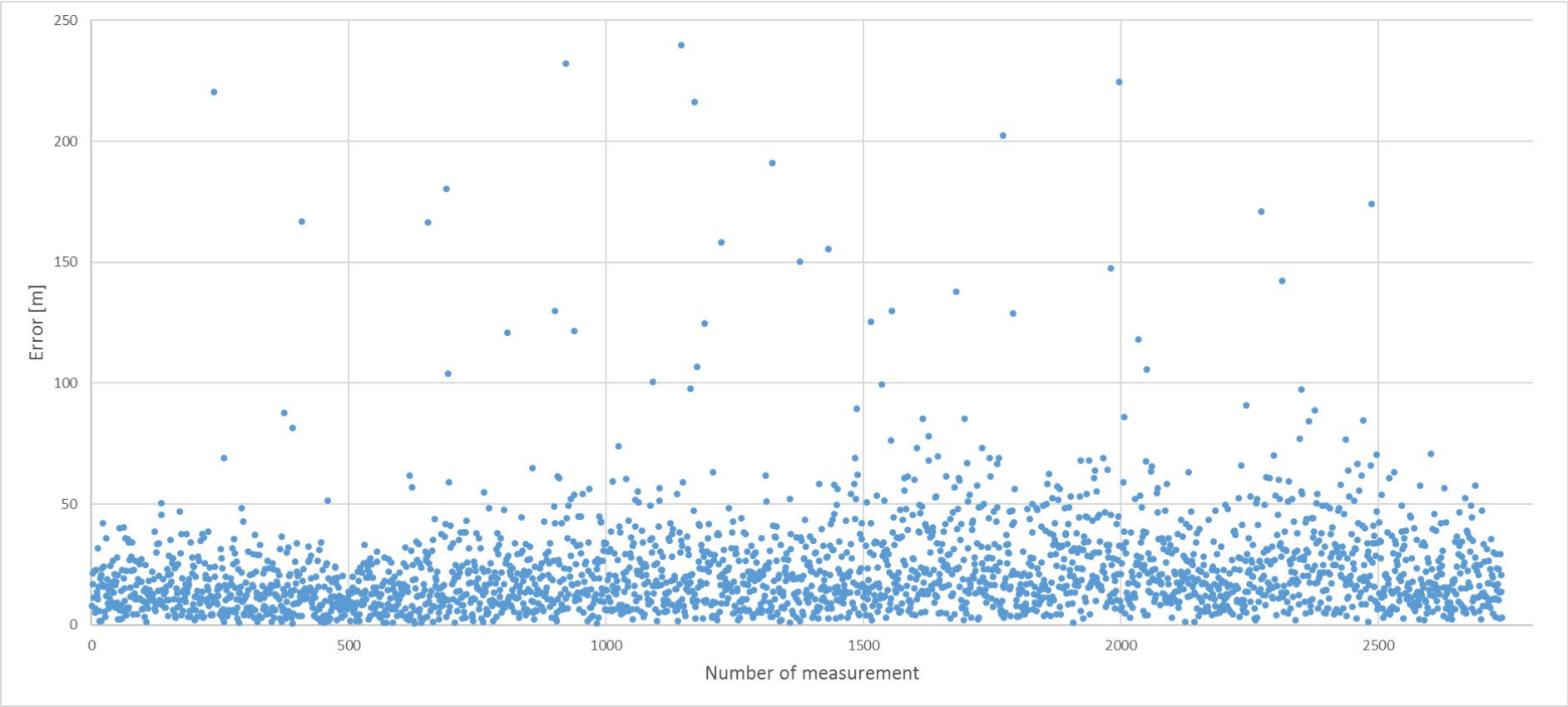

Figure 5-7: Positioning errors observed on 22.06.2021

Figure 5-7 shows the distribution of positioning errors obtained on 22.06.2021. Most errors are less than 50 meters.

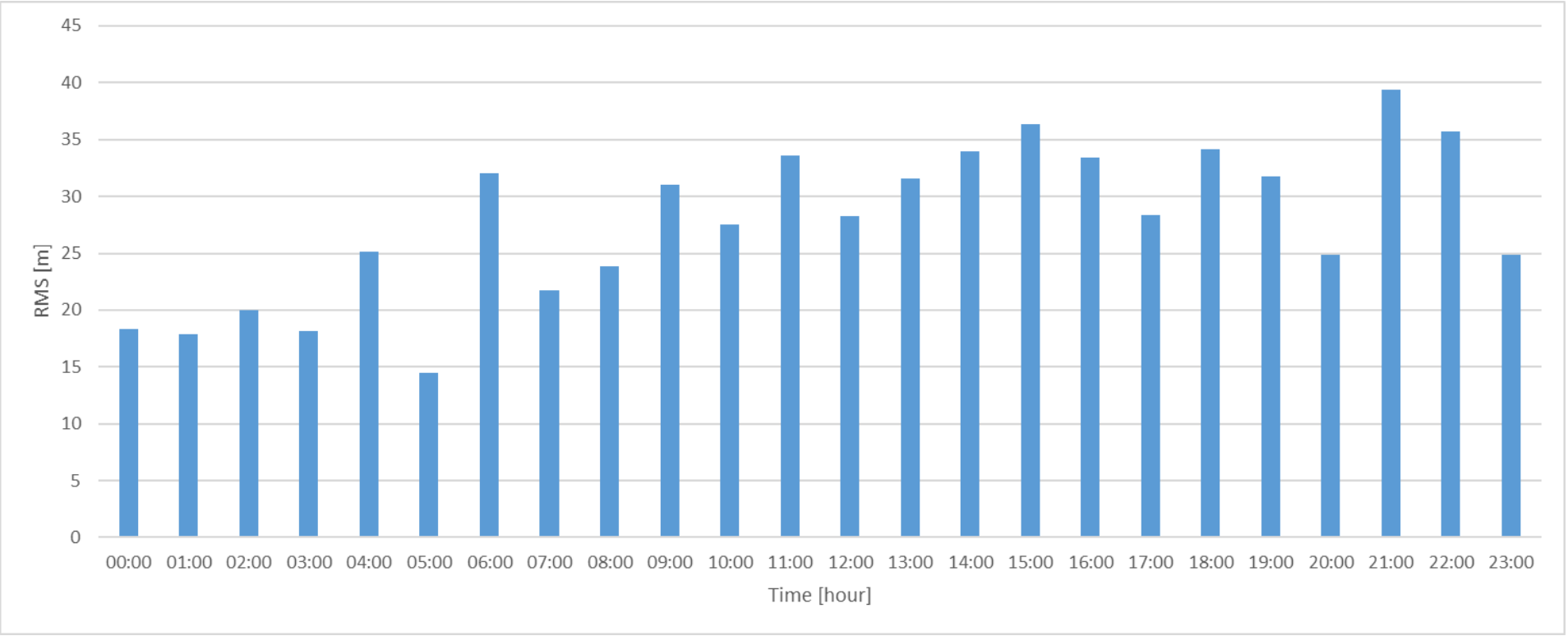

Figure 5-8: Measurements on 22.06.2021 - RMS positioning errors for each hour

The figures 5-8, 5-9 and 5-10 show the RMS values of the positioning error for each hour of measurements on: June 22, 2021, June 24, 2021 and June 27, 2021, respectively. It has been observed that during the night hours, especially between midnight and 8 am, the error values are slightly lower. This is in line with the observations discussed in section 4.1.

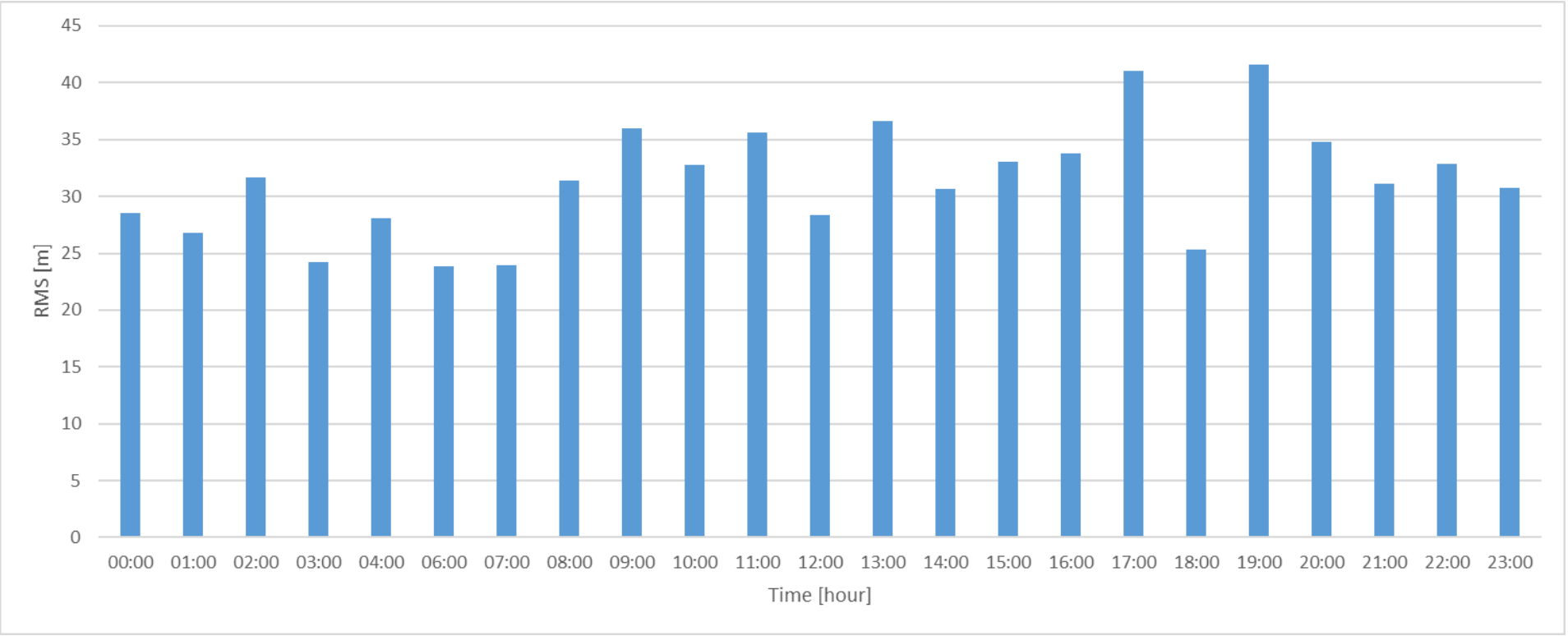

Figure 5-9: Measurements on 22.06.2021 - RMS positioning errors for each hour

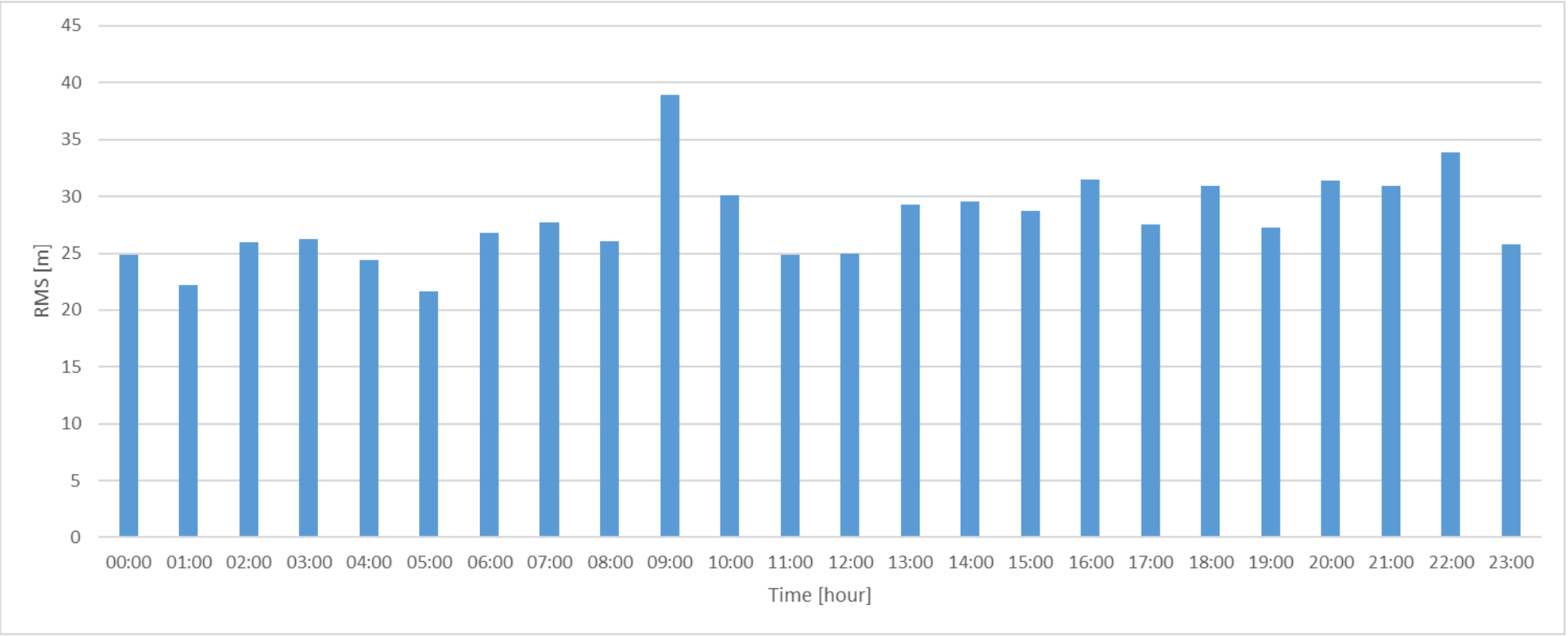

Figure 5-10: Measurements on 22.06.2021 - RMS positioning errors for each hour

5.2 Fluctuations of positioning accuracy and fluctuations of the range measurement accuracy due to weather conditions

Chapter 4.3 includes an extensive analysis of the dependence of the range measurement errors' RMS values on the prevailing meteorological conditions. It was shown that the most important meteorological factor influencing the accuracy of distance measurement is precipitation. Figure 5-11 shows the RMS values of positioning errors for each day and the respective sum of rainfall.

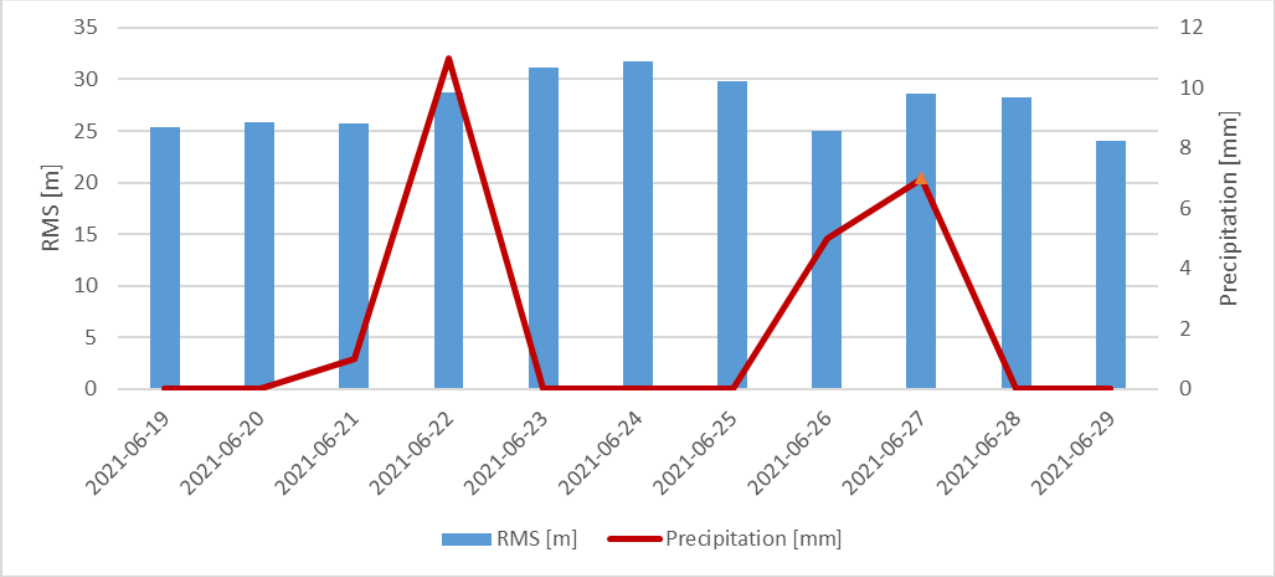

Figure 5-11: Summer campaign – RMS positioning errors for each day and the precipitation data

The dependence of the RMS value of positioning errors on the occurrence of rainfall is lower than in the case of range measurements. This may be due to the partial compensation of errors due to the fairly good reference stations geometry in relation to the receiving terminal.

5.3 Comparison of the positioning accuracy for various correlators

The positioning accuracy was analyzed for different correlation methods of the received reference signal during the range measurement. The correlators used will be discussed in more detail in an article to be published in the coming months. Only the results of the positioning results are presented below.
Three scenarios were implemented, the geometry of which is shown in Figure 5-12.

a)

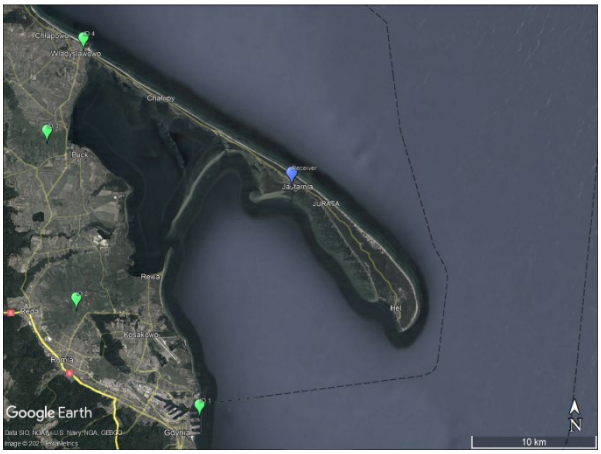

b)

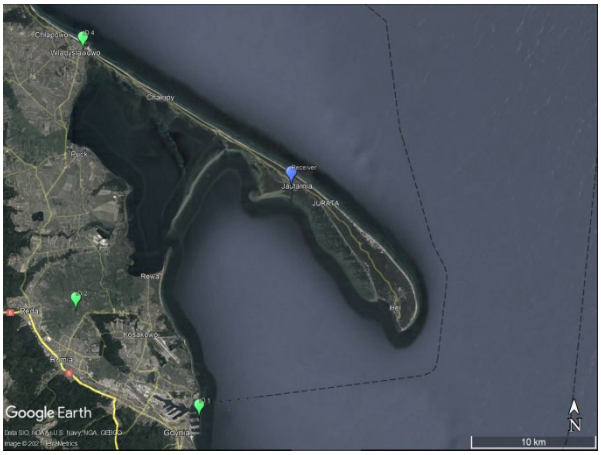

c)

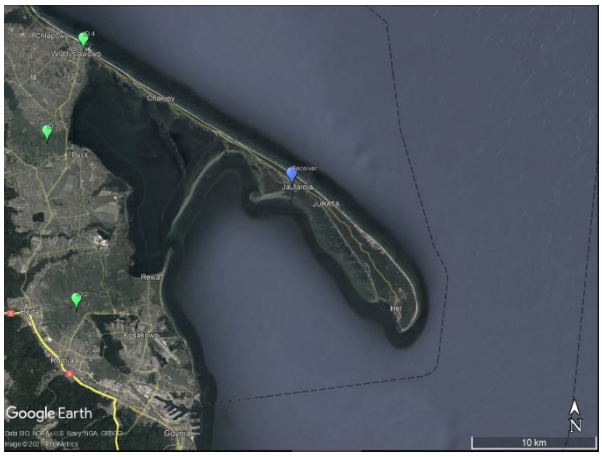

Figure 5-12: The geometry of reference stations distribution in the scenarios: a) scenario 1 – four stations and good geometry HDOP=3.39; b) scenario 2 - three stations and good geometry HDOP=3.73; c) scenario 3 - three stations and poor geometry HDOP=9.20

For the above scenarios 1, 2 and 3, the positioning results are presented in figures 5-13, 5-14 and 5-15, respectively.

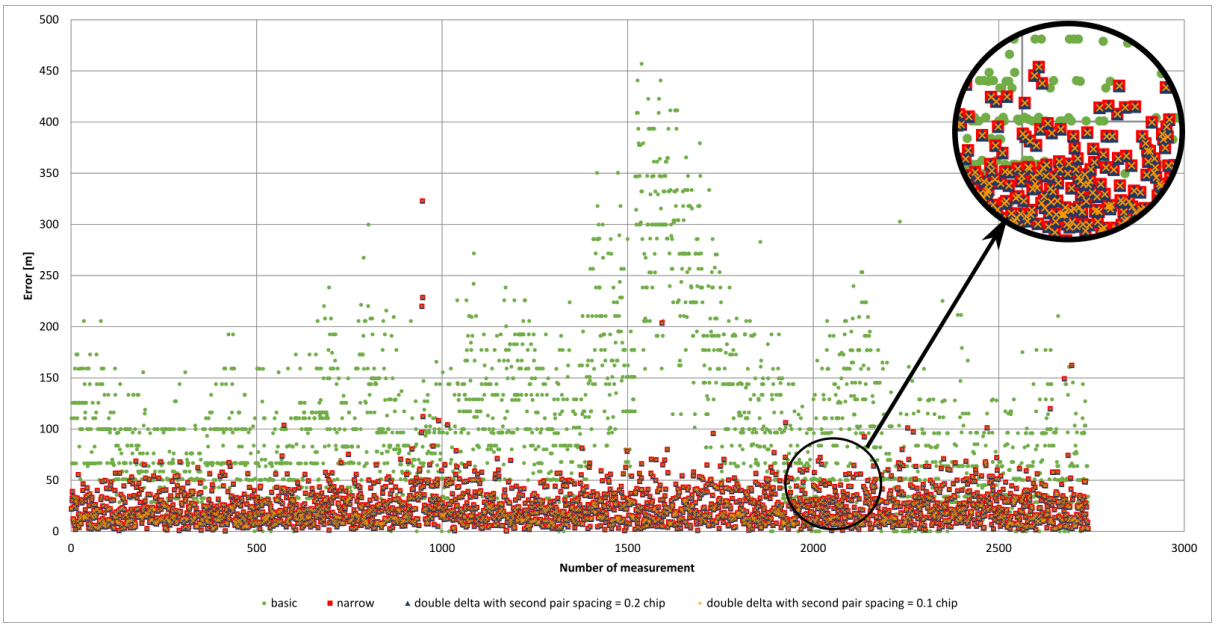

Figure 5-13: Scenario 1 - TOA positioning error for: basic correlator (green), narrow correlator (red), double delta correlator with second pair spacing = 0.1 chip (blue) and double delta correlator with second pair spacing = 0.2 chip (orange).

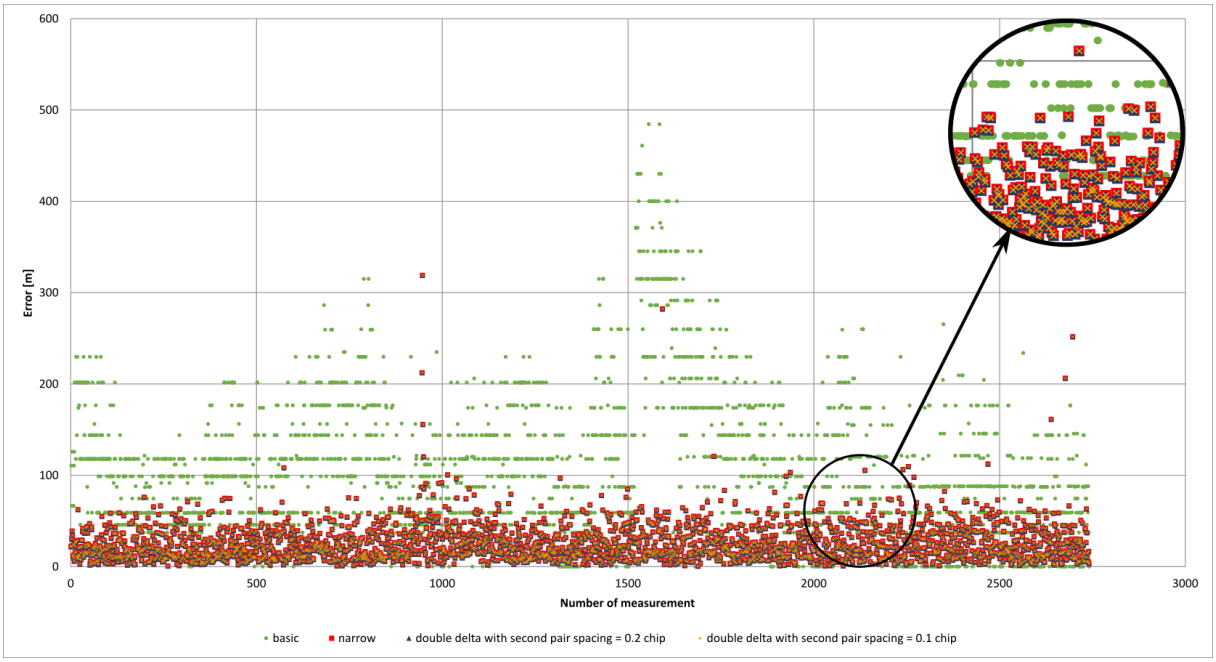

Figure 5-14: Scenario 2 - TOA positioning error for: basic correlator (green), narrow correlator (red), double delta correlator with second pair spacing = 0.1 chip (blue) and double delta correlator with second pair spacing = 0.2 chip (orange).

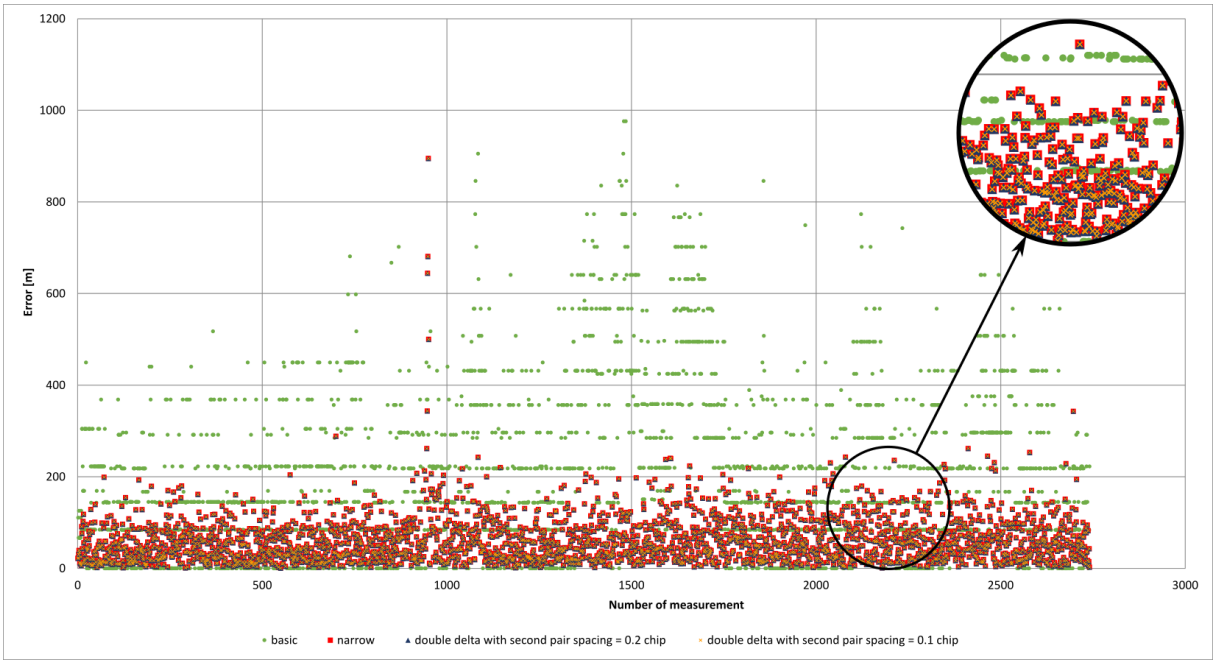

Figure 5-15: Scenario 3 - TOA positioning error for: basic correlator (green), narrow correlator (red), double delta correlator with second pair spacing = 0.1 chip (blue) and double delta correlator with second pair spacing = 0.2 chip (orange).

Among the used correlators, the basic correlator is characterized by the lowest accuracy. The accuracy of the other three correlators is at a similar level. Based on the research, it was decided to use one of them in the project.

To a large extent, the positioning accuracy also depends on the number of reference stations and the geometry of their arrangement. Attention should be paid to the error values: in scenarios 1 and 2, despite the use of four or three reference stations, respectively, the positioning accuracy remains at a similar level. The resulting RMS value of positioning errors in these scenarios differs only by about 3 meters. In the case of scenario 3, using three reference stations but with poor geometry, the obtained positioning errors are more than twice as high.

6 Real-time positioning demonstrator application

One of the tasks in the project was to develop a real-time positioning demonstrator. The aim was to ensure the possibility of ongoing observation of the determined position accuracy during dynamic measurements at sea.

6.1 Description of the software

The application provides the ability to observe the current location on the map. Reference stations are marked in red. Four points are marked for each measurement:

- position from GNSS (reference),
- position calculated on the basis of R-Mode measurements,
- position calculated on the basis of R-Mode measurements and subjected to Kalman filtration,
- position calculated from R-Mode measurements and then subjected to Kalman filtering using INS data.

In the upper left part of the application window, the exact coordinates of the above points and information about the error of the determined position (in relation to the position known from the GNSS system) are displayed. Moreover, for a position calculated only on the basis of the R-Mode data, the calculated ship clock bias value and DOP coefficients are provided. For items subjected to Kalman filtration, information about the calculated speed and course are also displayed. The lower left part of the application window is intended for the presentation of the positioning errors over time. Figure 6-1 shows the division of the demonstrator application window.

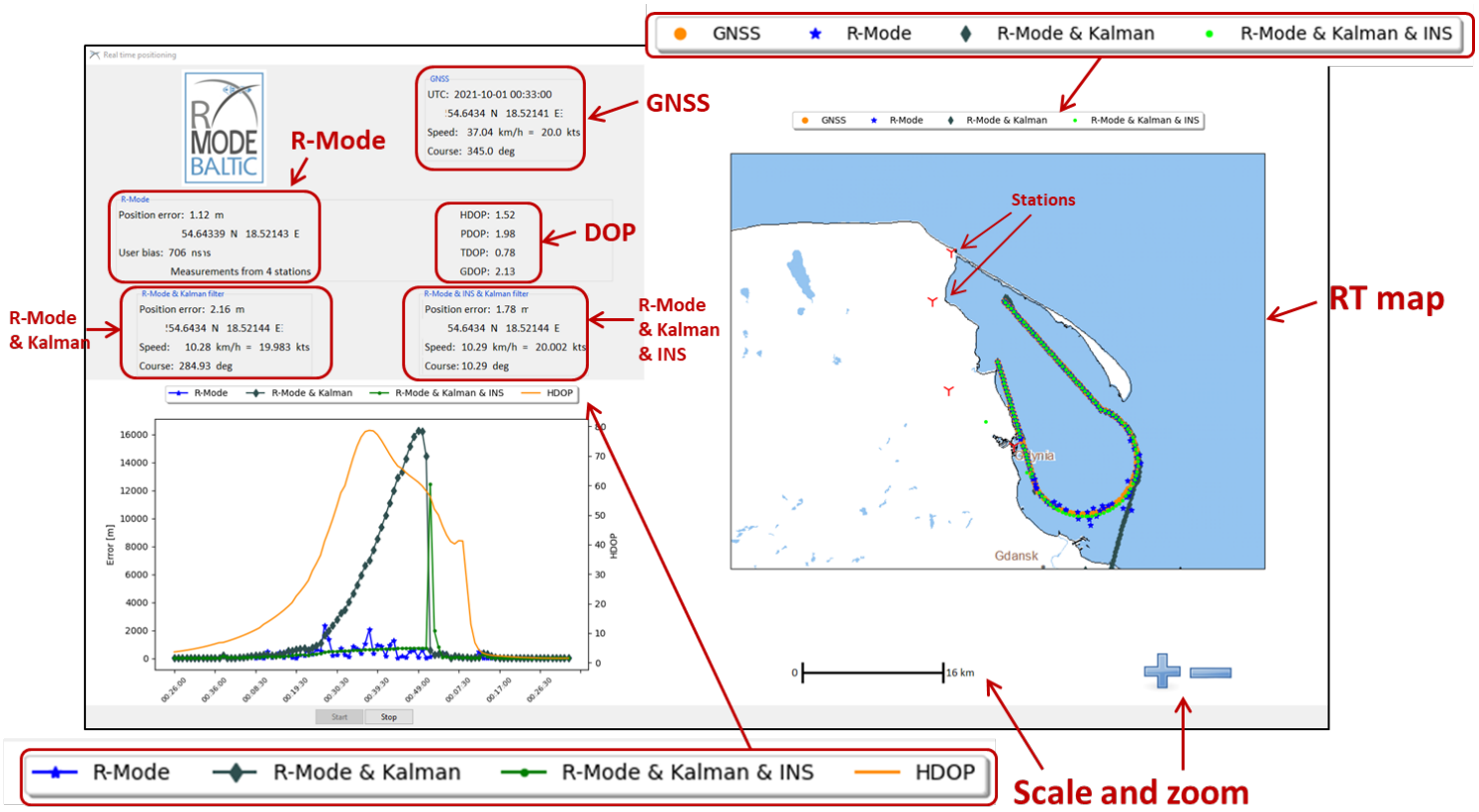

Figure 6-1: Real-time positioning demonstrator application window

6.2 Range measurement emulation

As part of the R-Mode Baltic 2 project, an emulator of range measurements was implemented. It was created on the basis of the research carried out in the previous part of the project [1-4, 1-5]. The emulator implementation was necessary for two reasons. The first goal was to conduct functional tests of the real time application, eliminate the bugs and improve its operation. The second goal was to test dynamic scenarios, which will be described in subsection 6.3.

In figure 6-2, the main window of the measurements emulator is presented. It enables the definition of dynamic scenarios with any number of reference stations, straight or circular motion, with a given ship speed and measurement frequency. Each station has defined, among others, its exact location, type of internal oscillator, power of the transmitted signal, which is shown in the figure 6-3 (station edition window)

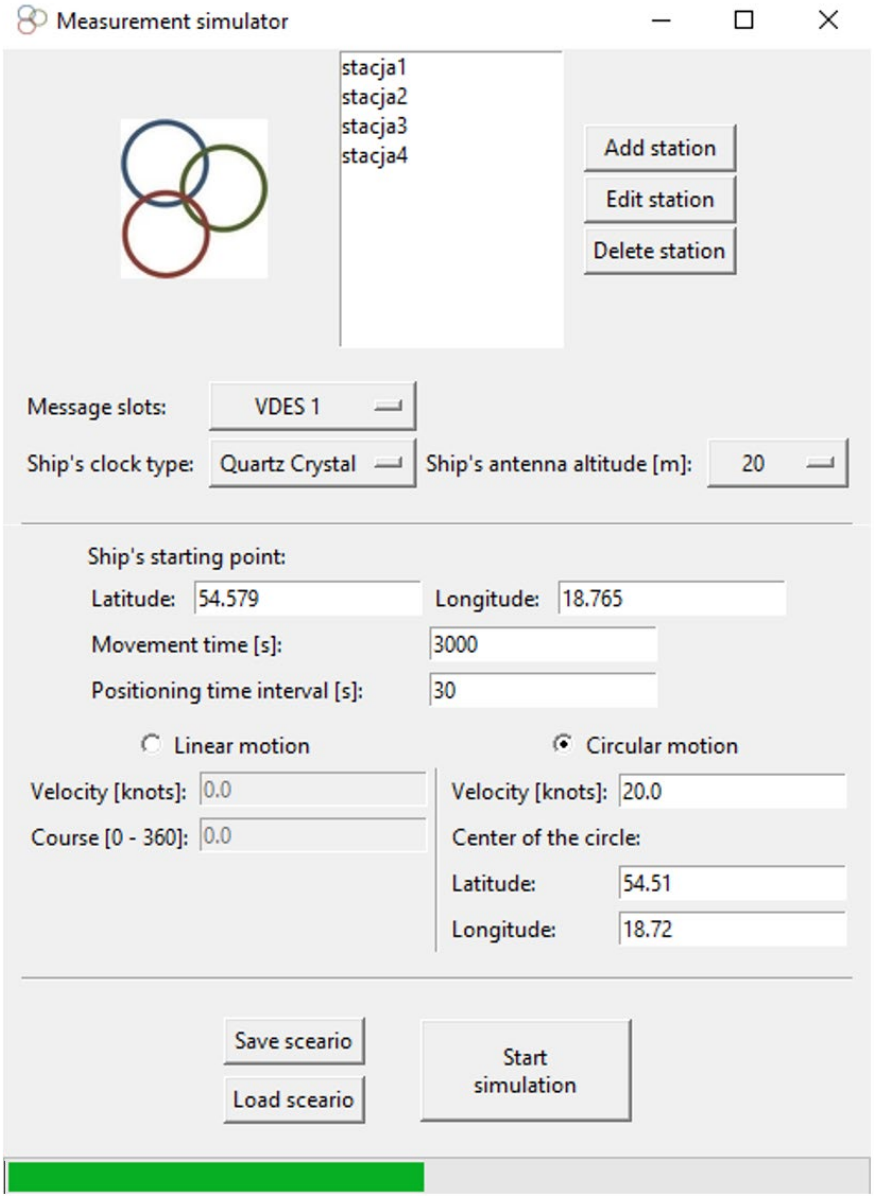

Figure 6-2: Range measurements emulator window

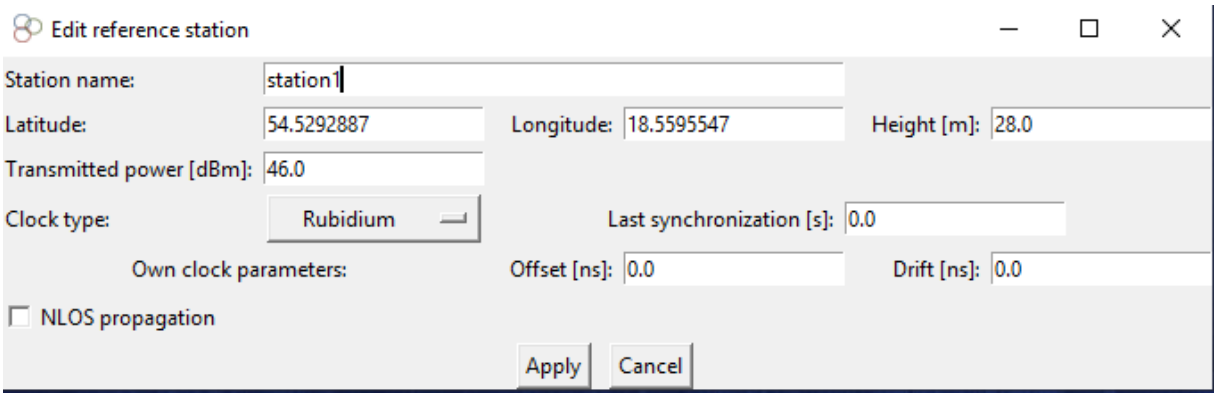

Figure 6-3: Station edit window

Based on the given parameters of the scenario, an output file is generated with the structure of the input file of the demonstrator application. The measurement results are emulated on the basis of the location data of each reference station and the location of the receiving terminal on the ship in accordance with its trajectory. Importantly, the followingerror models are included:

- propagation of the reference signal (SNR decrease with distance),
- errors of reference station clocks (drift and offset),
- receiving terminal clock errors (drift and offset).

6.3 Analysis of dynamic scenarios

During the R-Mode Baltic 2 project duration, only one real VDES R-Mode station in Gdynia was operational, built by the Institute of Telecommunications. Therefore, it was not possible to perform actual dynamic tests of the R Mode system. The evaluation of the system operation in dynamic scenarios was carried out on the basis of software emulation of measurement results, taking into account the models of distance measurement errors.

6.3.1 Line scenario with disappearing reference signal

The scenario was designed in a straight line for a ship moving away from the shore. As the unit fades away, the geometry of its location in relation to the reference stations changes. In addition, the signal fading successively from one and then from two reference stations has been added. As a result, over the distance, the position is calculated on the basis of signals from only two stations. The signals from these stations are then available again.

Figure 6-4 shows the route of the scenario - the ship moves away from the shore, which results in a change of geometry in relation to the reference stations and a decrease in the SNR of the received reference signals.

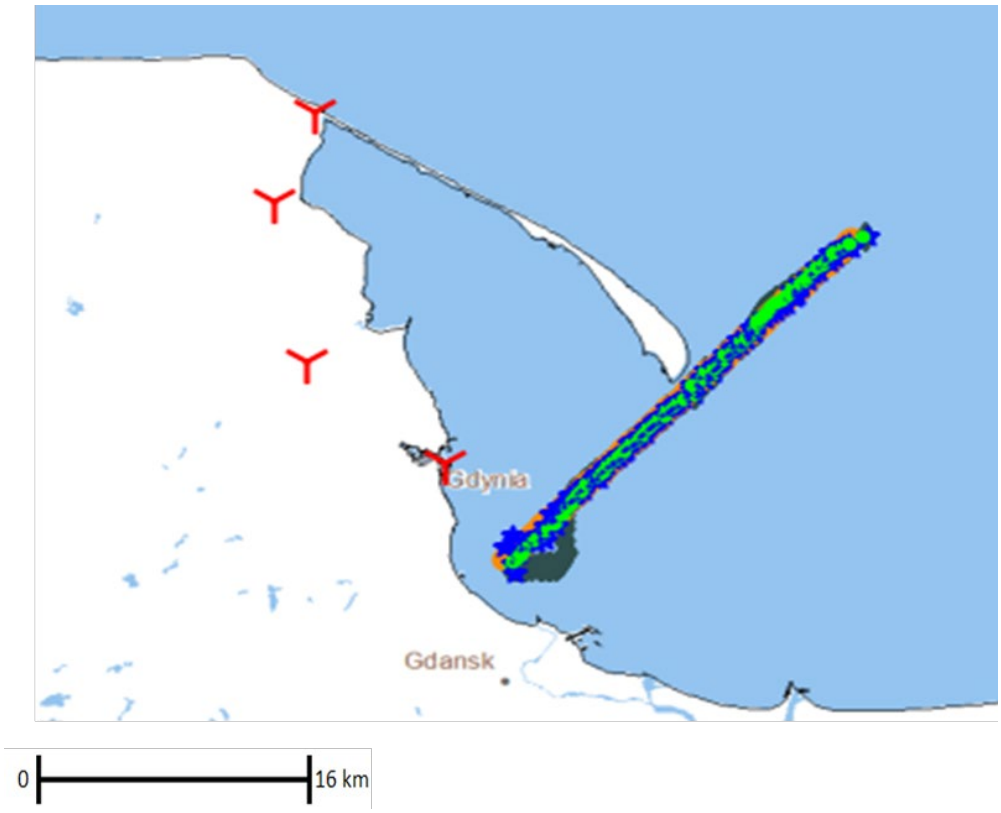

Figure 6-4: Line scenario with disappearing reference signal

Figure 6-5 shows the changes in positioning errors during unit movement, the change in geometry (HDOP) and the change in the availability of the number of reference stations. When analysing the position error values calculated only on the basis of R-Mode measurements, one can observe:

- In the case of poor geometry (large HDOP), it is possible to determine the position with an error of several dozen to several hundred meters,
- In the case of satisfactory geometry and good signal quality (SNR), the accuracy of the calculated position is much higher, even several meters,
- It is possible to calculate the position with only two reference signals available. It is associated with a positioning accuracy decrease because it is then impossible to determine the bias of the ship's clock,
- In the case of good geometry, but with poor quality (SNR) of the reference signal, which results from moving away from the station, the positioning error increases significantly,
- Kalman filter requires tuning based on actual measurement results (planned in the next stage),
- Kalman filter with INS data allows to obtain significantly more accurate positioning results.

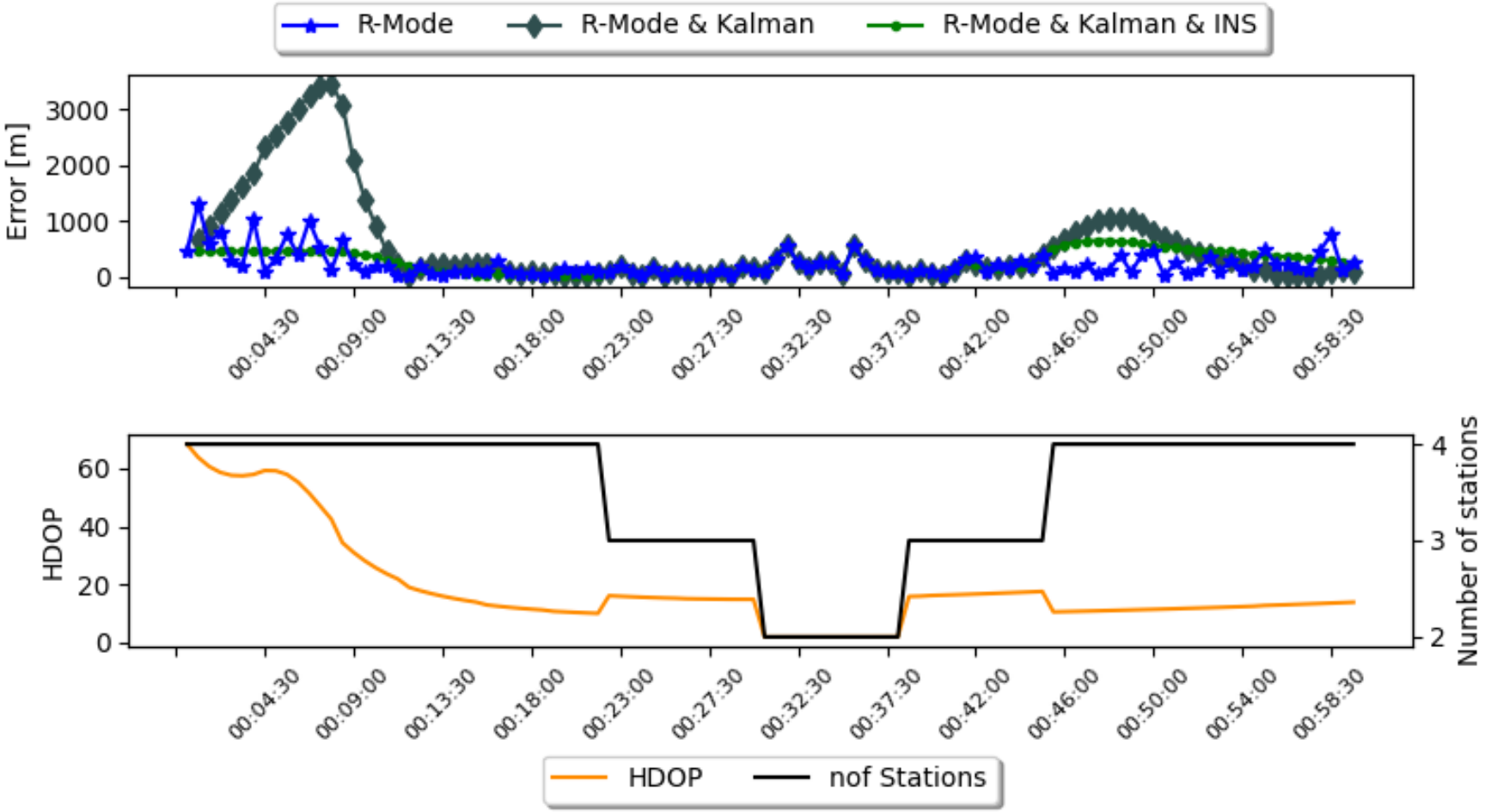

Figure 6-5: Line scenario positioning errors, geometry (HDOP) and number of available reference signals

6.3.2 Non-line scenario with HDOP changing

The scenario consists of three stages of the ship's movement: in a straight line, in a circle, and in a straight line along the coast. The course of the route is shown in Figure 6-6. For this scenario, there were four reference signals available at all times, while the movement changed the geometry - from very good to very poor and back to very good.

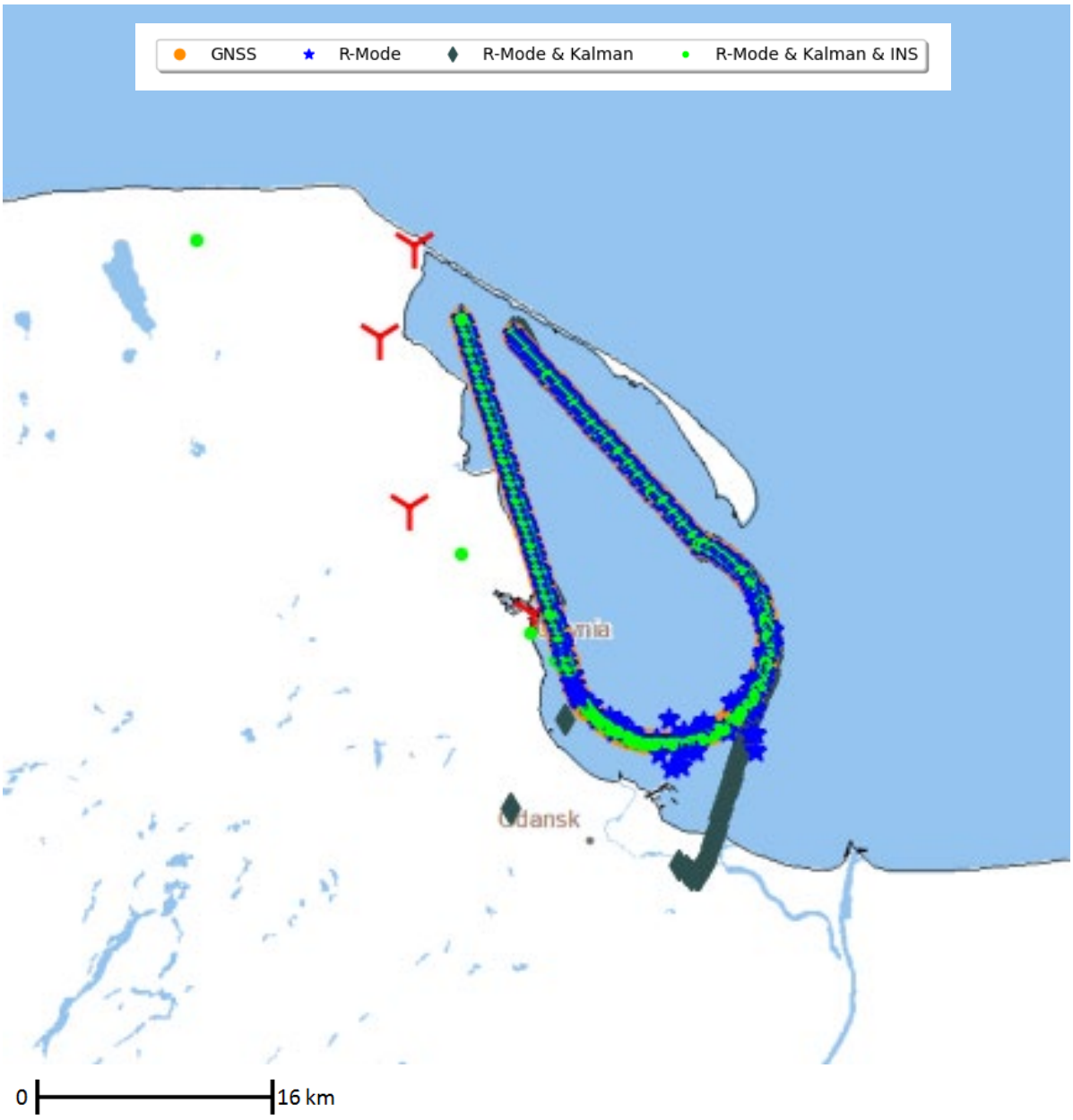

Figure 6-6: Non-line scenario with HDOP changing

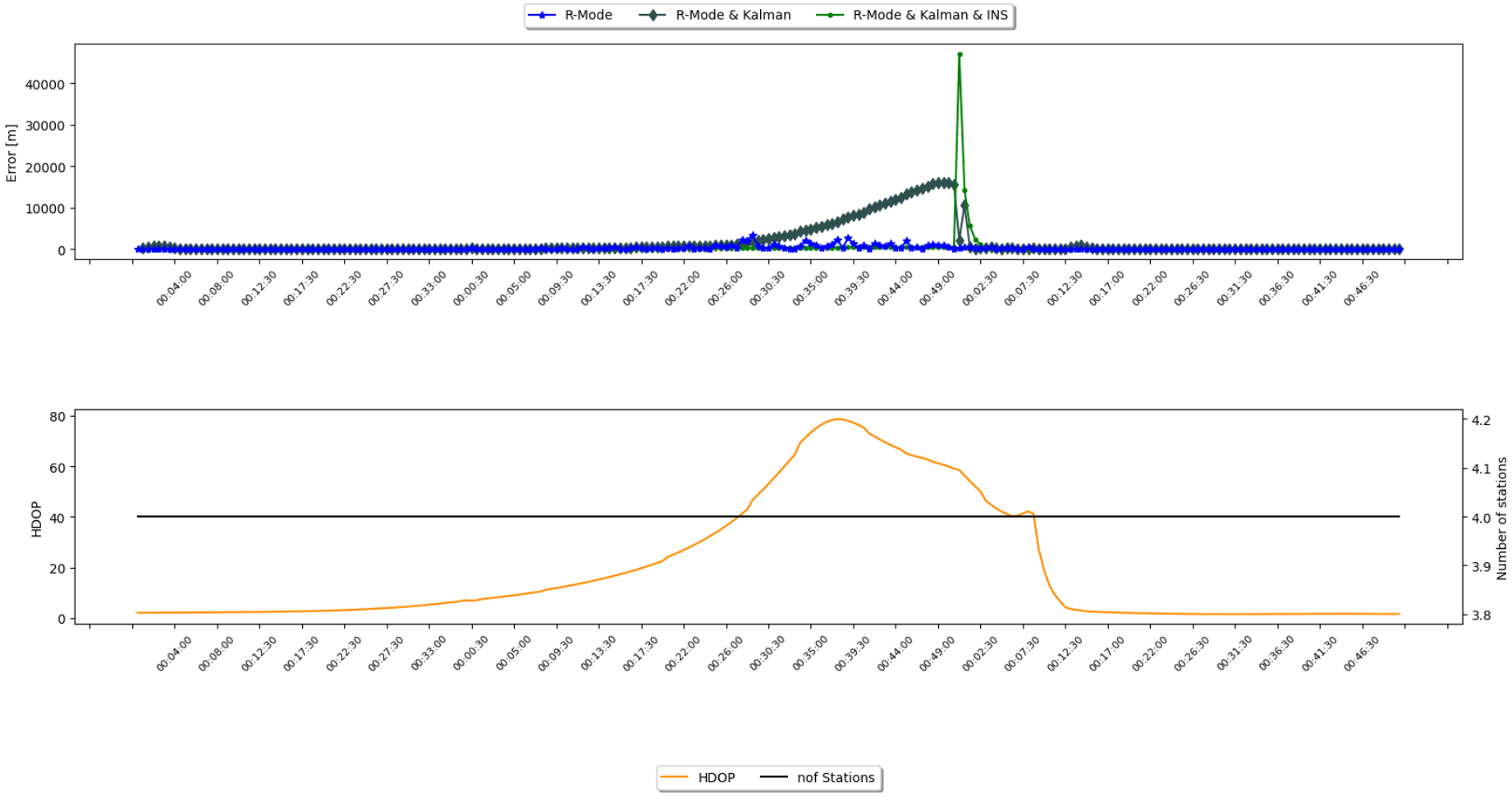

Figure 6-7: Non-line scenario positioning errors and geometry (HDOP)

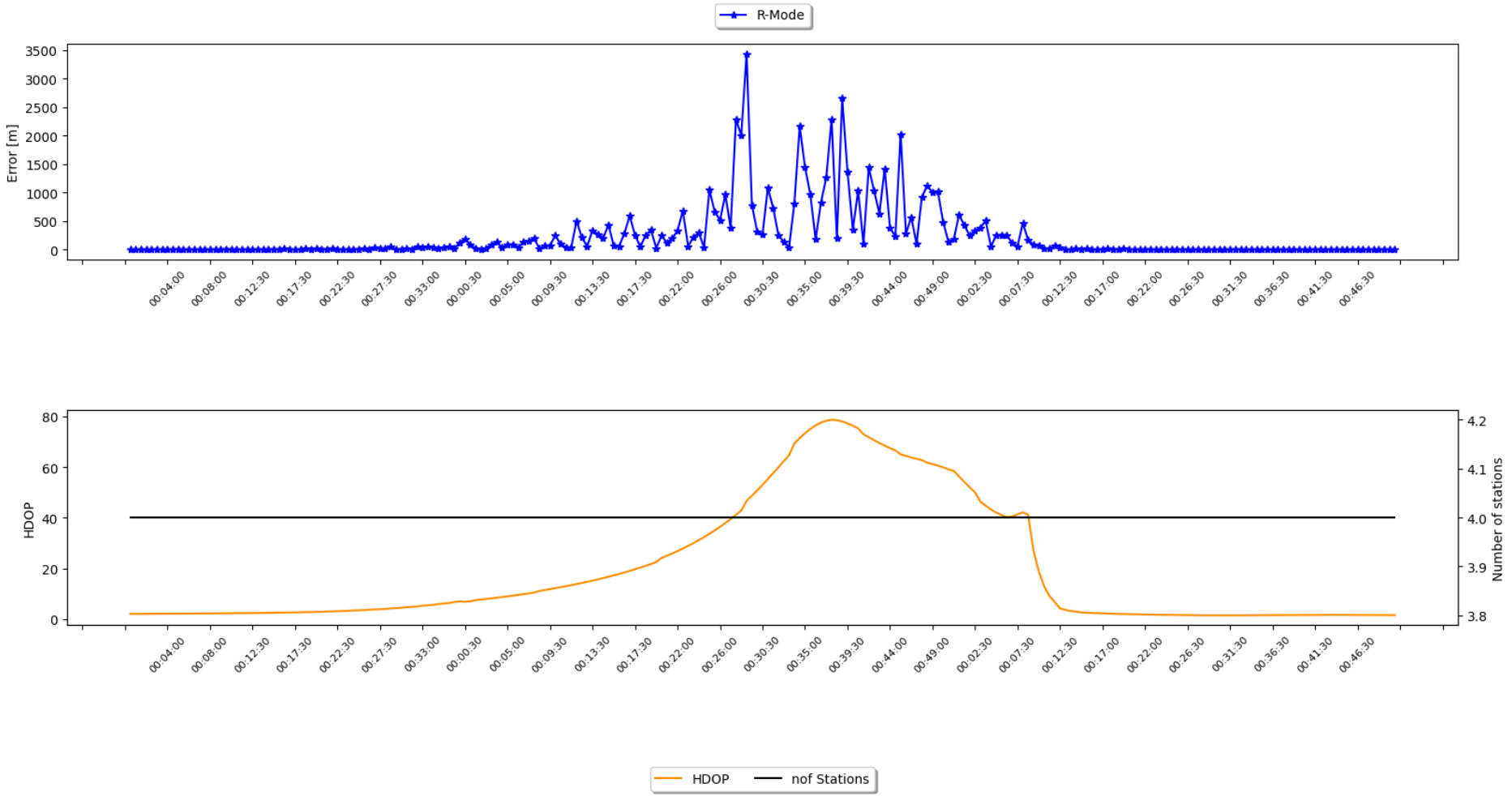

Figure 6-8: Non-line scenario R-Mode ranging positioning errors and geometry (HDOP)

Figure 6-7 shows the changes in the positioning errors while the vessel is moving and the simultaneous changes in the HDOP coefficient. A strong increase of the position error determined with the use of the Kalman filter indicates the necessity to tune this filter based on the actual results of a dynamic measurement campaign.

Figure 6-8 shows the positioning error values based only on R-Mode measurements. In the case of extremely poor geometry of the reference stations location and the receiving terminal - located almost in a straight line, the positioning error could reach 3.5 km. In areas with good geometry, the error value dropped to just several meters.

7 Summary and conclusions for the next measurement campaign

During the R-Mode Baltic 2 project, it was possible to create a fully functional system for a long-term, real-time position monitoring. This system allows to determine the receiver's position on the basis of static and dynamic measurements. The conducted measurement campaign, which took place in summer and autumn 2021, confirmed the effectiveness of such a system.

As previously described, at the beginning of the R-Mode Baltic 2 project, the initial task was to find the receiver's location for the purpose of static measurements. On the basis of the conducted analyzes, Jastarnia was identified as the target location. Based on this selection, radio planning was carried out, which allowed to determine detailed technical parameters on the transmitting and receiving side of the positioning monitoring system during the R-Mode Baltic 2 project.

During the conducted research, the focus was on the analysis of the obtained RMS errors between the determined pseudo-ranges from the VDES R-Mode positioning monitoring and the reference distance determined by the GNSS receiver. This approach allowed for the observation of the determined distance fluctuations over time and the analysis of the source of the distance errors.

In the measurement campaign, it was possible to collect data from approximately 474 hours, which translated into approximately 24 measurement days in which the samples were recorded. For the measurements carried out in the summer, the average RMS was 20.49 meters. It should be noted though that for some hours, the mean error was approximately 7.38 meters. The good news is that the RMS average for the hourly average error reset did not exceed the maximum value of 30 meters. The error had a tendency to go up on measurement days with rainfall. Such conditions also contributed to the observation of the phenomenon of tropospheric ducts, which was particularly visible in the graphs where the mean error was only reset at the beginning of the measurement campaign. The lack of accumulation of the average error was also a confirmation of the correct installation of the positioning monitoring system (on both the transmitting and receiving sides). Unfortunately, due to problems with the power amplifier, the summer measurement campaign had to be interrupted and resumed only in the fall. The autumn results are much worse compared to the summer measurements. In this case, the mean RMS of the distance was 43.22 meters and the maximum RMS value for the daily average error subtraction of the measurements reached 62.42 meters. These results were also correlated with the meteorological analysis, which, however, did not provide unambiguous conclusions. During the autumn measurement period, no weather anomalies occurred that would have contributed to such a discrepancy in the RMS error compared to the summer period. Long-term static measurements lasting several months would surely answer all the questions in that respect. Ultimately, however, thanks to the R-Mode Baltic 2 project, it was possible to create a positioning system that will be used in future measurement campaigns.

The obtained results and the created software are already being considered for future use. Discussions are underway on the continuation of the R-Mode project. On February 25, 2022 a meeting on "Project idea: Operational R-Mode System for Robust Maritime Traffic and New Maritime Applications" was organized under the chairmanship of Stefan Gewies (DLR). Our team from the National Institute of Telecommunications proposed the following tasks that could be included in the continuation of the project:

a) VDES R-Mode dynamic and static „long-term" positioning measurements:

- monitoring of the static accuracy of the ranging and position determined in the R-Mode system,
- collecting and analyzing long-term measurements,
- testbed at sea – dynamic positioning campaign at sea using real VDES R-Mode stations,
- VDES real-time demonstrator - further software development and tests of the Kalman Filter with inertial module for assessment of its potential future usage for R-mode,
- tracking positioning with temporary and periodic low station availability (just one or two R-Mode stations in range or even no station at all – predicted position).

b) Time and Frequency Transfer by use of Fiber Optic Cable [5-1]:

- potential utilization of the fiber-optic network and a cesium oscillator in cooperation with the Maritime Office in Gdynia,
- the verification of the possibility to transfer time and frequency from Gdynia to Jastarnia with a set time difference accuracy of <10 ns, with the elimination of the atomic standard in Jastarnia. This would require some sort of calibration actions, like using the GNSS carrier phase receiver or external reference clock, etc,
- distance/range measurements (accuracy, stability) on the Gdynia-Jastarnia route using VDES signals and a common time source - chance to compare stationary measurements using a cesium oscillator with measurements obtained for synchronization through a fiber optic solution. This would ensure a separation from the sources of time errors.

c) Sample applications for the R-Mode VDES system:

- Search and Rescue (SAR) service – application for supporting ongoing search and rescue operations. This service will improve the management of SAR units and will improve operations by distributing search areas and planned routes (designated by management) to individual SAR units participating in maritime operations.
- Maritime Safety Information (MSI) service – application for exchanging MSI messages between units. The information contained in the MSI may relate to potentially hazardous events in the Sea. For example, in the event of failure or unavailability of satellite navigation systems (global or local), the MSI distributor should send the message about GNSS outage with recommendation to use the R-Mode system for positioning.
- Nav Data service – a service for the distribution of navigation messages from the R-Mode system (such as reference data and time, Leap Second, R-Mode station parameters, including health status, clock offset, delay and clock uncertainty etc.) through VDES channel.

d) Develop real-time positioning application for hybrid receiver (VHF/MF):

- calculating the ship's position on the basis of the signal from MF and VHF reference stations simultaneously - this will enable the improvement of the accuracy of the determined position by increasing the number of reference stations and improving the geometry of their distribution,

- if the Project Partners shared models of the accuracy degradation for the distance measurement from MF reference stations along with the distance from these stations, it would be possible to conduct simulation tests to determine the impact of the use of a hybrid receiver on the improvement of positioning accuracy,
- if the project partners provide the results of distance measurements for the MF signal, it would be possible to perform a simulation-measurement analysis based on the actual distance measurements for VHF and MF measurements performed separately (simulation of a hybrid receiver based on previously recorded samples).

As a summary of the successful participation in the R-Mode Baltic and R-Mode Baltic 2 projects, the following achievements should be mentioned:

- Launch of the complete VDES R-Mode demonstration system.
- Performed sea trials (dynamic and long-term static monitoring) – measurements of the ranging accuracy based on the reception of the VDES R-mode signals transmitted from the station in Gdynia.
- Development of the multi-correlator concept and its implementation in the project (in order to reduce the multi-path phenomenon).
- Custom designed simulator which offers the accuracy predictions of the R-Mode System under various conditions and is capable of using previously measured and recorded signals.
- Launch of the real-time VDES R-mode positioning in laboratory conditions (and at Jastarnia) based on live signals received from one physical station in Gdynia (transmitted signal emulates messages from 4 stations).
- First software implementation and initial tests of the Kalman Filter with inertial module for assessment of its potential, future utilization in the R-mode.

References

[1-1] EfficienSea 2 project official website: http://www.efficiensea2.org.

[1-2] Ranging Mode for the Baltic Sea project official website: http://r-mode-baltic.eu/.

[1-3] R-Mode Baltic 2 project official website: https://projects.interreg-baltic.eu/projects/r-mode-baltic-2-253.html.

[1-4] AIS and VDES Ranging – concept and signal design, https://www.r-mode-baltic.eu/publications/

[1-5] AIS and VDES Ranging – measurements results, https://www.r-mode-baltic.eu/publications/

[1-6] R-Mode positioning system demonstrator, https://www.r-mode-baltic.eu/publications/

[2-1] Niski R, REPORT ON THE SELECTION OF THE POSITION for the VDES RECEIVER on the HEL Peninsula, Gdańsk, 2021

[2-2] Bronk K, Lipka A, Niski R, Radio project: R-Mode Gdynia base station, Gdańsk, 2021

[2-3] ITU-R P.1546-6, Method for point-to-area predictions for terrestrial services in the frequency range 30 MHz to 3 000 MHz, 08/2019,

[2-4] ITU-R M.2092-0, Technical characteristics for a VHF data exchange system in the VHF maritime mobile band, 10/2015

[3-1] Bronk K, Koncicki P, Lipka A, Rutkowski D, Wereszko B. Simulation and measurement studies of the VDES system's terrestrial component. Polish Maritime Research. 2019;1(101) Vol. 26:95-106. DOI: 10.2478/pomr-2019-0011.

[3-2] IALA Guideline G1139. The Technical Specification of VDES, Edition 5.0. September 2019.

[3-3] Bronk K, Januszewska M, Koncicki P, Niski R, Wereszko B. The concept of the R-Mode Baltic System using AIS Base Stations (in Polish). *Przegląd Telekomunikacyjny i Wiadomości Telekomunikacyjne*. 2019;6:257-260. DOI: 10.15199/59.2019.6.27.

[3-4] Bronk K, Koncicki P, Lipka A, Niski R, Wereszko B. Concept, signal design, and measurement studies of the R-Mode Baltic system. Navigation. 2021. DOI: 10.1002/navi.443.

[3-5] National Instruments, "NI USRP™-USRP 2954 ,https://www.ni.com/pl-pl/support/model.usrp-2954.html

[3-6] PROCOM BPF 2/2-250, https://amphenolprocom.com/products/filters/654-bpf-2-250

[4-1] GMV, Multicorrelator,2011,https://gssc.esa.int/navipedia/index.php/Multicorrelator

[4-2] Weather forecast archives, https://jastarnia.eu, 2021

[4-3] Benachenhou K, Sari E, Hammadouche, Multipath Mitigation in GPS/Galileo Receivers with Different Signal Processing Techniques, Aeronautic department of BLIDA, SETIT 2009, International Conference: Sciences of Electronic, Technologies of Information and Telecommunications.

[4-4] Tamazin M, Noureldin A, Korenberg M, Kamel A, A New High-Resolution GPS Multipath Mitigation Technique Using Fast Orthogonal Search, The Journal Of Navigation, 2016.

[4-5] Rogers L, Likelihood estimation of tropospheric duct parametrs from horizontal propagation measurements, Radio Science, Volume 32, Number 1, pages 79-92, 1997.

[4-6] ITU-R Recommendation P.834-7. Effects of tropospheric refraction on radiowave propagation. 2015.